Hi-Gain Spacecraft Antenna Modification Program

final report

GER 12856

OCTOBER 1966

PURCHASE ORDER 950905
(SUBCONTRACT UNDER NAS7-100)

PREPARED FOR
JET PROPULSION LABORATORY
CALIFORNIA INSTITUTE OF TECHNOLOGY
PASADENA, CALIFORNIA

GOODYEAR AEROSPACE
CORPORATION

CODE IDENT NO. 25500

GOODYEAR AEROSPACE
CORPORATION

AKRON 15, OHIO

HI-GAIN SPACECRAFT ANTENNA
MODIFICATION PROGRAM

(Reference: GER 11156 - Purchase Order 950467)

GER-12856

Final Report

October 1966

J. W. Haylett
R. S. Wilson

Prepared For

Jet Propulsion Laboratory
California Institute of Technology
Pasadena, California

Purchase Order 950905
(Subcontract Under NAS7-100)

This work was performed for the Jet Propulsion Laboratory, California Institute of Technology, sponsored by the National Aeronautics and Space Administration under Contract NAS7-100.

ABSTRACT

Goodyear Aerospace Corporation has concluded a follow-on design study, to the initial design and development contract 950467 (Reference GER 11156). This follow-on study has resulted in development, fabrication, and delivery of a modified 9-foot advanced development model of an expandable, directive, high-gain spacecraft antenna for Jet Propulsion Laboratory (JPL). The model demonstrated the feasibility of the design approach resulting from the follow-on design study.

This final report documents the following programs:

(1) preliminary design and analysis

(2) model re-design and fabrication, and

(3) model testing

It also outlines antenna ground deployment procedures, and presents conclusions and recommendations.

Work was performed under JPL contract No. 950905. The effort is a subcontract under Prime Contract NAS 7-100.

TABLE OF CONTENTS

TABLE OF CONTENTS (Cont'd)

TABLE OF CONTENTS (Cont'd)

TABLE OF CONTENTS (Cont'd)

TABLE OF CONTENTS (Cont'd)

TABLE OF CONTENTS (Cont'd)

LIST OF ILLUSTRATIONS

LIST OF ILLUSTRATIONS (Cont'd)

LIST OF ILLUSTRATIONS (Cont'd)

LIST OF TABLES

SECTION I

INTRODUCTION

A. BACKGROUND

Goodyear Aerospace Corporation has concluded a follow-on design study, to the initial design and development contract 950467 (Reference GER 11156). This follow-on study has resulted in development, fabrication, and delivery of a modified 9-foot advanced development model of an expandable, directive, high-gain spacecraft antenna for Jet Propulsion Laboratory (JPL). The model demonstrated the feasibility of the design approach resulting from the follow-on design study.

This final report documents the following programs:

(1) preliminary design and analysis,

(2) model re-design and fabrication, and

(3) model testing.

It also outlines antenna ground deployment procedures, and presents conclusions and recommendations.

Work was performed under JPL Contract No. 950905. The effort is a subcontract under Prime Contract NAS 7-100.

The program was initiated by JPL primarily to improve the conformance of the screened antenna to the true paraboloid and, also, to conduct a weight-saving

investigation. The principal objectives were:

(1) Reduce the screened antenna surface tolerance to less than ± 0.20 of an inch with respect to the ribs, by attaching 0.006 inch diameter stainless steel wire to the bottom of adjacent ribs. This wire is to be passed through and along the screen surface, and by applying tension to the wire, literally lower this surface closer to the paraboloid. This effort shall result in no greater than 0.3 db gain reduction as compared to the true paraboloid surfaces. The total weight increase shall be less than 0.1 pounds.

(2) Reduce the rib tip deflections to less than ± 0.10 of an inch under ± 1 g loading. The weight of a redesigned rib shall not exceed the weight of the present rib. Thermal deflections shall be less than ± 0.050 inches at one astronomical unit.

(3) Develop a concept of analytical investigation which will insure that the total screen surface shall not deviate more than ± 0.30 of an inch from a true paraboloidal surface under ± 1 g loading. This tolerance shall include those listed under preceding items (1) and (2).

(4) Investigate the electrical, physical and thermal properties of material suitable for the antenna screen. The objective shall be to select a material physically and thermally compatible with the antenna. In addition, the material shall have an average reflectivity of

95 percent and shall yield an overall loss of 0.2 db or less.

(5) Install an operational feed and associated coaxial line in accordance with JPL drawing J 124930 and with modifications to match the existing deployment system.

(6) Conduct a study of the existing welded-truss boom structure. Determine the structural advantages and the weight advantages of the new configuration.

(7) Achieve antenna deployment with no loose parts other than the cannister.

(8) Conduct a design review of potential weight savings for the hub structure, feed support and deployment system.

(9) Design, fabricate and install drum locks which will positively restrain the rib deployment cable drum in its fully-opened position, thereby maintaining screen contour in the event of subsequent damage to the deployment actuator or cable.

(10) Minimize the electrical blockage of the antenna hub caused by loose screen between antenna ribs when the antenna is in the packaged configuration.

B. APPROACH

Design and development approaches were guided toward reliability, simplicity, and acceptable radio frequency performance, in that order. The desired characteristics included the following:

(1) The antenna must be capable of being erected, checked out, aligned, and packaged on earth; and must retain the specified operating characteristics when deployed in space environment.

(2) The antenna shall have a 95 percent probability of accurate deployment to the performance requirements of the contract (see Section 1, paragraphs A(1), A(2), and A(3)).

Goodyear Aerospace first initiated a preliminary design and analysis program to establish guide lines for material selection, to select a contour control configuration, to establish possible weight savings, and to reduce the design approaches. The preliminary design is discussed in Section II of this report.

The model re-design and fabrication stage followed the preliminary design task. A description of the selected design, the findings of structural, thermal, and weight analysis, and the modification techniques are discussed in Section III.

Before delivery of the model, Goodyear Aerospace performed contour, electrical and vibration tests. Section IV reports results of the tests.

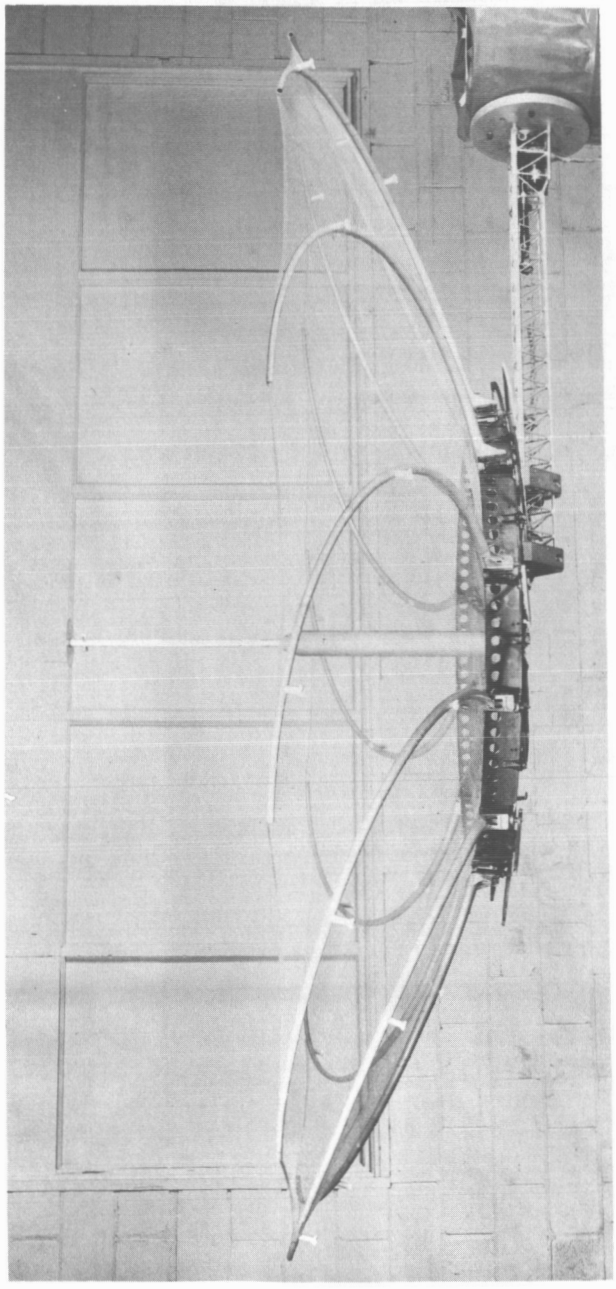

DEPLOYED CONFIGURATION

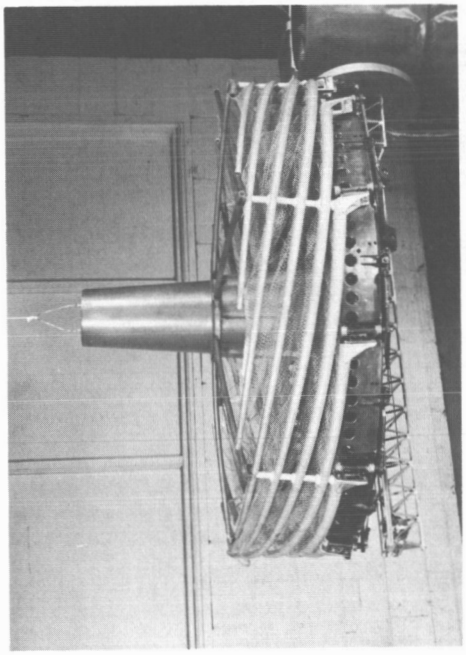

PACKAGED CONFIGURATION

Figure 1. High-Gain Spacecraft Antenna

Section V contains the ground operational instructions for the antenna.

C. RESULTS

Figure 1 shows the high-gain spacecraft antenna model in the packaged and in the deployed configurations.

The model was delivered to JPL in August 1966. Photographs and color movies of antenna deployment at Goodyear Aerospace have been prepared and delivered to JPL.

The antenna design basically consists of curved, tapered ribs that extend radially outward from the hub to the 9 foot diameter periphery. The ribs support a reflector screen and establish parabolic contour. The ribs are pivoted at the hub rim and nest circumferentially around the hub rim in the packaged condition. The screen material is a lightweight mesh of 0.003 inch diameter tin-plated copper wire that is attached to the ribs. This wire mesh is made to conform closely to the parabolic contour by means of attaching restraining wires to the back edges of the ribs with epoxy cement as shown in Figure 2. The center one-third of each of the eight rib-to-rib wires is interwoven in the screen mesh prior to placing the wires under the tension required to meet the contour requirements. Note that pairs of radial wires are also attached between the parabolic face of the hub and the outboard end of each rib. These radial wires are also interwoven into the screen mesh.

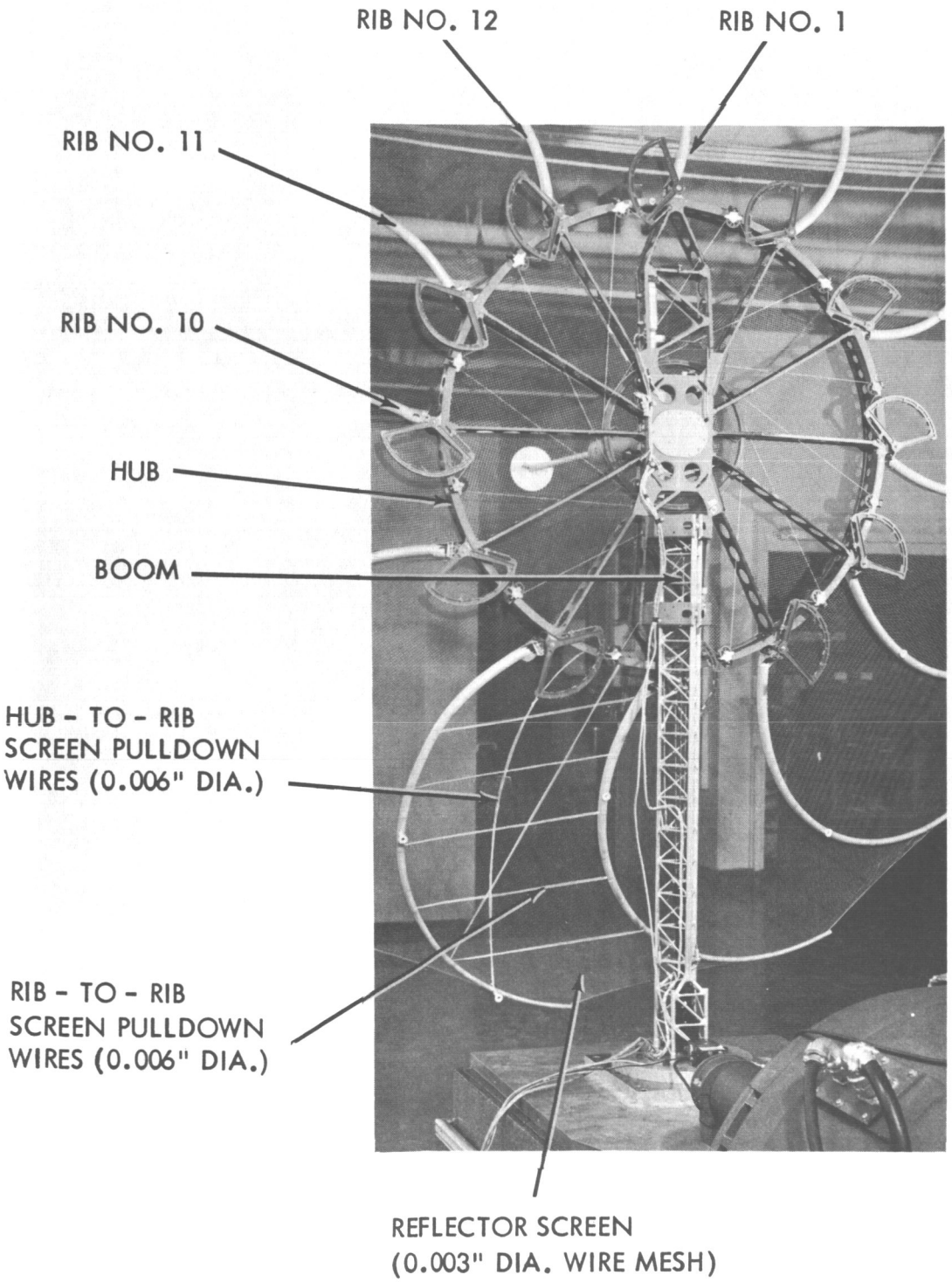

FIGURE 2. SCREEN CONTOUR WIRES

SECTION II

PRELIMINARY STUDY AND ANALYSIS

A. GENERAL

The initial task included investigation of structural and mechanical parts design, shape retention methods, screen reflectance characteristics, feed integration methods, weight-reduction methods, elimination of loose deployed parts, and elimination of electrical blockage at the hub. The initial task report in this section is grouped under eleven major paragraph headings, as follows:

B. RIB TOLERANCE

C. SCREEN TOLERANCE

D. SURFACE TOLERANCE

E. SCREEN REFLECTANCE

F. FEED INTEGRATION

G. BOOM STRUCTURAL ANALYSIS

H. LOOSE PARTS

I. WEIGHT REDUCTION

J. SECTOR LOCKS

K. ELECTRICAL BLOCKAGE

L. RECOMMENDED CONFIGURATION

Data obtained in the investigation was used as basic data for the re-designed configuration described in Section III of this report.

B. RIB TOLERANCE

1. General

The conducted study of new rib designs included the following considerations for reducing tip deflections to less than ± 0.10 inch with ± 1 g loading:

a. Filling the ribs with low density foam

b. Tapering the ribs from root to tip

c. Altering the rib cross-section

d. Changing the rib material

e. Thermal Analysis

Secondary objectives of the rib design study were to:

a. Reduce thermal deflections to less than ± 0.050 inches at one astronomical unit.

b. Maintain the weight of the new ribs equal to or less than the weight of the ribs fabricated under JPL Purchase Order 950467.

Many materials were considered during this study, and the three best materials were considered in detail. Invar was considered because of its low thermal expansion; Aluminum was considered because it is a well-known material with established fabrication techniques; and Lockalloy was considered the best of the new materials which will be available in the next few years. The results

Table I. Rib Material and Cross-Section Data

Tube Construction		Deflections Perpendicular to Contour			Root Yield Moment (Inch - Pounds)	Total Tube Weight (Pounds)
Material	Wall Thickness (Inches)	Dead Weight (Inches Per g)	Thermal Gradient			
			Degrees F	Inches		
1" O.D. TUBES:						
INVAR	0.007	0.0736	25	0.023	110	3.96
2014 T6 ALAL	0.016	0.0536	1.5	0.0245	692	3.12
	0.020	0.0536	1.1	0.0180	865	3.89
LOCKALLOY	0.016	0.0141	1.2	0.0145	504	2.27
	0.020	0.0141	0.8	0.0096	629	2.84
Tapered Diameter Tubes: 1" ROOT DIA., 0.5" DIA. TIP						
INVAR	0.007	0.0691	Root 25 Tip 6.5	0.0192	110	2.97
2014 ALAL	0.016	0.0504	Root 1.5 Tip 0.4	0.0208	692	2.34
	0.020	0.0504	Root 1.1 Tip 0.3	0.0154	865	2.92
LOCKALLOY	0.016	0.0132	Root 1.2 Tip 0.3	0.0120	504	1.70
	0.020	0.0132	Root 0.8 Tip 0.2	0.008	629	2.12

Table I (Continued)

Tube Construction		Deflections Perpendicular to Contour			Root Yield Moment (Inch - Pounds)	Total Tube Weight (Pounds)
Material	Wall Thickness (Inches)	Dead Weight (Inches Per g)	Thermal Gradient Degrees F	Thermal Gradient Inches		
Tapered Diameter Tubes: 1.5" ROOT, 0.5" TIP:						
INVAR	0.007	0.0288	Root 40 Tip 6.5	0.0214	248	3.96
2014 T6	0.016	0.0210	Root 3.3 Tip 0.4	0.0296	1560	3.12
	0.020	0.0210	Root 2.7 Tip 0.3	0.0246	1950	3.89
LOCKALLOY	0.016	0.0055	Root 2.5 Tip 0.3	0.0169	1130	2.27
	0.020	0.0055	Root 2.0 Tip 0.2	0.0132	1410	2.84
1" O.D. Tubes With Tapered Wall Thickness:						
INVAR	0.014 to 0.007	0.0515	Root 15 Tip 25	0.0183	220	5.94
2014 T6	0.036 to 0.012	0.0306	Root 0.7 Tip 2.0	0.022	1560	4.67
LOCKALLOY	0.036 to 0.012	0.0076	Root 0.5 Tip 1.5	0.0121	1130	3.42

Table I (Continued)

Tube Construction		Deflections Perpendicular to Contour			Root Yield Moment (Inch - Pounds)	Total Tube Weight (Pounds)
Material	Wall Thickness (Inches)	Dead Weight (Inches Per g)	Thermal Gradient			
			Degrees F	Inches		
0.75" O.D. Tubes With Tapered Wall Thickness:						
INVAR	0.014 to 0.007	0.091	Root 10 Tip 17	0.0165	123	4.40
2014 T6	0.036 to 0.012	0.055	Root 0.3 Tip 1.2	0.0163	875	3.50
LOCKALLOY	0.036 to 0.012	0.015	Root 0.3 Tip 0.9	0.0097	636	2.54
Foam Filled Tubes:						
INVAR, 1" O.D.	0.007	0.084	34	0.0312	110	4.52

are shown in Table I, and the subsequent paragraphs discuss the approach used to obtain the data.

2. Filling the Ribs With Foam

A curved, thin-walled tube, when loaded by bending in the plane of its curvature, deflects more than is calculated using conventional beam theory. This increased deflection results from a change in the cross-sectional shape of the tube. Page 110 of Reference 1 gives a detailed discussion of the problem and an approximation for the deflection of a curved tube. This deflection may be written as:

$$\delta_c = k\delta$$

where δ_c is the deflection of the curved tube, δ is the deflection from conventional theory, and k is a correction factor.

The expression for k may be approximated as:

$$k = \frac{10 + 12 \left(\frac{t R}{r^2}\right)^2}{1 + 12 \left(\frac{t R}{r^2}\right)^2}$$

Figure 3 shows the variation of k with t for these tube diameters (2 r) and the 21 inch radius of curvature (R) of the JPL deployable spacecraft antenna ribs.

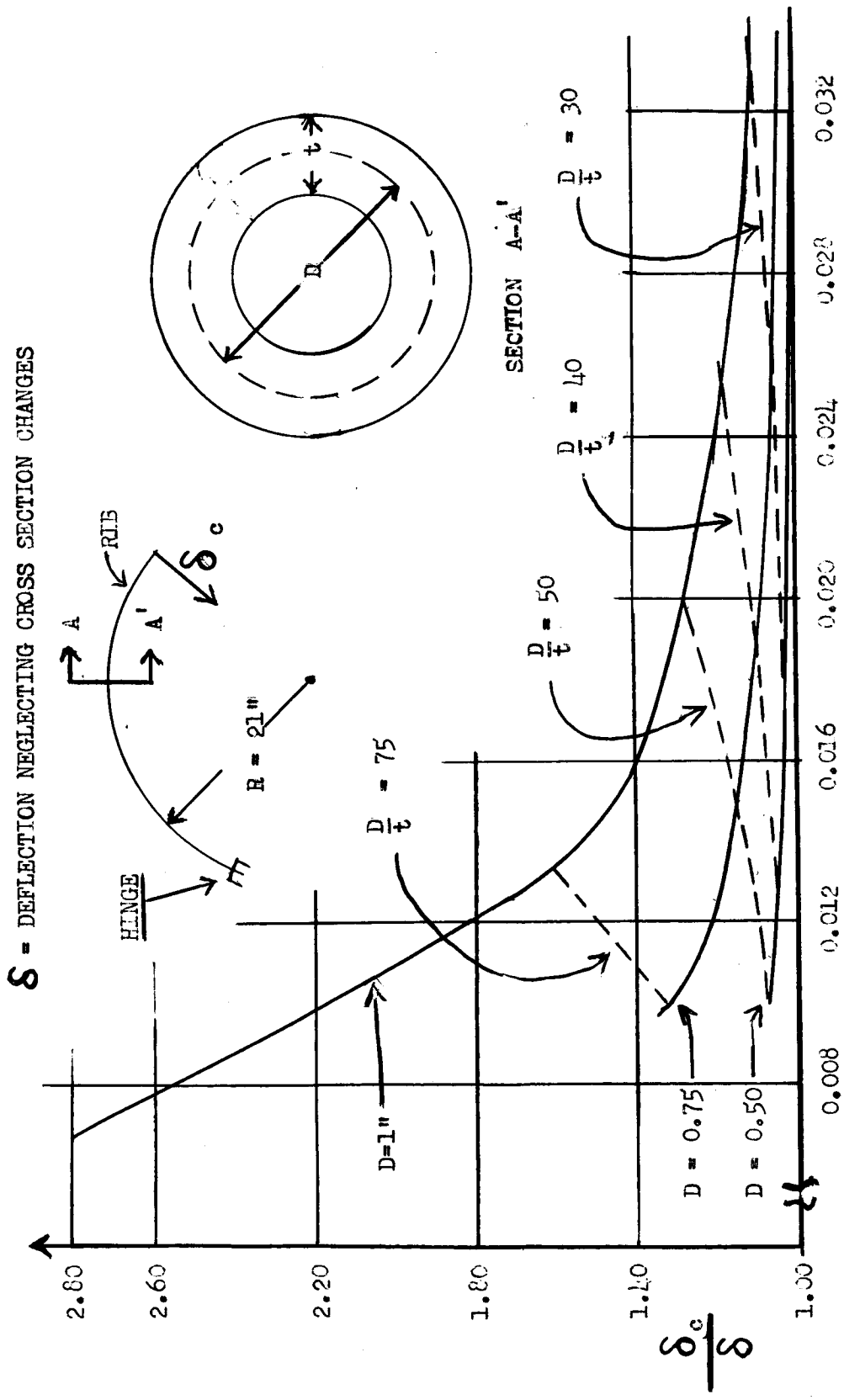

Figure 3. Deflection Correction Factor Vs Rib Thickness

Filling thin tubes with foam reduces the deformations of the tube cross-section, and results in deflections in the plane of curvature which can approach those derived from conventional theory neglecting the curvature. The same results may be obtained by an increase in the tube wall thickness and/or a decrease in the radius of the cross section.

The conclusion is drawn from the preceding that a less dense tube wall material offers a better solution to the problem. These materials have a better density-to-modulus ratio than the Invar as originally used. This is also desirable. The foam appears as an increase in material density for dead weight deflections perpendicular to the plane of curvature of the rib, without an appreciable increase in stiffness.

3. Tapering The Rib Diameter From Root to Tip

Tapering the rib diameter from root to tip is suggested as a way of reducing the dead weight deflections perpendicular to the planes of the ribs. The deflection integral for a curved, tapered-radius tube is given by:

$$\delta_{1G} = \frac{2\gamma R^4}{E r_o^2} \left\{ \int_0^B \left[\frac{1 - \cos\phi + n(\phi - \sin\phi)}{(1 + n\phi)^3} \right] \sin\phi \, d\phi \right.$$

$$\left. + 1.25 \int_0^B \frac{(\phi - \sin\phi) + n(\phi^2/2 + \cos\phi - 1)}{(1 + n\phi)^3} (1 - \cos\phi) \, d\phi \right.$$

where:

$$n = \frac{1}{\beta}\left(\frac{r_B}{r_o} - 1\right)$$

r_B = radius at root

r_o = radius at tip

β = included angle

R = rib radius

γ = material density

E = Young's modulus

A closed form solution is not possible for this deflection equation. A numerical evaluation, utilizing Simpson's Rule, is made with the approximate geometry of the High Gain Spacecraft Antenna ribs. Two assumptions are used for the boundary conditions: First, the diameter of 1-inch for the root, and one half inch for the tip, was selected for a numerical evaluation of the deflection equation.

$$\delta_{1G} = \frac{\gamma R^4}{E r_o^2}(.885 + .797)$$

$$r_o = \frac{r}{2}$$

where r is the radius of the present tube

$$\delta_{1G} = 6.73 \frac{\gamma R^4}{E r^2} \text{ inches}$$

A tube of constant radius cross section using the same included angle has a deflection of:

$$\delta_{1G} = 7.17 \frac{\gamma R^4}{E r^2} \text{ inches}$$

The taper provides a 6 percent reduction in deflection for this condition.

The second assumption is that the root radius may be increased above the present one inch in diameter. The maximum possible root diameter appears to be about 1.5 inches, or possibly a little less. When a tube having a 1.5 inch root diameter and a 0.5 inch tip diameter is used, a numerical evaluation of the deflection equation is made as follows:

$$\delta_{1G} = \frac{\gamma R^4}{E r_o^2} (.374 + .327)$$

$$r_o = \frac{r}{2}$$

where r is radius of present tube

$$\delta_{1G} = 2.804 \frac{\gamma R^4}{E r^2} \text{ inches}$$

This assumption provides a tube whose deflection is 39 percent of the present tube for the dead weight deflection perpendicular to the plane of the tube. Note that this is an upper limit for physical space available and that there is doubt as to whether this extreme could be attained in the taper of the tube. This taper has an adverse effect on the deflections in the plane of the

tube. The loading in this plane is essentially independent of the weight. The decreased bending section outboard and the increased root radius both adversely affect the deflection in this plane, as shown in Figure 3. The reduction in dead weight deflection is desirable, but the other effects are less desirable.

4. Tapering the Tube Wall-Thickness From Root to Tip

Tapering the rib wall-thickness from root to tip and maintaining a constant mean radius is another way of reducing the dead weight deflections perpendicular to the planes of the ribs. The deflection integral for a curved tube having tapered wall-thickness and a constant mean cross section radius is given by:

$$\delta_{1G} = \frac{2\gamma R^4}{E\ r^2}\left\{\int_0^{\beta} \frac{1 - \cos\phi + k(\phi - \sin\phi)}{1 + k\phi} \sin\phi\, d\phi \right.$$

$$\left. +1.25 \int_0^{\beta} \frac{\phi - \sin\phi + k\left[\frac{\phi^2}{2} + \cos\phi - 1\right]}{1 + k\phi} (1 - \cos\phi)\, d\phi \right\}$$

where $k = \frac{1}{\beta}\left(\frac{t_B}{t_o} - 1\right)$

t_B = thickness at root

t_o = thickness at tip

β = included angle

R = rib radius

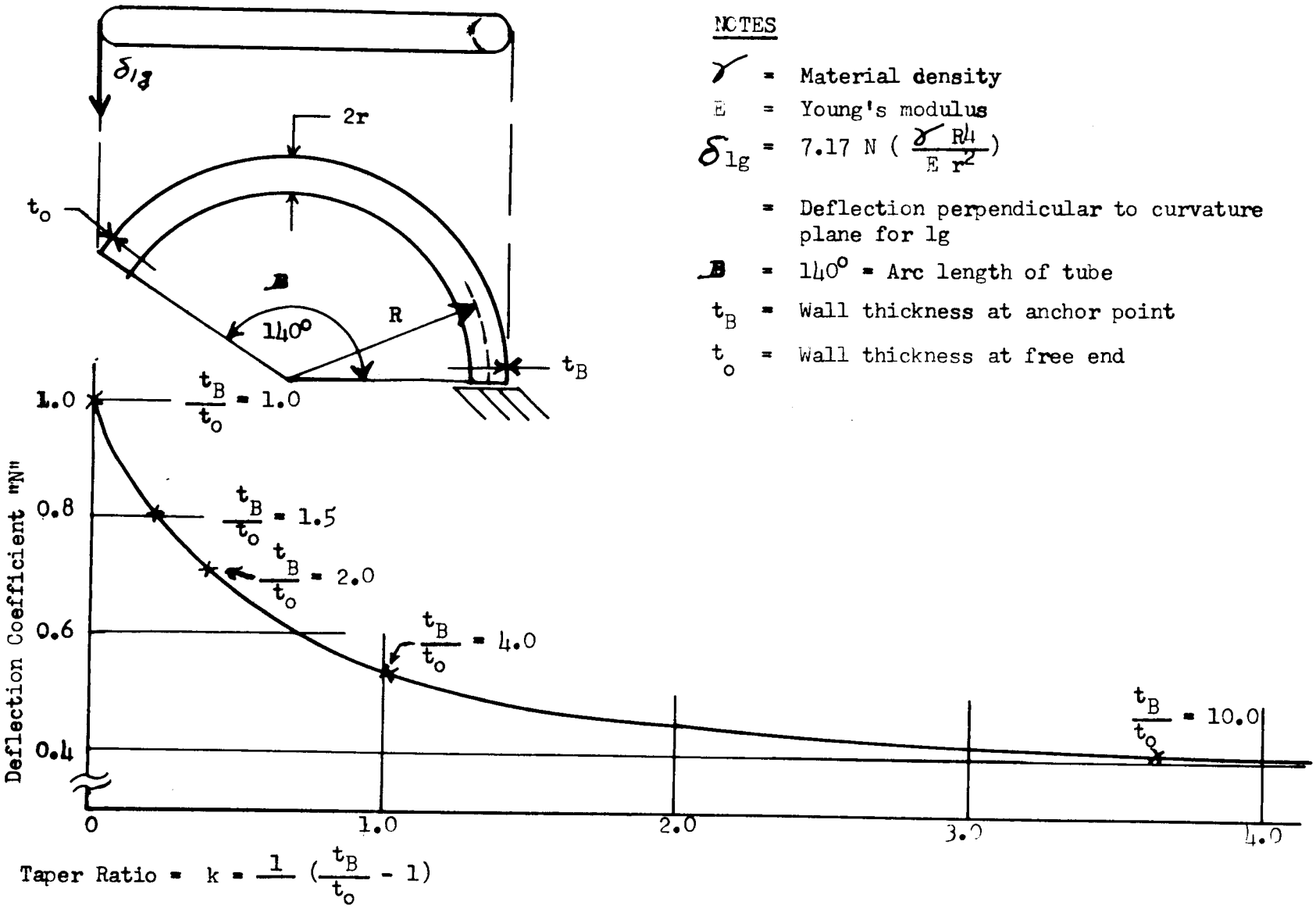

NOTES

γ = Material density

E = Young's modulus

δ_{lg} = 7.17 N ($\frac{\gamma R^4}{E r^2}$)

= Deflection perpendicular to curvature plane for lg

B = 140° = Arc length of tube

t_B = Wall thickness at anchor point

t_o = Wall thickness at free end

Figure 4. Dead Weight Deflection Of Constant Diameter Cylindrical Tubes Having Tapered Wall Thickness

GOODYEAR AEROSPACE CORPORATION
GER-12856

r = cross section radius

γ = material density

E = Young's modulus

A closed form solution of the deflection equation is not possible. A numerical evaluation, utilizing Simpson's Rule is made with geometry approximating that of the high gain spacecraft antenna ribs. Value of $\frac{t_B}{t_o}$ used are 1.5, 2.0, 4.0 and 10.0. The ratios of the coefficients of $\frac{\gamma_R 4}{E\ r^2}$ to that of a tube of constant cross section are given in Figure 4.

The equation for tubes with tapered walls and constant radius is:

$$\delta_{1G} = N\ 7.17\ \frac{\gamma_R 4}{E\ r^2}$$

where N = deflection coefficient ratios.

Figure 4 is a plot of N for various values of k. Inspection of Figure 4 shows that a ratio of $\frac{t_B}{t_o}$ of about 3, or k = .80 would result in 42 percent reduction in dead weight deflection. The corresponding increase in thickness at the root would be beneficial to the in-plane bending problem. The reduction in the outboard bending inertia is small, also desirable for the in-plane bending.

5. Altering the Rib Cross-Section

The rib has significant bending requirements about both axis of the cross section. In addition, approximately half of the deflection perpendicular to the plane of the rib comes from torsional deformation. The design requires a maximum bending

stiffness about two perpendicular axis and a minimum torsional deflection. A thin circular cylinder and a thin hollow square could meet the requirements. Using the radius of the tube as the standard, the bending moment inertia-to-area of section ratios are developed and the perimeter-to-enclosed area is also determined. The bending deflections are inversely proportional to the $\frac{I}{A}$ ratio and the torsional deflections are proportional to the ratio of the perimeter to the enclosed area.

Equal Perimeter Thin Tube Circular	Thin Tube Square
$A = 2\pi r t$	$A = 4th = 2\pi r t$
$I = \pi r^3 t$	$I = \frac{2}{3} h^3 t$
$\frac{I}{A} = r^2$	$\frac{I}{A} = \frac{h^2}{6} \frac{\pi^2 r^2}{24} = .411\, r^2$
$\oint d s = 2\pi r$	$\oint d s = 4 h = 2\pi r$
$A_s = \pi r^2$	$A_s = h^2 = \frac{\pi^2 r^2}{4}$
$\frac{\oint d s}{A_s} = \frac{2}{r}$	$\frac{d s}{A_s} = \frac{8}{\pi r} = \frac{2.55}{r}$

The preceding data shows clearly that the circular tube cross section is best for the present rib configuration.

6. Changing the Rib Material

The equation for the dead weight deflection contains the quantity of $\frac{\gamma}{E}$ which are material properties. Figure 3 indicates that a thicker tube is desirable to reduce deformations in the plane of a rib. A decrease in density

of the structural material permits an increase in wall-thickness, with no increase in weight. This increase in wall-thickness gives better performance in the plane of the rib. Practically all conventional structural materials have a better $\frac{\gamma}{E}$ ratio than the Invar which was originally used. This improved ratio may be used either to decrease the deflection at a given weight; or to decrease the weight a limited amount for a given deflection, by effecting a decrease in the cross-section radius "r".

The best material of a practical nature found to date is "Lockalloy", a 62 percent beryllium 38 percent aluminum alloy. Its density modulus ratio is

$$\frac{.0756}{28.5 \times 10^6} = 2.56 \times 10^{-9} \text{ in.}$$

The best of the currently available aluminum alloys is 2014ST. This aluminum alloy has a density modulus ratio of

$$\frac{.101}{10.5 \times 10^6} = 9.62 \times 10^{-9} \text{ in.}$$

The presently used Invar has a density-to-modulus ratio of

$$\frac{.29}{22 \times 10^6} = 13.2 \times 10^{-9} \text{ in.}$$

The ultimate strength and yield strength are 55 and 40 ksi for the Lockalloy and 65 and 55 ksi for 2014 T6 aluminum alloy which compare favorably with the 60 and 20 ksi of Invar. The increase in thickness possible with Lockalloy or

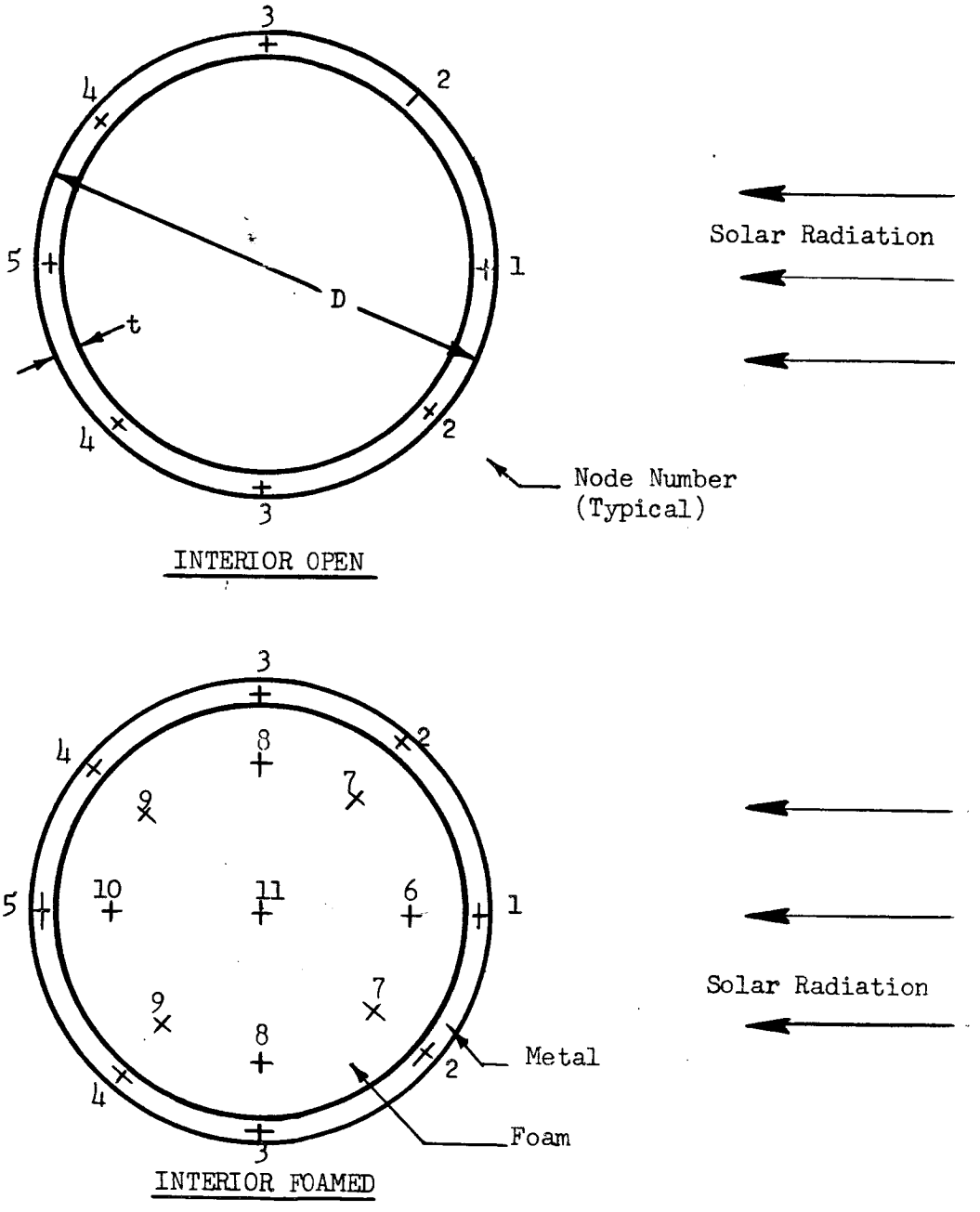

Figure 5. Thermal Schematic of Rib

or Aluminum, in conjunction with their higher yield strengths, should provide ribs which are more resistant to physical damage.

7. Thermal Analysis

The tube thermal schematic is shown in Figure 5. The tube and foam are divided into a number of nodes. A heat balance on each node results in a set of simultaneous nonlinear equations which, when solved, produce the node temperatures. An IBM 1410 Digital Computer was used to perform the computations.

The results of the thermal study are presented in Figures 6, 7, and 8. The temperature differential reported is the difference between the temperatures of nodes 1 and 5. Figure 6 considers a hollow tube, and presents the temperature differential as a function of the ratios of wall thickness-to-diameter, and thermal conductivity-to-diameter. Figures 7 and 8 consider an Invar tube filled with foam, and present the temperature differential as a function of wall thickness and diameter. Figure 7 presumes a foam thermal conductivity of 0.04 BTU-in/hr-ft^2-°F, which approximates evacuated foams. Figure 8 shows the effect of increasing the foam conductivity to 0.4 BTU-in/hr-ft^2-°F by unspecified means; only slight improvement in thermal deflections would be realized.

The results of the thermal analysis study indicate Invar will produce larger thermal gradients than either Aluminum or Lockalloy, assuming the same physical construction and environment. If the weight of the tubes is increased by

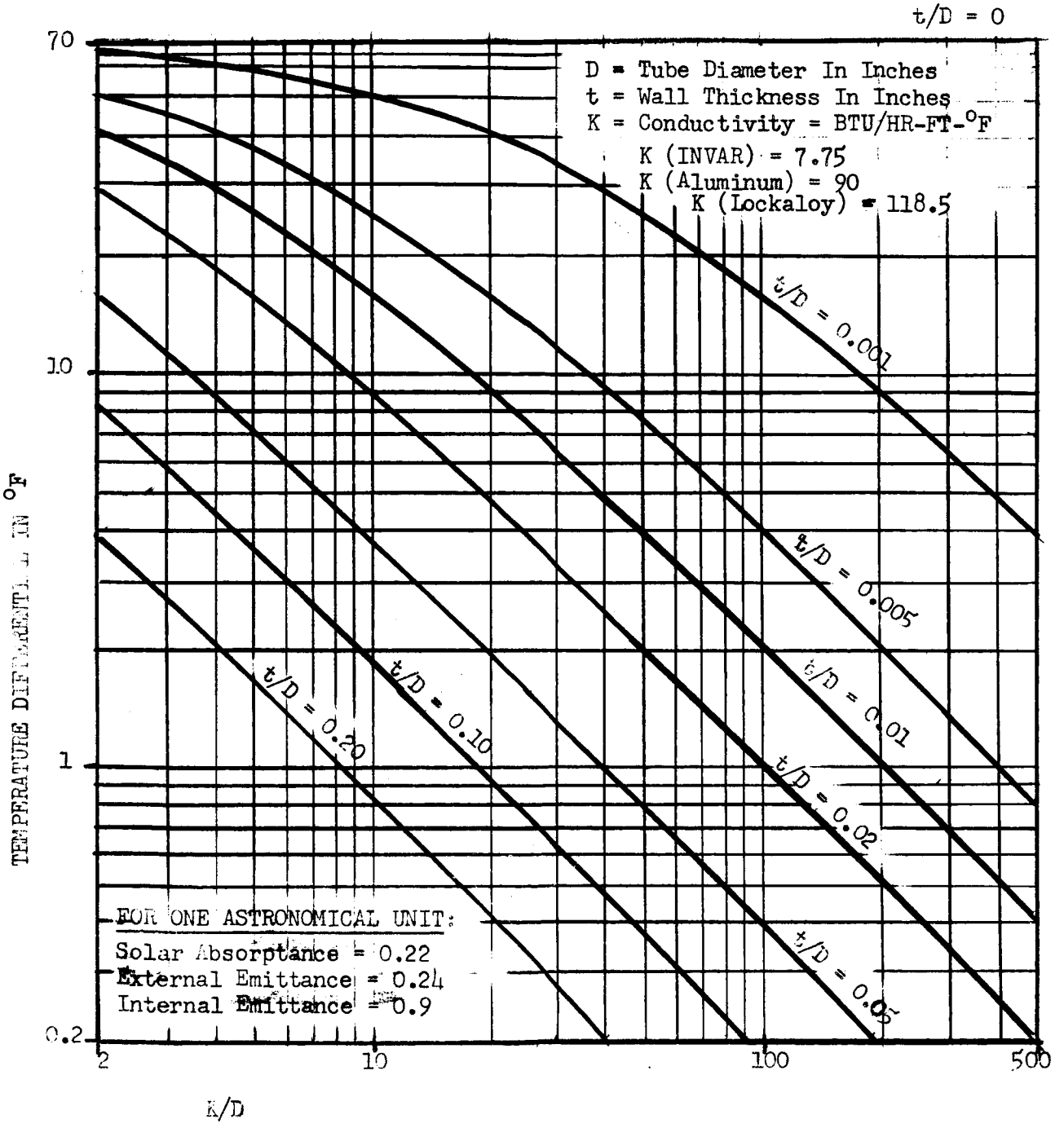

Figure 6. Temperature Differential Across Rib With Internal Radiation

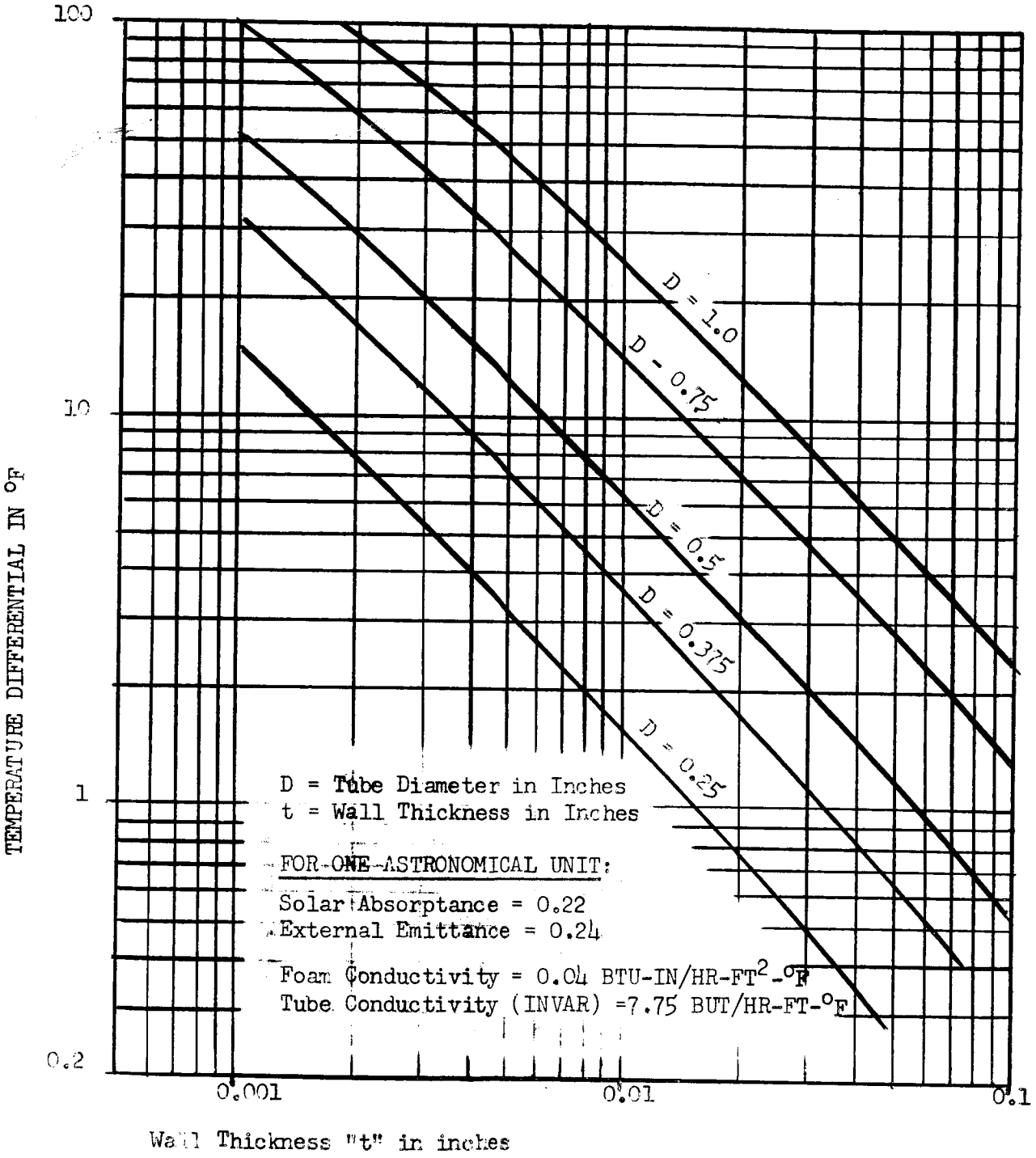

Figure 7. Temperature Differential Across Rib Filled With Low-Conductivity Foam

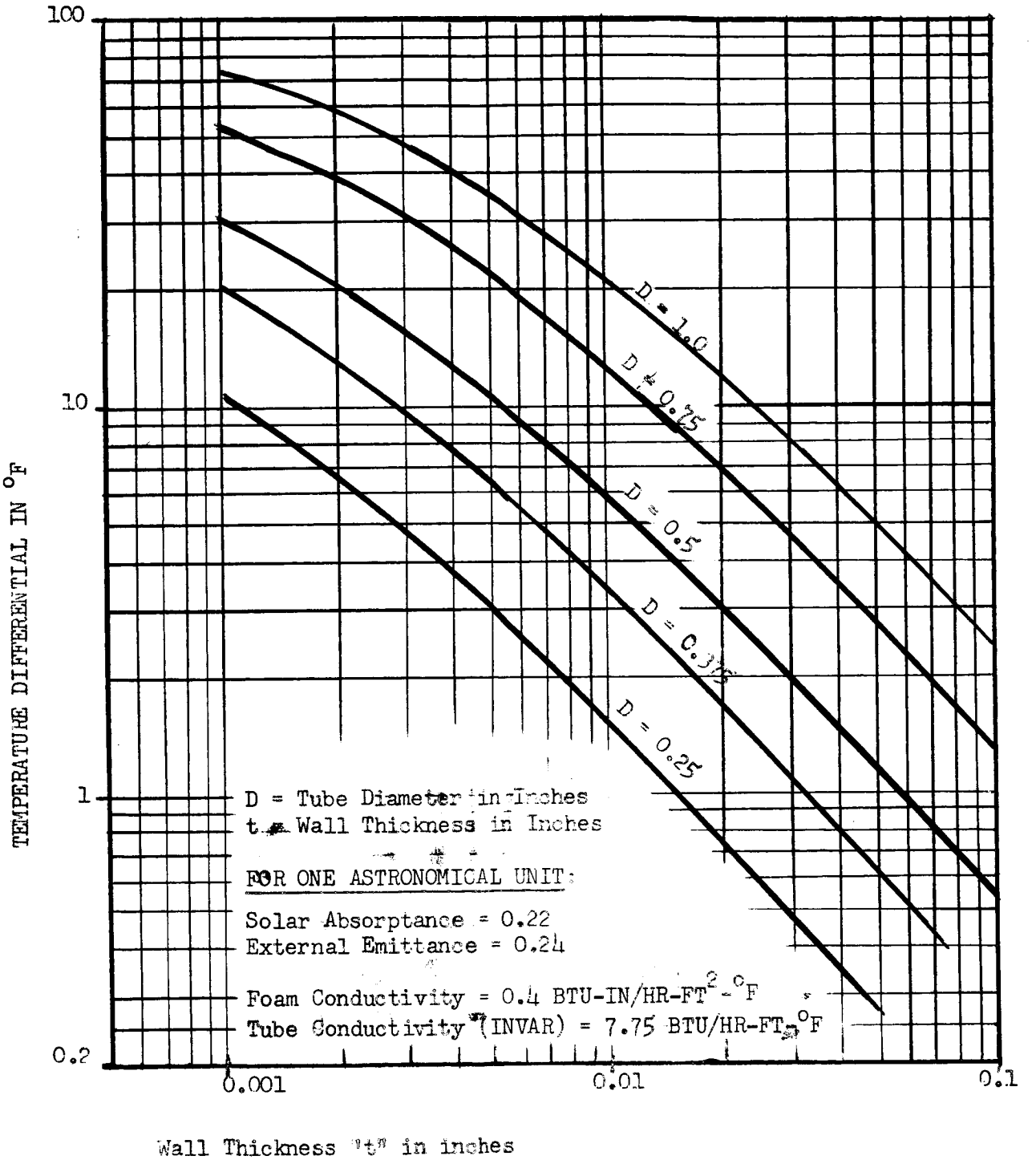

Figure 8. Temperature Differential Across Rib Filled With Low-Conductivity Foam

varying the aluminum or Lockalloy tube wall-thickness inversely as their density ratios (to equalize the weight of the three configurations) the thermal gradient difference for Invar will be even greater.

The ultimate consideration, however, is the deflection associated with the thermal gradients. The results of this consideration is shown in Table I, and in general, indicates Lockalloy as the most desirable material, with aluminum second, and Invar third. It should be noted that all thermal deflections are below the $\pm$ 0.050 inches required by the specification.

8. Selected Design

The data in the preceding study was used to select the rib for incorporation into the modified antenna. The selected rib design uses 2014 T6 aluminum tubing with a tapered diameter (1 inch root and 0.5 inch tip) and a constant wall thickness (.020 inch). The new configuration meets or exceeds the specification in all respects. This construction, as compared to the original 1 inch diameter Invar rib, has the following advantages:

1. Lighter weight
2. Lower 1 g deflections
3. Lower thermal deflections
4. Improved structural characteristics
5. Less susceptible to handling damage

Lockalloy configurations were superior to the selected design in all respects, however, design and fabrication information was not available on processes or limitations. Lockalloy material was therefore considered as too advanced to be incorporated into a current antenna program.

C. SCREEN TOLERANCE

1. General

A study of various methods for using the elements to reduce the contour error of the screen surface was conducted. The design objective was to reduce the contour error to less than $\pm$0.200 inch with respect to the ribs.

2. Screen at Antenna Deployment

When the antenna is deployed, the screen is drawn taut between adjacent ribs. Because a screen element is a straight line in the direction of stretch, the screen assumes a single, radially curved surface between ribs. Therefore, even if the ribs are exactly to contour, the screen contour will be stretched flat from rib-to-rib and will not match the paraboloid. The maximum error will be midway between the ribs, and cross section of the antenna will appear as shown in Figure 9.

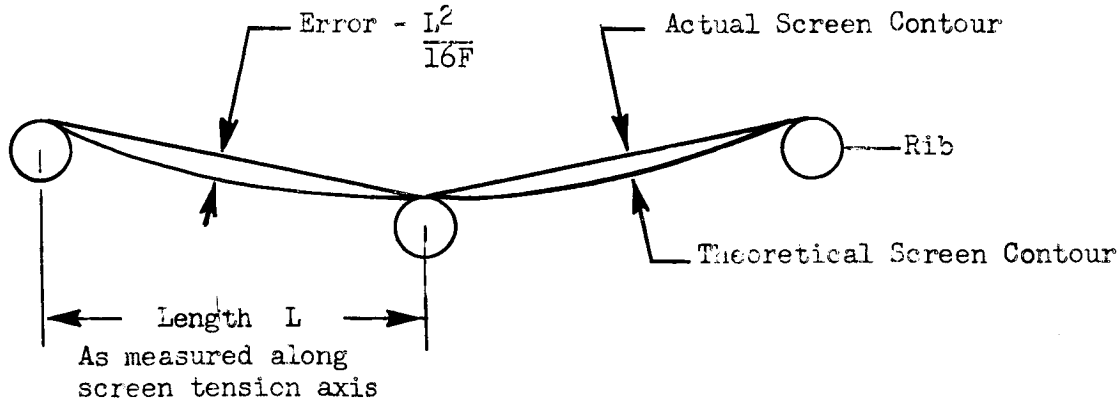

Figure 9. Cross Section Through Deployed Screen

3. Proposed Solutions

To make the actual screen contour more closely approximate the theoretical contour, tie wires were run from the underside of the ribs to the screen. As the tie wires were tensioned, it pulled the screen down closer to the theoretical contour. Various tie methods were tried. Several of these initial methods are shown in Figure 10.

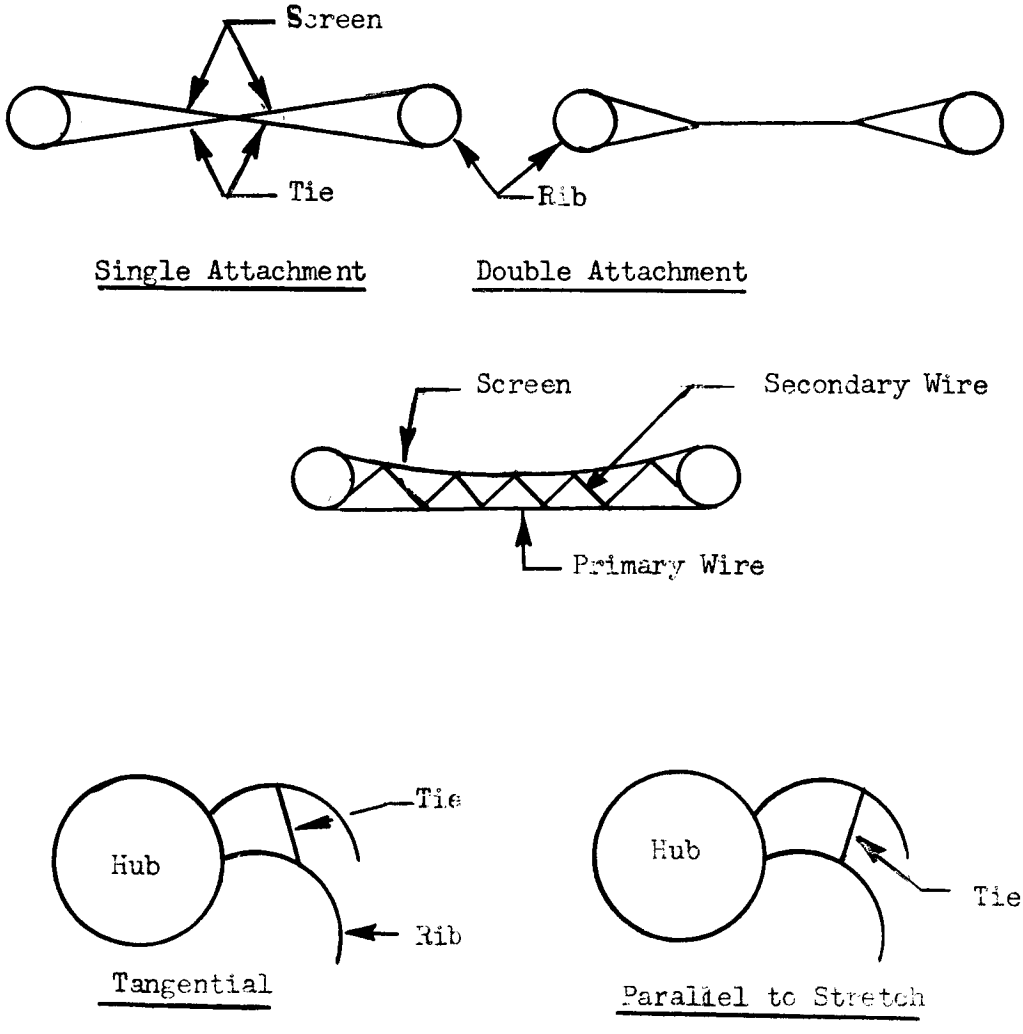

Figure 10. Screen Pulldown Using Tie Elements

The method determined most feasible and accurate was what might be termed "a double attachment parallel to the direction of screen stretch." Actually, a single wire was fed from the underside of a rib through the screen at a point approximately one third the distance to the adjacent rib. The wire was then intertwined with the screen for another third of the distance, and then fed to the underside of the adjacent rib.

4. Installation of Wires

One bay on the original antenna was modified to incorporate tie wires. These were spaced four inches apart, tensioned to decrease the contour error, and fastened to the ribs with tape. By sighting along the screen, it was apparent that the screen was presenting a wavy surface in a direction perpendicular to the wires. The contour variation at crests and troughs appeared too large. Accordingly, wires were installed every two inches and the surface then seemed quite uniform.

5. Test Procedure

To determine the surface accuracy, the antenna was mounted aperture face-down, with its axis perpendicular to a surface table. A height gage was used to measure the distance from the surface table to any point on the parabolic antenna. An electrical contact was used to determine when the gage point just touched the screen. Readings were taken at different radii in four-inch increments. At each radius, the gage was moved in the arc of a circle and five readings taken;

one at each rib and at three equidistant points on the screen. In this manner the points measured would be random insofar as the tie wires were concerned. At times the electrical contact would be at a wire and at other times between wires. It is apparent that at any radius, the variation in readings between the ribs and the screen is the contour error measured parallel to the antenna axis.

6. Test Data

Four sets of measurements were taken:

(a) Original setting; wires installed and tensioned

(b) After antenna was closed and opened once

(c) After antenna was closed and opened a second time

(d) After tie wires were removed

Table II shows the readings obtained.

7. Summary

From an analysis of the data, it is evident that the screen contour error can be reduced to within ±0.200 inches with respect to the ribs by using tie wires. Without these wires, the maximum error recorded was 0.637 inches. It should be noted that these tests were made using one-inch diameter ribs. There may be a slight compromise of the results shown when tapered tubes are installed. However, it is believed that the required accuracy can be met with the tapered tubes.

Table II. Screen Contour Measurements* With Aperture Face-Down

* Radius	** Measurement Condition	Rib #10	Left	Screen Center	Right	Rib No. 9	Low Spot In Screen	Rib Mean	*** Maximum Error Plus	*** Maximum Error Minus	Total Error
24	A	20.230	20.100	20.220	20.120	20.290	20.100	20.260	+0.030	-0.160	0.190
	B	20.290	20.100	20.200	20.110	20.290	20.095	20.290	+ 0	-0.195	0.195
	C	20.295	20.095	20.225	20.120	20.285	20.090	20.290	+ 0	-0.200	0.200
	D	20.270	19.975	19.890	19.875	20.290	19.865	20.280	+0.010	-0.415	0.425
28	A	18.950	18.765	18.850	18.895	18.920	18.760	18.935	+0.015	-0.175	0.190
	B	18.965	18.760	18.845	18.865	18.940	18.750	18.955	+0.012	-0.202	0.215
	C	18.955	18.740	18.860	18.900	18.935	18.700	18.945	+0.010	-0.245	0.255
	D	18.950	18.410	18.350	18.420	18.945	18.350	18.947	+0.003	-0.597	0.600
32	A	17.395	17.440	17.335	17.410	17.395	17.280	17.395	+0.045	-0.115	0.160
	B	17.400	17.380	17.280	17.365	17.405	17.250	17.402	+0.003	-0.152	0.155
	C	17.400	17.425	17.315	17.390	17.395	17.240	17.397	+0.002	-0.157	0.160
	D	17.385	16.860	16.765	16.860	17.420	16.765	17.402	+0.018	-0.637	0.655
36	A	15.630	15.570	15.580	15.675	15.630	15.510	15.630	+0.045	-0.120	0.165
	B	15.625	15.520	15.540	15.620	15.640	15.465	15.632	+0.008	-0.167	0.175
	C	15.615	15.570	15.585	15.660	15.630	15.510	15.622	+0.038	-0.112	0.150
	D	15.570	15.055	15.030	15.110	15.645	15.005	15.607	+0.038	-0.602	0.640
40	A	13.600	13.680	13.665	13.605	13.630	13.525	13.615	+0.065	-0.090	0.155
	B	13.590	13.625	13.590	13.550	13.605	13.500	13.597	+0.028	-0.097	0.125
	C	13.580	13.650	13.615	13.555	13.625	13.510	13.602	+0.048	-0.092	0.140
	D	13.560	13.105	13.070	13.135	13.645	13.065	13.602	+0.043	-0.537	0.580
44	A	11.395	11.470	11.435	11.420	11.375	11.300	11.385	+0.085	-0.085	0.170
	B	11.395	11.395	11.350	11.320	11.385	11.220	11.390	+0.005	-0.170	0.175
	C	11.380	11.410	11.335	11.345	11.380	11.250	11.380	+0.030	-0.130	0.160
	D	11.375	10.970	10.940	11.005	11.420	10.910	11.397	+0.023	-0.487	0.510

* All measurements and radii are given in inches

** Measurement Condition Legend: A = Original Setting, wires installed and tensioned; B = Antenna Closed and Opened Once; C = Antenna Closed and Opened a Second Time; D = Tie Wires Removed.

*** MINUS errors are deviations toward surface table; PLUS errors are deviations away from surface table.

The results indicate that repeatability of the measurements was achieved. The small discrepancies can be attributed to reading accuracy and to the possibility of a slight give where the wire end was fastened to the rib with tape. A cement, such as epoxy, would be used on the production antenna.

The maximum error and "total error" noted in Table II was determined by comparison of the readings with the "rib mean" readings. Although this is not rigorous, the rib readings are very close together and thus the small error introduced by using the rib mean can be neglected.

The loose tie wires in the packaged condition give an unorganized appearance. It was initially believed that a problem would exist with fouling or tangling of these tie wires. However, in addition to the closing and opening tests noted, the antenna was operated several times during the preliminary installation of the tie wires. At no time did these wires foul. Therefore with normal packaging care this should not be a problem.

The test was made using 0.008 inch diameter stainless steel tie wires. The weight of these wires for the complete antenna would be less than 0.05 pounds. If the weight of the cement was added, the net weight increase would still be less than 0.1 pounds.

8. Conclusions

The preceding study and tests indicate the feasibility of utilizing tie wires to

obtain the desired contour accuracy. The large number of wires will, however, be a major installation problem in that each wire must be installed individually, tensioned separately and remain fixed in tension, yet be adjustable throughout the complete test program. Approaches to solving these problems appeared straight forward and were solved in the design phase of the program. The final optimized design is presented in Section III.

D. SURFACE TOLERANCE

The specification requires that the surface shall not deviate more than ±.30 inches from a true paraboloidal surface under ± g loading. The ±0.05 inch thermal deflection is included in the ±0.30 inches which leaves ±0.25 inches as the total tolerance deviations for ground measurements.

The preliminary design and study reported in paragraphs B and C indicate the tolerance requirements will be met. A summary of the requirements versus calculated deviations are given below. The summary does not include manufacturing and repeatability tolerances, but adequate tolerance reserve is present to compensate for these omissions.

	Requirement	Calculated
Thermal deviation	± 0.050 inches	± 0.015
Gravitational deviation	± 0.100 inches	± 0.050
Screen tolerance	± 0.2 inch	± 0.130

E. SCREEN REFLECTANCE

1. General

An investigation of the electrical, physical and thermal properties of various antenna screen materials was conducted. The objective was to select a material which would be physically and thermally compatible with the antenna, and which would also have an average reflectivity of 95 percent which is an overall loss of 0.2 db or less.

Previous experience on the original contract indicated the Raschel lace material physically and thermally compatible with the antenna, but the material was only 80 percent reflective at 2295 MHz. The material was 3 mil diameter silver-plated Invar wire which theoretically should have reflected 90 to 95 percent of the RF energy. At first, the original samples operated at 90 to 95 percent efficiency, but their efficiency degraded continuously, reaching a low of 60 percent after several months. Cleaning the degraded material restored the reflectance to 80 percent and above.

The major problem with previous antenna screening materials appeared to be contact resistance between adjacent wire elements of the screen. The current program was therefore initiated with a literature search for dry circuit contact resistance data, and with waveguide testing of various materials to verify the theoretical approach. The materials were tested with various tensions, before and after cleaning, before and after exposure to a corrosive environment, and at

periodic intervals up to one year.

The program resulted in the selection of 3 mil diameter tinned copper wire knitted into a Raschel lace pattern which, when deployed on the antenna, would orient into a rectangular pattern having spacings 0.25 by 0.13 inch. The subsequent paragraphs of this sub-section detail the results of the study.

2. Literature Survey

The most pertinent discussion regarding dry circuit contact was found in references 2 through 5.

The "dry circuit contact" is defined as an electrical contact in which only mechanical forces are used. Thus, no dielectric breakdown of insulating films or no heating effect of current flowing in a concentrated area assists in making the contact. In the case of the knitted wire material, these mechanical forces are small and will not disturb tarnish films which are normally insulating. Depending on the metal, these insulating films may be oxides, sulfides, chlorides, or other alien, multi-molecular films.

The following is a summary of information obtained from literature on dry circuit contact for the metals considered for this program:

a. Aluminum. With Aluminum wire, an aluminum oxide (Al_2O_3) film is formed very rapidly, with a thickness of 20 angstroms attained in a few seconds.

In a short period, even at room temperature, the thickness becomes too great for electrical conduction. The Al_2O_3 is securely bonded to the aluminum and can not be disturbed with light mechanical forces.

b. Copper. With copper wire, copper oxide (C_2O) film is formed at room temperature in about 30 minutes. This film is extremely thin. However, after a period of time, the oxide film will exhibit resistivities sufficiently large to act as insulators. Copper sulfide films can also be formed where the copper is exposed to an industrial environment. Both of the films increase the contact resistance, with copper sulfide being the most severe.

c. Gold-Plated Copper. Gold is extremely stable under ambient conditions. An adhesion monolayer of oxygen is deposited on gold in air, but this deposit does not affect the dry circuit contact. If the gold plating is 100 micro-inches or less, the copper will migrate or diffuse thru the gold. An insulating film of copper oxide or copper sulfide may then be formed, thereby increasing the contact resistance.

d. Tin Plated Copper. Tin is an excellent corrosion-resistant coating which has a very low contact resistance. As in the case of gold, the copper will migrate or diffuse thru the tin, but the migration process is very slow. Only a trace of migration was found after 28 months in ambient conditions.

3. Test Specimens

All test specimens were commercially knitted Raschel lace having a pattern as close as feasible to the antenna material pattern. The only obvious difference

occurred in the aluminum screen sample which had a spacing slightly larger than the required 0.25 by 0.13 inch. This difference may have caused a slight degradation but it was not considered a significant factor in the final selection.

Knitted samples of each of the following materials were tested:

Aluminum	5 mil diameter
Invar	3 mil diameter
Copper	3 mil diameter
Tinned Copper	3 mil diameter copper with greater than 20 x 10^{-6} inches of tin plating
Gold-Plated Copper	3 mil diameter copper with 20 x 10^{-6} inches of gold plating

4. Test Setup and Procedures

The screen samples were mounted on holding fixtures which could apply a varying load to the screen. The screen and fixtures were then inserted into a waveguide test set-up which was calibrated to indicate the reflection characteristics of the sample. From this data, the free space reflection characteristics were calculated.

The cells of the screen material are rectangular in shape when tensioned. The long dimension of the rectangles tend to form continuous parallel lines. The short dimension of the rectangles tend to form discontinuous parallel lines. Because of this non-symmetry in the cell structure, the tests were conducted with the long dimension of the rectangle oriented in two different positions: (1) parallel to the electric field vector in the waveguide, and (2) perpendicular to the electric

field vector in the waveguide. The free space reflection data obtained with parallel orientation and perpendicular orientation were averaged to obtain the reflected power characteristic of each sample.

A detailed discussion of the test set-up and calculation procedure is given in Appendix A.

5. Test Results

The screen tension test results are given in Table III; the environment test results are given in Table IV, and the life test results are given in Table V.

Table III. Screen-Tension Test Results

Material	Tension (Pounds/Inch)	Average Relected Power (percent)
Aluminum	0	57
	0.12	51
	0.25	50
	0.37	54
Invar	0	55
	0.06	54
	0.25	53
Copper	0	78
	0.06	85
	0.12	90
	0.25	89
Tinned Copper	0	96
	0.06	97
	0.12	97
	0.37	97
Gold-Plated Copper	0	67
	0.06	79
	0.12	90
	0.25	89

Table IV. Environment Test Results

Material	(Pounds/Inch)	Average Reflected Power (Percent)	Condition
Copper	0.12	58	Before Cleaning
	0.12	96	After Cleaning
	0.12	94	After Sulfide Exposure
	0.12	87	5 Days After Sulfide Exposure
Tinned Copper	0.12	97	Before Exposure
	0.12	94	After Chloride Exposure
	0.12	94	5 Days After Chloride Exposure
Gold Plated Copper	0.12	74	Before Cleaning
	0.12	96	After Cleaning
	0.12	96	5 Days After Cleaning

Table V. Life Test Results

Material	(Pounds/Inch)	Average Reflected Power (Percent)	Elapsed Time
Tinned Copper	.12	97	Initial
	.12	94	1.5 Years

6. Summary

The theoretical hypothesis and test results were in excellent agreement in that the tin-plated copper proved to be the highest reflecting material and showed very small degradation with time. The bare copper improved in reflectance after cleaning, but subsequently degraded as insulating films increased on the surface of the wire. The gold-plated wire also improved after cleaning and, as would be expected, remained high for at least five days. Although not tested, it is believed the gold-plated copper would have returned to its low reflectance in a relatively short period of time, due to the migration of the copper through the gold plating. After the tension tests, the Aluminum and Invar were eliminated as possible candidate materials because of their extremely low reflectance values.

Based on the test data and the theoretical evaluation, 3 mil tin-plated copper wire was selected as the screening material for the modified antenna.

F. FEED INTEGRATION

1. General

An operational feed designed by JPL (Dwg. J-126352) and produced by GAC (Dwg. SK-DW-33065) was installed on the antenna (See Figure 1). The feed operated satisfactorily, but it was not optimized as part of this program. The feed patterns and resulting antenna patterns are discussed in Section IV.

2. Coaxial Conductor

The 82 inch long coaxial conductor is fabricated from RG-142/U. It is terminated

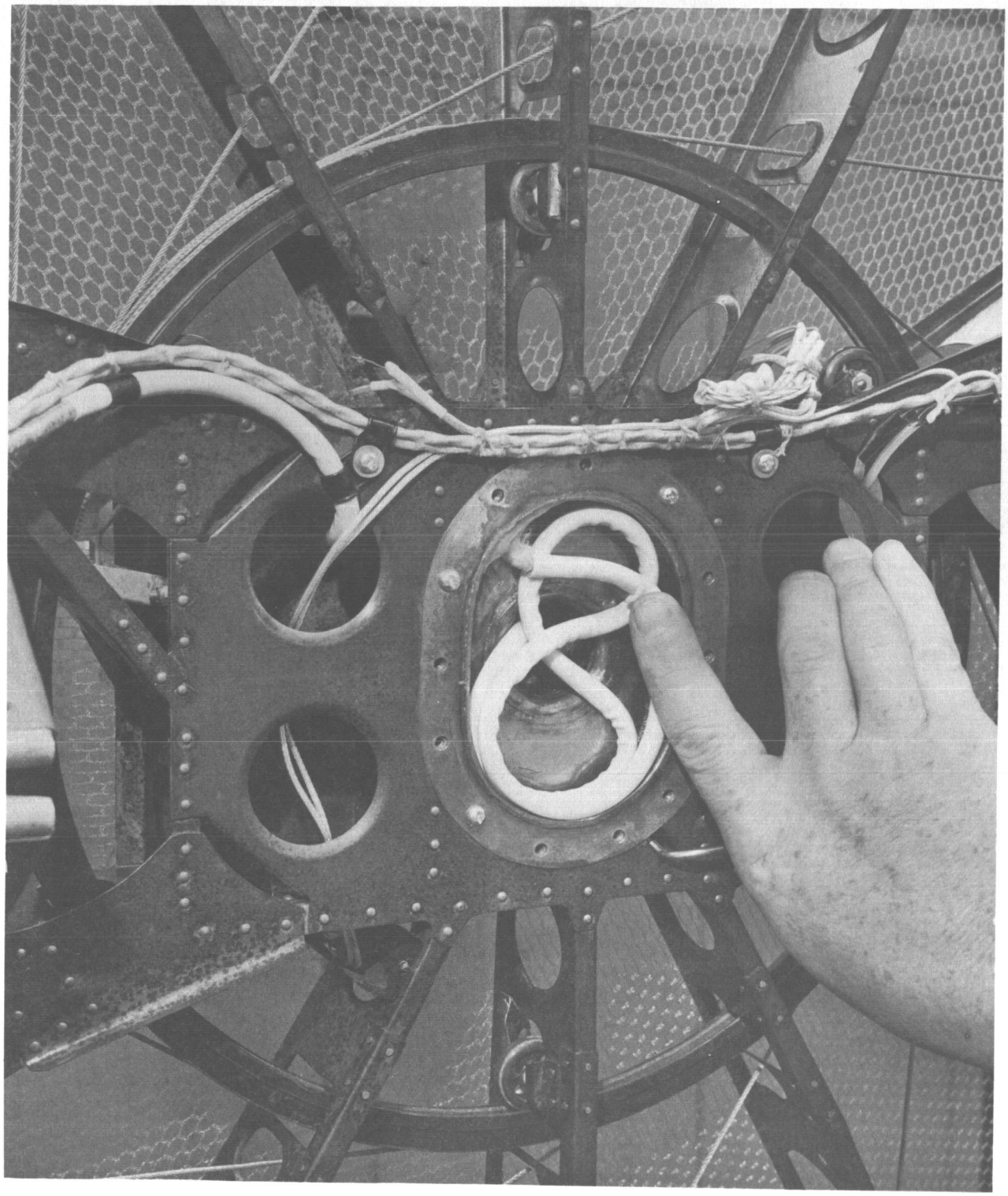

Figure 11. COAX "Figure 8"

at the feed in a GRIFF 166B connector and at the boom in an FXR 97875-1000 connector. The section passing through the bellows chamber of the feed support is encased in a 0.010 wall teflon sleeve to facilitate low friction withdrawal from the "Figure 8" packaged configuration of the conductor. See Figure 11. The "Figure 8" eliminates the torsional twist in the conductor which would be inherent for coil packaging.

G. BOOM STRUCTURAL ANALYSIS

1. General

In accordance with the requirements of JPL Contract No. 950905, item 6, GAC conducted a study of the welded-truss boom structure in comparison with a riveted sheet metal boom structure. The welded truss can be seen in detail in Figures 1 and 2. The sheet metal version is shown in Figure 12.

2. Structural and Weight Comparison

The boom in Figure 12 has the same geometric configuration as the welded truss boom. The truss chord members are replaced by shear webs for the riveted design. The riveted construction offers two advantages:

(a) The riveted boom has greater strength because this construction permits the use of higher strength aluminum alloys.

(b) The riveted construction has a higher structural damping coefficient, resulting in a 20 percent reduction in the dynamic response of the system to resonant frequencies.

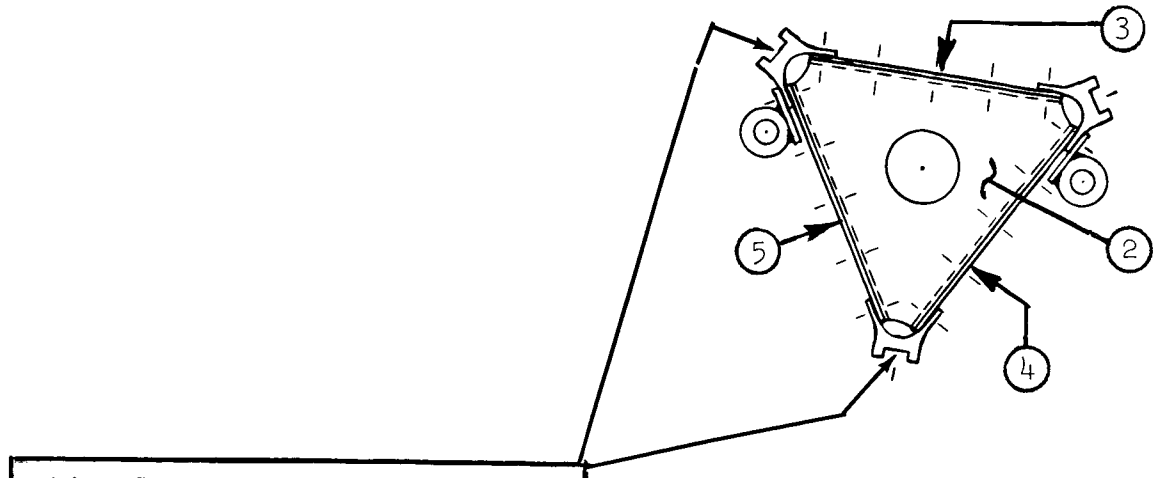

SECTION B-B
(2/1)

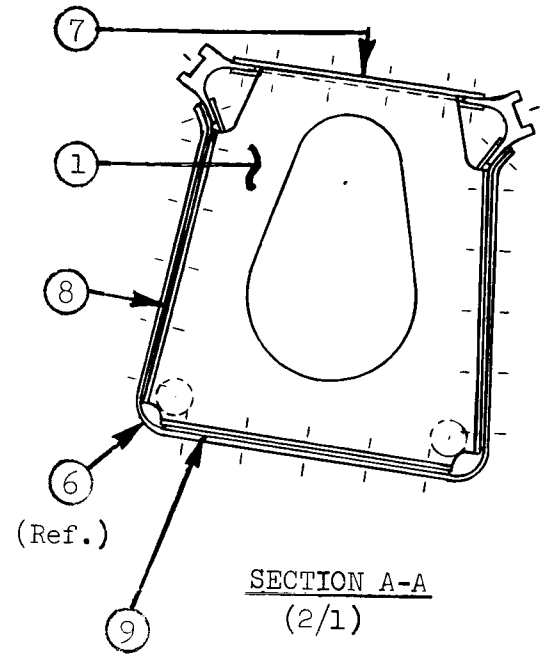

SECTION A-A
(2/1)

MATERIAL THICKNESS CODE FOR 7178-T6 ALUMINUM ALLOY PRIMARY STRUCTURE:

1	BULKHEAD	.025
2	BULKHEAD	.025
3	WEB	.025
4	WEB	.025
5	WEB	.025
6	TRANSITION	.040
7	WEB	.040
8	WEB	.025
9	WEB	.025

TRAVERSING SURFACES ON THE THREE TRACKS WILL HAVE SAME GEOMETRICAL RELATIONSHIP AS ON WELDED-TRUSS BOOM

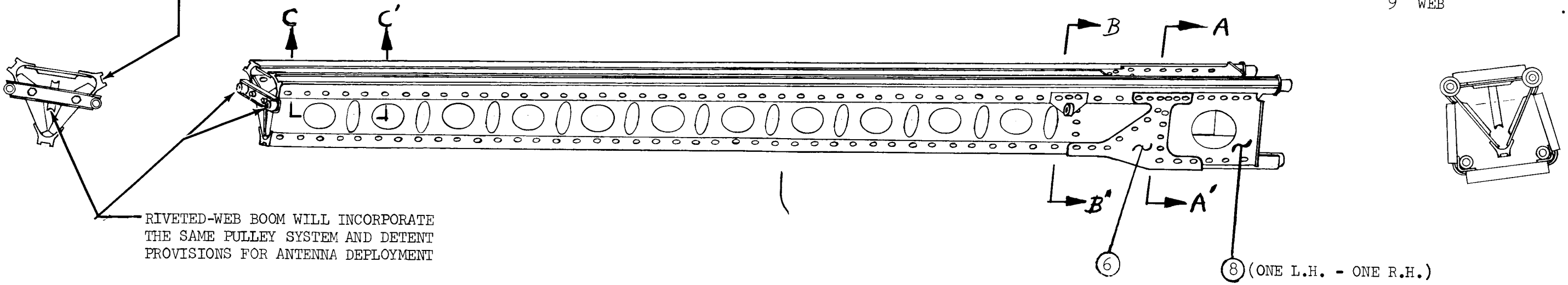

RIVETED-WEB BOOM WILL INCORPORATE THE SAME PULLEY SYSTEM AND DETENT PROVISIONS FOR ANTENNA DEPLOYMENT

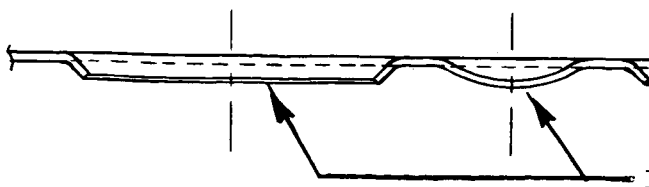

SECTION C-C'
(4/1)

1.500 DIAMETER LIGHTENING HOLES AND .750 WIDE X 1.900 LONG WEB-STIFFENING BEAD PATTERN IN WEBS 3, 4 and 5

Figure 12. Aluminum Web (Riveted) Boom

These two advantages are obtained with no change in the weight or in the natural frequencies of the system. A comparison of these two boom designs is given in Table VI.

Table VI. Comparison Summary of Boom Designs

Design Description	Welded Truss	Riveted Webs
MATERIAL	6061-T6 Al. Alloy	7178-T6 Al. Alloy
REFERENCE	Figures 1 and 2	Figure 12
STRENGTH:		
Allowable Stress	$F_{col.}$ = 20000 psi*	F_{tu} = 83000 psi**
Factor of Safety (Ult.)	1.25	1.50
Allowable Load (Launch Configuration)	16 g's (Any Axis)	50 g's (Any Axis)
STIFFNESS:		
Calculated Natural Frequency In Deployed Configuration	2 CPS	2 CPS
WEIGHT (Calculated)	2.726 Lb (Final)	2.727 Lb (Prelim.)

*$F_{col.}$ = Column Yield Stress

**F_{tu} = Ultimate Tensile Stress

H. LOOSE PARTS

1. General

In accordance with the requirements of JPL Contract No. 950905, item 7, GAC conducted a study to eliminate all loose parts. The problem arises in deployment of the antenna and involves the following parts:

(a) Rib supports in the packaged configuration must remain captive after deployment.

(b) Teflon shims separating adjacent screen faces entrapped between ribs and rib supports must remain captive after deployment.

(c) The break away tie cords used to secure the deployment cables to the quadrants and tie the electrical cables along the surface of the boom must be held captive.

The following solutions to the problem areas were derived.

2. Captive Rib Supports

The captive rib supports, consisting of a silicone rubber bumper and an aluminum tube having an 0.50 inch diameter and an 0.020 inch wall thickness, were cemented to the ribs with epoxy cement as shown in Figure 1.

3. Teflon Shims

The teflon shims, which are 0.004 inches thick and 1.25 inches in diameter, contain an 0.06 inch diameter hole. The shims are inserted in the required positions on the ribs as shown in Figure 13.

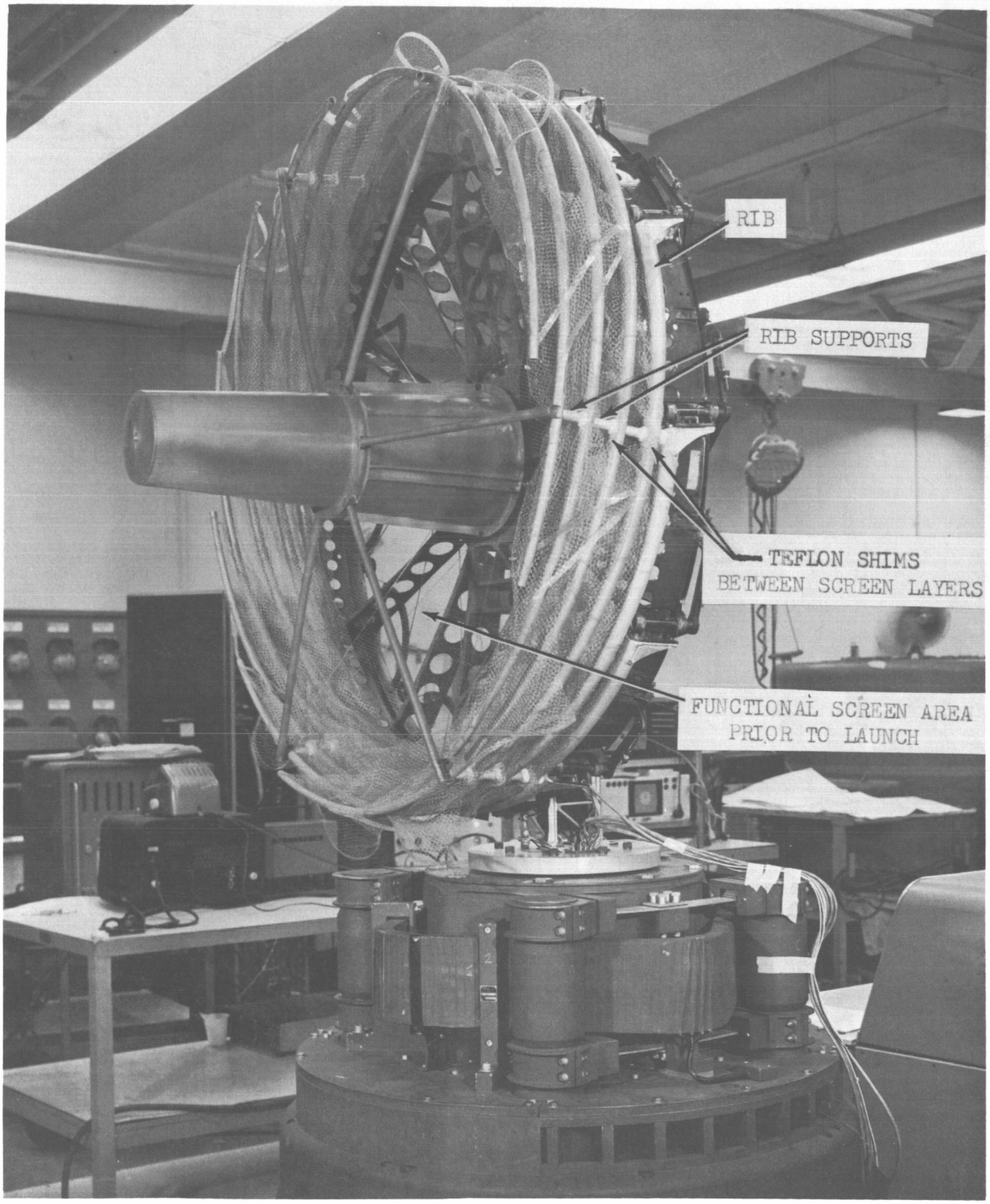

Figure 13. Teflon Shims And Rib Supports

After positioning, each shim is attached to the rib by a drop of epoxy cement. The cement is allowed to form a small button over the 0.06 inch diameter hole. A permanent captive installation of the shim to the rib is thereby accomplished.

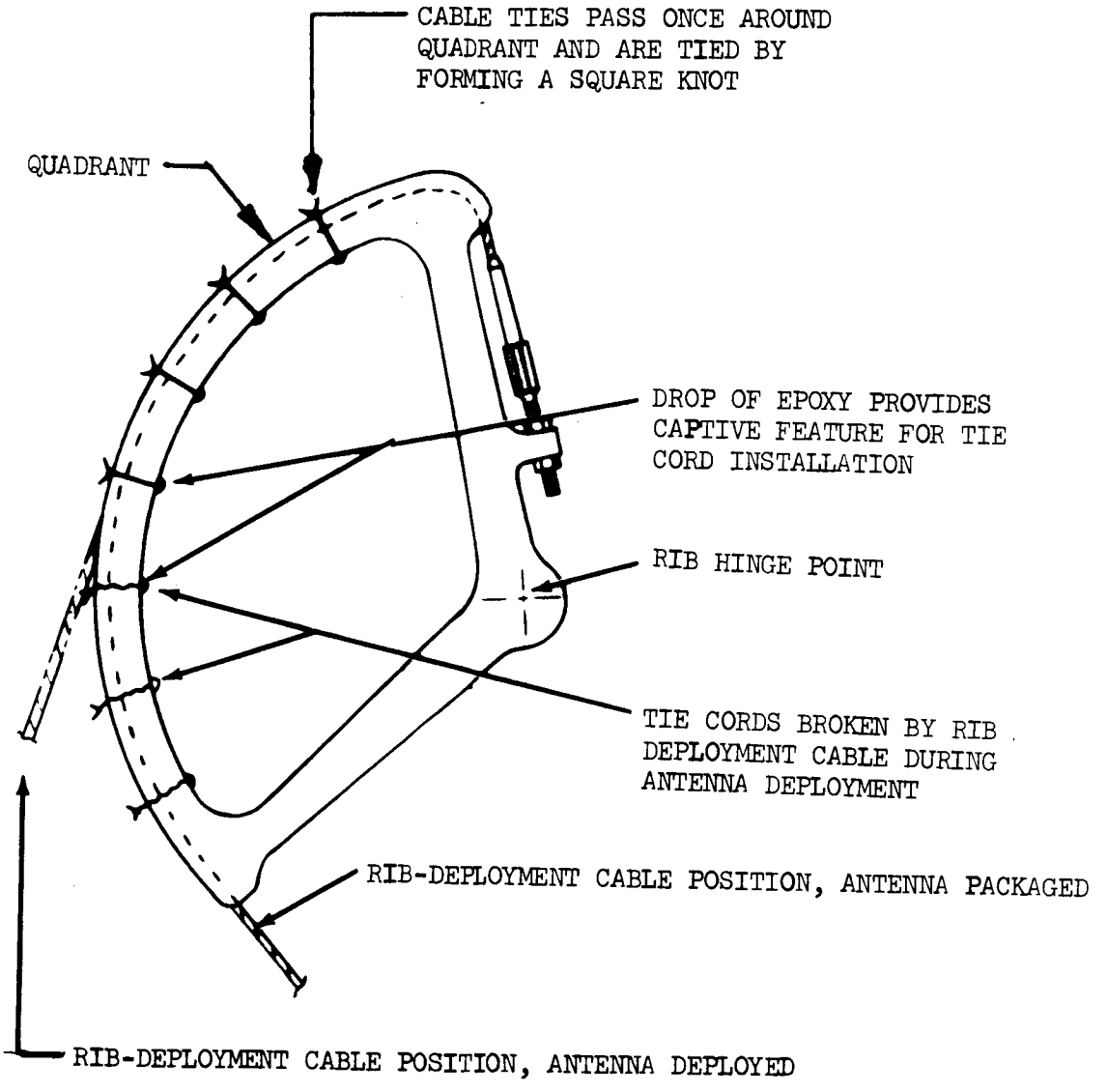

Figure 14. Quadrant Cable Ties

4. Cable Ties

Each cable tie consists of a single thread (Federal Specification V-T-295, Type II, Class 1, Size 00) which is tied off at seven equally-spaced positions along a quadrant when the deployment cables are in place. Each thread is then permanently attached to the quadrant by a drop of epoxy cement, thereby preventing loss of the ties when they are broken by the cable during deployment. Figure 14 shows the ties before and after deployment. The same method of tie instllation is also used to capture the electrical cables along the side of the boom.

I. WEIGHT REDUCTION

1. General

In accordance with the requirements of JPL Contract No. 950905, item 8, GAC conducted a design study to further reduce the weight of the antenna in the areas of the deployment system, hub structure, and feed support. Descriptions of the various proposals, together with comments noting the advantages and/or disadvantages of each, are given in the following paragraphs 2 through 6.

2. Deployment System

a. Screw Deployment of the Hub. The present linear actuator and cable system inside the boom can be replaced by a screw and nut mechanism as shown in Figure 15. A long screw is mounted on top of the boom and is supported at its outboard end by a bearing. The inboard end of the screw is coupled to a geared

motor, and a nut is fastened to the hub structure. As the motor rotates the screw, the nut and hub will travel axially along the boom.

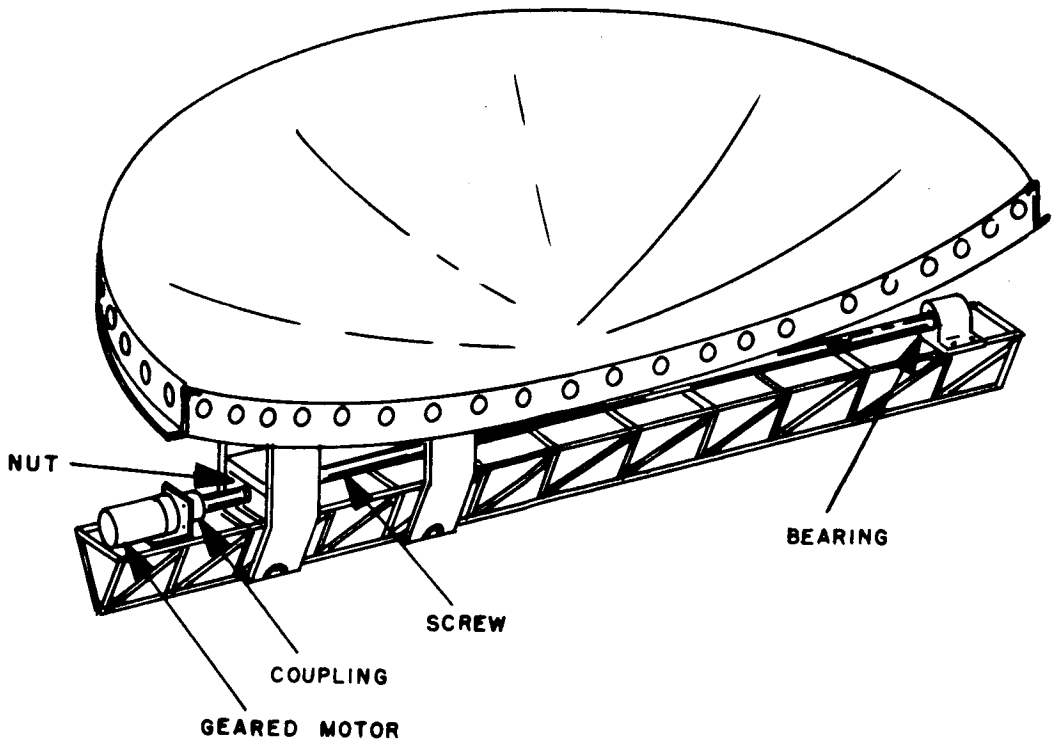

Figure 15. Deployment System Using Rotating Screw And Nut

In addition to an estimated weight reduction of 0.5 lbs., this system provides positive positioning of the hub at all times; that is, the hub cannot lead the actuator. To accommodate the screw, the distance between the hub and boom will have to be increased. Possible problem areas are lubration of the screw and bearing, and vibratory effects. Bumpers will probably be required to limit the screw vibration amplitude.

b. Drum and Quadrant Size Reduction. Study showed that the drum and the quadrants may be reduced to approximately 70 percent of their present size. A smaller drum will interfere with the hub rib attachments and with the area allocated to the feed support. A smaller quadrant will require the addition of turnbuckles to provide additional cable adjustment.

The overall weight reduction will be approximately 0.3 lbs. The decrease in the size of the quadrant will cause a corresponding decrease in cable travel and an increase in cable load. This will necessitate a revision of the actuator and pulley system within the boom. Structurally, the idler pully brackets may have to be reinforced, and the flanged holes in the hub structure may have to be relocated to accommodate the new position of the cables.

c. Change Quadrants to Arms. Study showed that it is not feasible to change the quadrants to arms because the plane of the quadrant is not in the plane of the idler pulley. Thus, as the hinge rotates, the cable will no longer lie in the plane of the pulley. The resulting misalignment is too great to use a fixed

pulley. This condition may be partly alleviated by using a loose swivel-type pulley. However, for this application, a loose pulley does not appear to be too reliable because of the vibratory forces present; also, if a cable slackens the pulley could swivel and bind the cable.

d. Rotary Actuator To Deploy Hub. It is possible to remove the linear actuator and travel-multiplying pulley system from the boom and replace it with a rotary-actuated cable, as shown in Figure 16. A rotary actuator, mounted at the inboard end of the boom, drives a straddle-supported reel. One end of the cable is fastened to the reel, and, after passing over the outboard idler pulley in the boom, the other end is attached to the hub. As the motor rotates and reels in the cable, the hub travels along the boom. By adding a secondary cable from the reel to the hub, the hub could be positively positioned at all times. The estimated weight change is 0.10 pounds increase. A disadvantage is the accommodation of the actuator, since it is at right angles to the boom and to the plane of the cables. The problem of cable alignment may be eliminated by substituting a sprocket and a punched steel strap in place of the reel and cable. The weight difference will be 0.02 lbs. less.

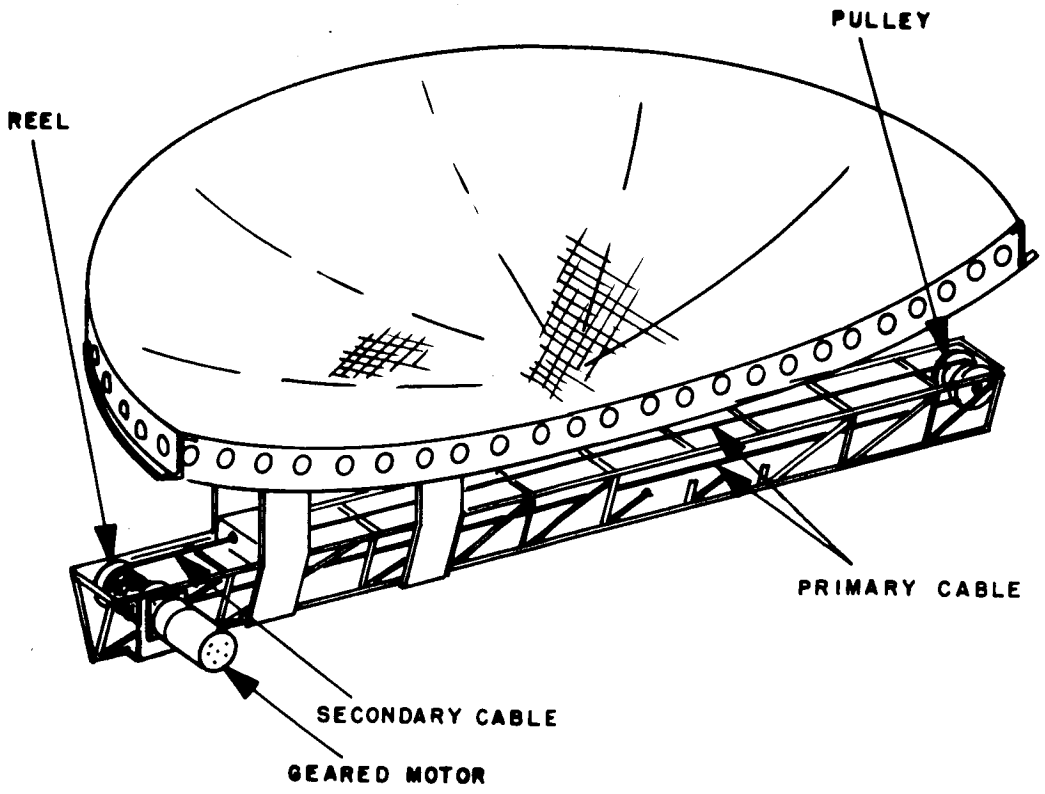

Figure 16. Hub Deployment System Using Rotary-Actuated Cable

e. Actuate Six Ribs Only. It is possible to deploy the antenna by actuating six alternate ribs. With this system, dependence is placed upon the screen mesh to deploy the other ribs. However, the mesh tension will vary between adjacent bays. Also, it will approximately double the cable tension and

hinge loads at the actuated ribs. Estimated weight reduction is 0.5 lbs.

f. Eliminate The Center Drum. A study was made to determine if the center drum could be eliminated, requiring all twelve rib cables to be individually connected to the boom. Twelve additional idler pulleys will be required. No feasible arrangement can be devised.

g. Eliminate One Interface At The Hinge. Elimination of one interface at the hinge is possible. The rib must fit the parabolic contour of the antenna when it is deployed and fit the hub when it is packaged. To adjust one position of the rib, without disturbing the other, requires two interfaces. However, since the packaged condition of the rib does not have to be held to accurately, it would be possible to eliminate one interface if adequate tooling was available to establish a precise hinge line. Estimated weight saving will be 0.6 lbs. It is noted that, during initial erection at GAC, both interfaces were utilized.

3. Hub Structure

a. Configuration Change. In the weight reduction study of the hub, no basic change in configuration was devised which would result in a weight savings. More lightening holes could be added, but the resulting weight reduction would be less than 0.1 pounds.

b. Material Change. Considerable weight savings could be achieved if the hub material was changed to aluminum. To meet the strength requirements, it

would be necessary to increase the material thickness above that presently used for Invar (.012 and .015 to .015 and .020 gage). The net weight saving would be approximately 3 lbs. An additional increase in gage size for aluminum would be necessary to attain the thermal deflection constant provided by Invar. The new gage size is determined as follows:

$$\text{deflection} = K\,(\Delta t)\,C$$

where K = physical constants; t = temperature differential; C = thermal coefficient of expansion; $C_I = 0.7 \times 10^{-6}$ (Invar); $C_A = 12.5 \times 10^{-6}$ (Aluminum).

Considering the same physical dimensions,

$$(\Delta t_I)\,C_I = (\Delta t_A)\,C_A$$

then

$$\Delta t_A = \frac{\Delta t_I \times .7 \times 10^{-6}}{12.5 \times 10^{-6}}$$

Substituting $\Delta t_I = 24.88$ (from Figure 17):

$$\Delta t_A = \frac{24.88 \times .7 \times 10^{-6}}{12.5 \times 10^{-6}}$$

$$\Delta t_A = 1.39°F$$

The graph in Figure 17 shows that 1.39°F can be maintained with .020 gage aluminum. Thus, to maintain a constant deflection, the minimum gage of aluminum must be

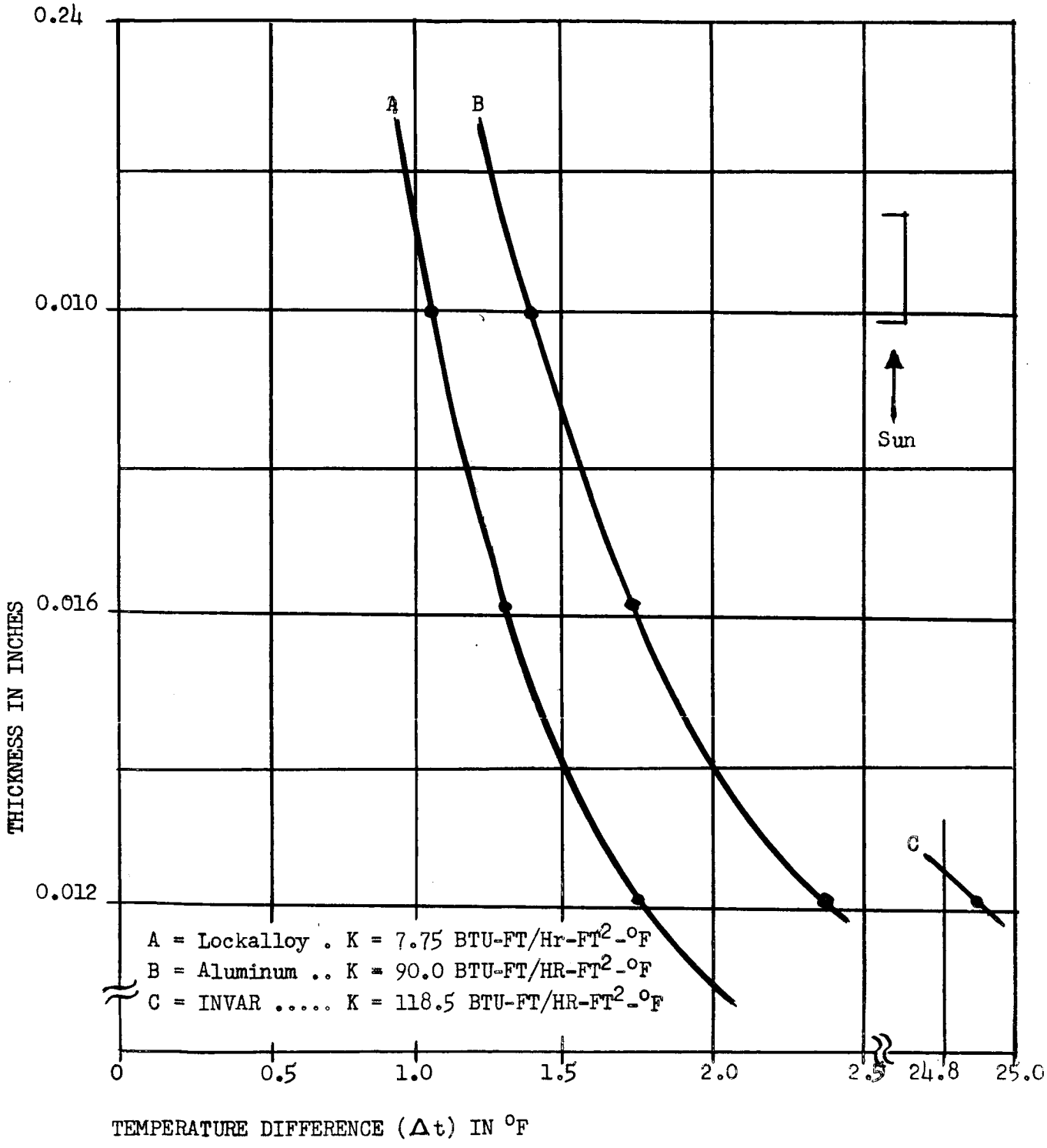

Figure 17 Thickness Vs. Temperature Differe

increased to .020; but use of .020 gage aluminum decreases the total weight savings to approximately 2.5 lbs. This study was conducted using a generalized channel structure to show the trend of material changes. Optimizing studies conducted during a hub redesign could possibly save additional weight by using improved thermal coatings or thermal shields.

c. Hardware Material Change. At present, steel nuts and bolts are used to fasten the hinge brackets. If these were changed to aluminum alloy, a weight reduction of 0.4 lbs. would be achieved.

d. Thermal Analyses. The thermal analysis of a hub-rib was performed to determine the temperature distribution throughout the member. This information enabled the calculation of thermal deflections.

The typical member analyzed was a channel 18 inches in length, with a 2-1/2 inch web and 3/8 inch flanges. The web had five 1-1/2 inch diameter lightening holes, spaced 2-3/10 inches center-to-center along its length.

Three materials were considered; Invar, Aluminum, and Lockalloy. The thermal conductivity and thickness of each member analyzed is shown in Table VII.

Table VII. Thermal Conductivity of Channel Material

Material	Conductivity	Thickness In Inches		
Invar	7.75 Btu-Ft/Hr-Ft^2-°F	0.012	-	-
Aluminum	90.0 Btu-Ft/Hr-Ft^2-°F	0.012	0.016	0.020
Lockalloy	118.5 Btu-Ft/Hr-Ft^2-°F	0.012	0.016	0.020

A thermal model of the channel was programmed on the IBM 1401 Digital Computer. Heat transfer due to conduction and radiation exchange between sections of the rib was considered, and the temperature distribution was determined. To provide a minimum temperature differential between the flange facing the sun and the opposite flange, special coatings were used on each member. The exterior surface of the flange facing the sun was coated with a material having a high emittance ($\epsilon = 0.91$) and a low absorptance ($\alpha = 0.22$). The interior surface of this flange and the remaining surface area of the member was coated with a material having a low emittance ($\epsilon = 0.05$) and a low absorptance ($\alpha = 0.15$). The results of this analysis are presented in the thickness versus temperature-difference graph shown in Figure 17.

The relationship of the aluminum (.016") and Invar (.012") thermal gradients for this specific structural configuration was further evaluated by varying the solar position. The maximum conditions for an isolated channel (no shield) and for a member enclosed between two non-radiating shields (shielded) were considered. The non-radiating shields would simulate blockage of solar radiation by other support members of the antenna. The results are presented in Table VIII. The relatively constant ratio of $\frac{\Delta t_I}{\Delta t_A}$ shown for the shielded condition indicates that solar position has little or no effect on the advantages or disadvantages of the two metals considered.

Table VIII. Thermal Gradients Vs Solar Position

Solar Angle (Degrees)	Aluminum (0.016 Inch Thick)				Invar (0.012 Inch Thick)				Ratios	
	No Shield		Shield		No Shield		Shield		No Shield	Shield
	T_{avg}	ΔT_A	T_{avg}	ΔT_A	T_{avg}	ΔT_I	T_{avg}	ΔT_I	$\frac{\Delta t_I}{\Delta t_A}$	$\frac{\Delta t_I}{\Delta t_A}$
0	-33	1.8	-33	1.8	-38	25	-38	25	13.9	13.9
20	133	9.6	-40	1.7	155	110	-44	23	11.5	13.6
40	165	11.5	-60	1.4	180	126	-63	19	11.0	13.6
60	179	11.1	-101	0.9	193	117	-102	13	10.6	14.4
80	173	9.3	-184	0.3	182	97	-185	5	10.4	16.7

4. Feed Support and Deployment

a. Truss. Study showed that there is no weight saving attained by substituting a truss or a tripod support structure for the present tubular structure.

b. Cable Actuation. The compressed gas-and-bellows type feed deployment system could be replaced by a cable type system, as shown in Figure 18. One end of the cable is attached to the inner tube and the other end is attached to the boom. As the hub travels along the boom, the cable is pulled, causing deployment of the feed.

Since the travel of the hub exceeds that of the feed, a travel-proportioning device or a delay device is required. The coaxial cable is packaged in essentially the same manner as at present. However, it will have to be rerouted so it will

not interfere with the actuation cables. The estimated weight reduction is 0.20 pounds.

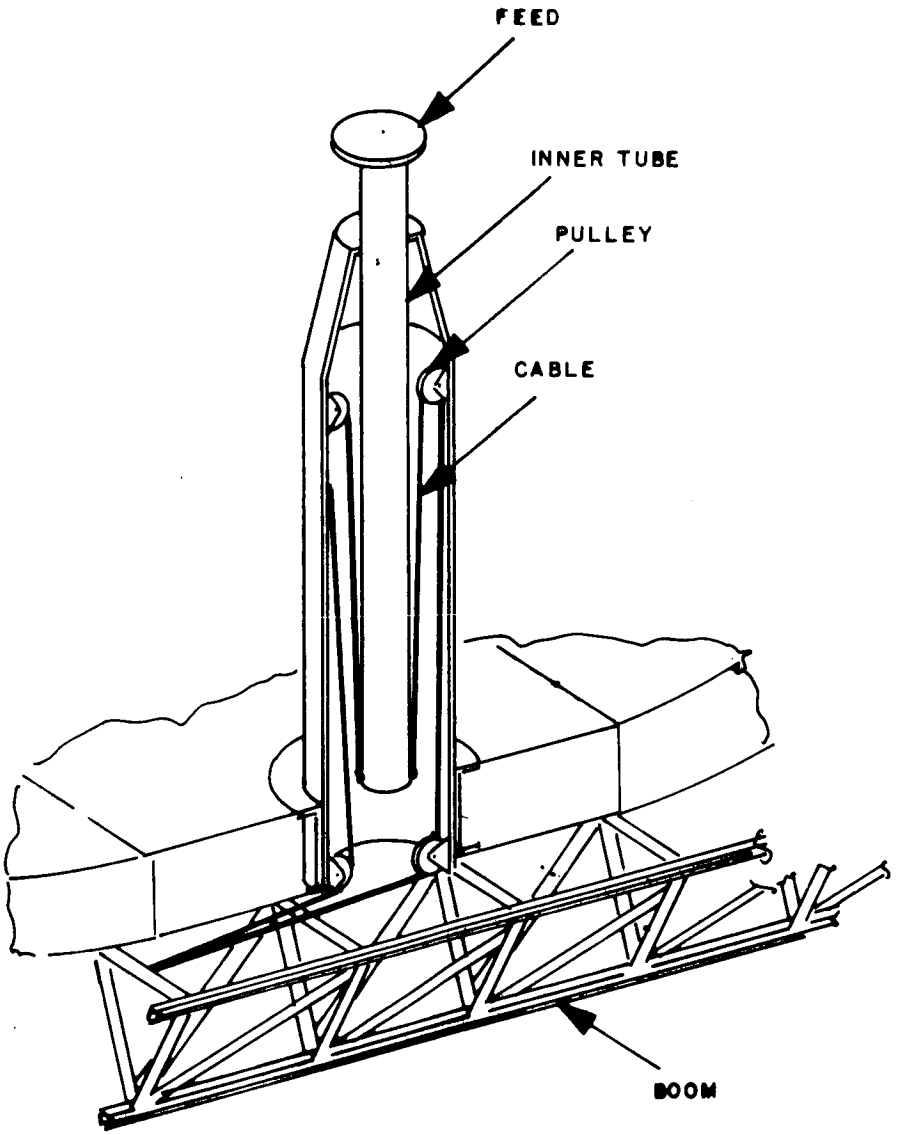

Figure 18. Cable Type Feed Deployment System

c. Pantograph. A pantograph and screw could be used to replace the present feed actuation system and support. Rotating the screw by an actuator causes the feed to rise to its deployed position. An automobile jack is a variation of this design.

With the number of links and joints in these designs, it is unlikely that the support would be rigid enough to satisfy the operational requirements. The one major advantage is that the coaxial cable would not be confined and could be fastened to the links.

d. Screw Jack. In the screw jack type feed deployment system (Figure 19) the gas system is eliminated and the inner tube is replaced by a hollow screw. The outer tube supports a bearing and a rotary actuator. The bore of the inner race of the bearing is threaded and mates with the screw. The inner race also incorporates an integral external gear which meshes with a pinion mounted on the actuator output shaft. As the gearing rotates the inner race of the bearing, the screw (which is feather-keyed to prevent its rotation) move axially to deploy the feed. The weight saving is small, but if a plain bearing is substituted for the ball bearing, the weight saving will be approximately 0.3 lbs.

An alternative to this design is to use a special low-speed hollow-armature motor. The bore of the armature is threaded to mate directly with the screw. This eliminates the need for gearing. As the motor rotates, the feed is deployed.

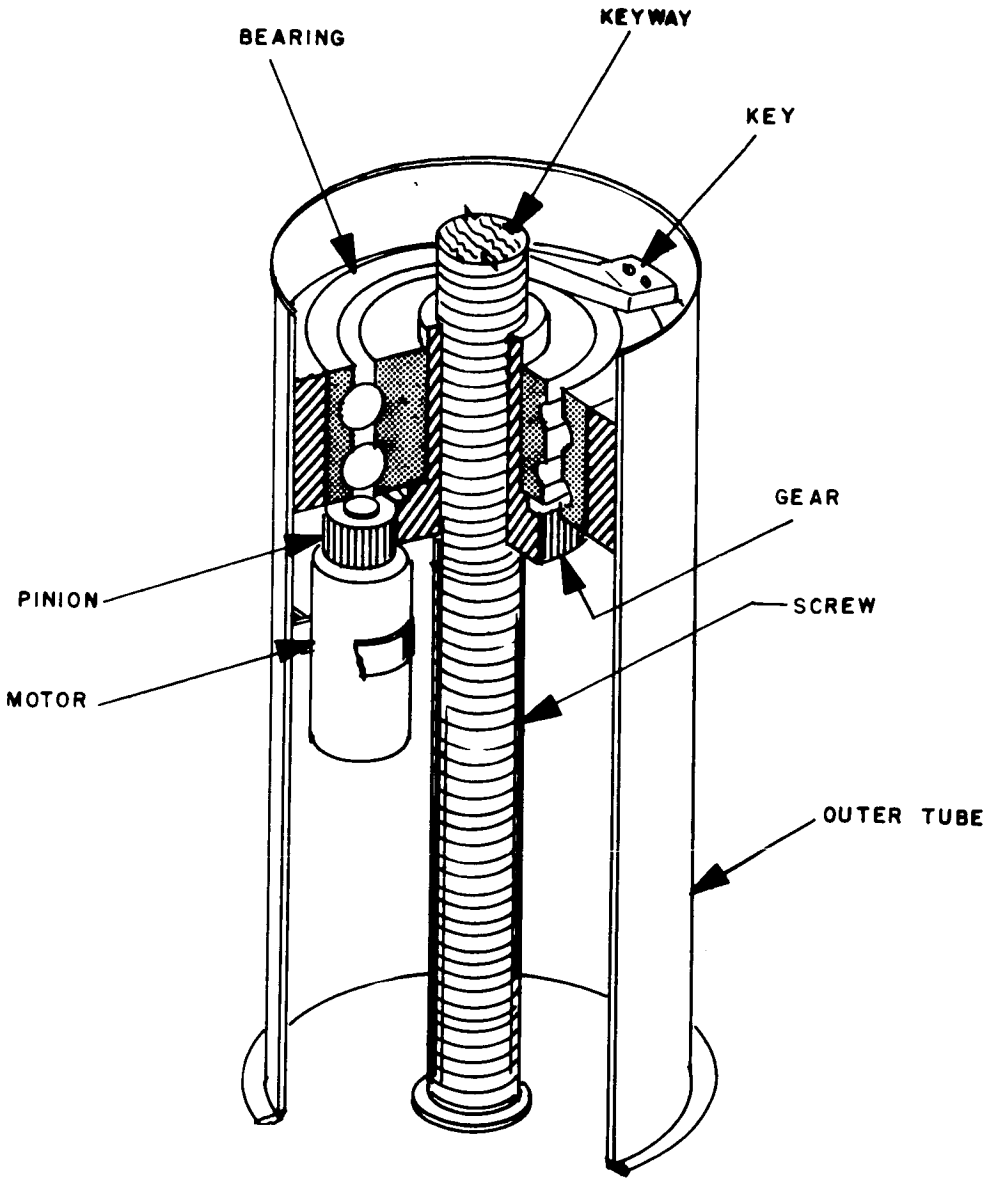

Figure 19. Screw Jack Type Feed Deployment System

The estimated weight savings is 0.3 lbs.

In either design, the outer support tube could be replaced by a tripod arrangement. This would permit access to the bottom of the hollow screw. The coaxial cable

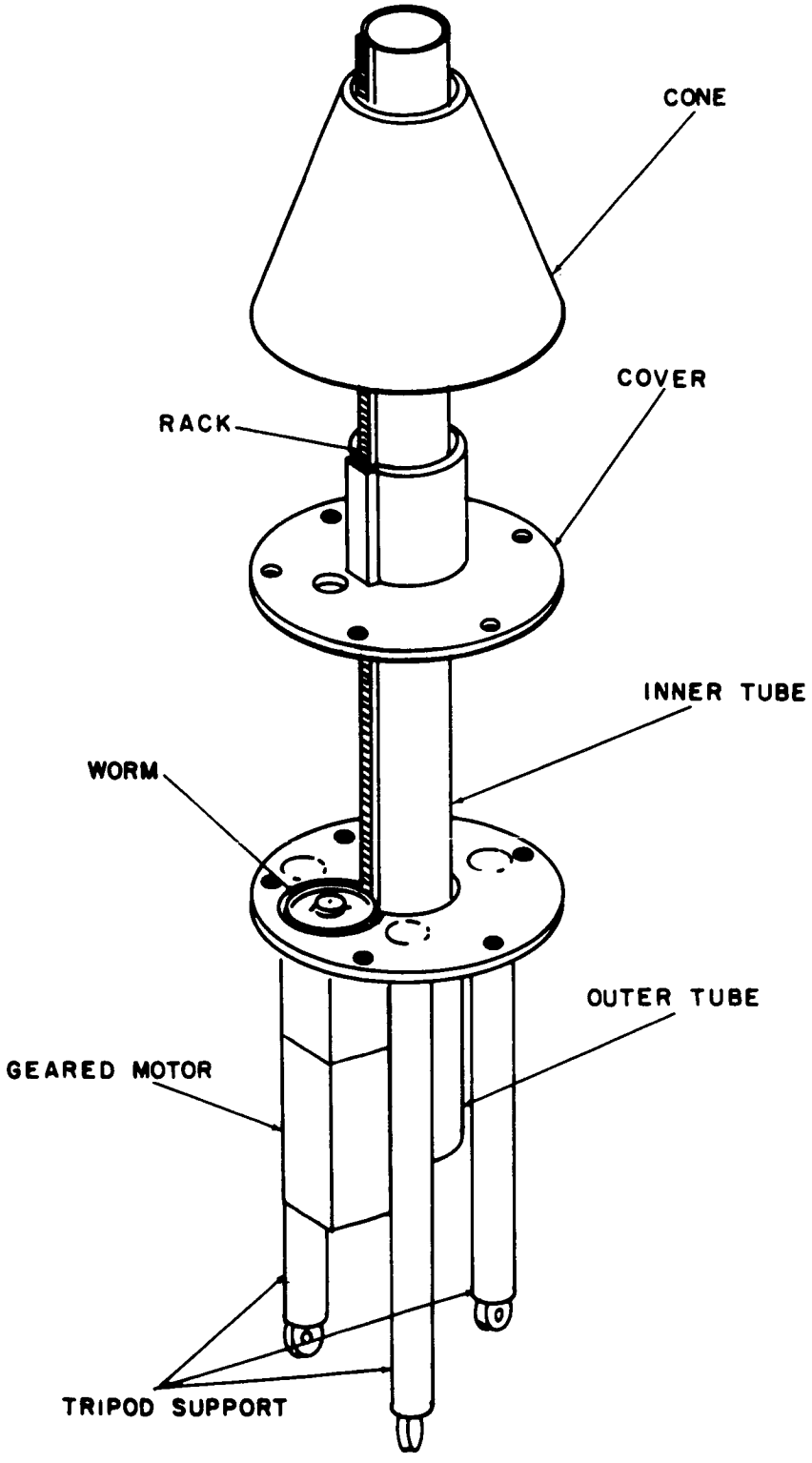

Figure 20. Rack Type Feed Deployment System

could then be packaged in a "Figure 8" with sufficient slack to permit deployment of the feed.

e. Rack. In the rack type feed deployment system, a worm and rack replaces the gas actuation system, as shown in Figure 20, A helical rack is cut on the inner tube. A geared motor, supported by the outer tube, drives a straddle-mounted worm which meshes with the rack. As the worm is rotated, the keyed inner tube moves axially and deploys the feed. Weight savings is estimated at 0.5 lbs.

This design also permits use of a tripod support. If the packaged height of the antenna is increased approximately 1.3 inches, the coaxial cable stowage will be greatly simplified because the increased height will permit stowage above the parabolic contour.

5. Recommendations For Additional Weight Savings

a. Deployment. The most promising weight saving modification is utilization of a screw to effect hub deployment, as discussed in paragraph 2-a.

b. Hub Structure. Weight savings in hub structure material and hardware material (paragraphs 3-b and 3-c) appear to be feasible.

c. Feed Support and Deployment. The feed deployment system which appears most feasible is the system using a rack-and-worm drive to deploy the feed (paragraph 4-e). Problem areas may be lubrication and vibration effects.

6. Summary of Weight-Savings Study

The weight savings recommendations fall into two categories. These are:

(a) Recommended savings which would have been incorporated into a redesign of the applicable hardware items, if this redesign had been contractually negotiated and authorized.

(b) Recommended savings which were actually incorporated into the redesign of the applicable hardware items.

Table IX itemizes these weight savings studies.

Table X defines the JPL spacecraft antenna weight. The calculated weight was based on production drawings. The actual weight was determined by weighing the complete assembly. This actual weight includes the 0.99 pound incorporated weight savings shown in Table IX, and appears as a reduction in the weight for the Reflector. The projected weight represents the weight of a new antenna with all modifications incorporated.

Table IX. Weight Savings Studies Summary

Recommended Changes			Weight Savings (Pounds)		
Status	Paragraph	Item	Not Incorp'd	Incorporated	Total
Not Incorporated	Section II Par. G-2	Change welded truss boom structure to a riveted web boom structure	0.2		0.2
	Section II Par. I-2-a	Change to an electrically actuated screw drive to accomplish hub deployment	0.5		0.5
	Section II Par. I-3-b	Change hub material from Invar to Aluminum	2.5		2.5
	Section II Par. I-3-c	Change screws, nuts and bolts from steel to aluminum	0.4		0.4
	Section II Par. I-4-e	Change feed deployment operation from a gas actuation system to a rack and worm actuation system	0.5		0.5
Incorporated	Section II Par. B-3	Change ribs from .007 inch wall x 1.00 inch dia. Invar tubes to .020 inch wall x 0.5 to 1.00 inch dia. tapered aluminum tubes		1.04	1.04
	Section II Par. G-4	Add screen pulldown wires between adjacent ribs in order to improve contour with respect to paraboloid		-0.05	-0.05
		TOTAL	4.1	0.99	5.09

Table X. Weight Breakdown

Item	Weight (Pounds)		
	Calculated	Actual	Projected
Hub Structure (Including Hinges)	11.391	18.27	14.87
Deployment Mechanism (Hub and Ribs)	3.663		
Feed (Including Support Structure and Actuation Hardware)	2.640		
Boom (Including Actuator, Guide Support, Rollers, Brackets, and Hardware)	6.979	6.45	5.95
Protective Canister	1.671	2.10	1.67
Reflector (Ribs, Screen and Pulldown Wire)	4.156	4.16	4.16
Totals	30.500	30.98	26.65
Actual Unit Aperture Weight For Antenna (Total Weight Less Canister and Boom)	$= \frac{22.43}{63.61} = 0.353$ psf.		
Projected Unit Aperture Weight For Antenna (Total Weight, Less Canister and Boom)	$= \frac{19.03}{63.61} = 0.299$ psf.		

J. SECTOR LOCKS

1. General

In accordance with task number 9 of JPL Contract No. 950905, GAC conducted a design study of various methods for locking the ribs in place after deployment of the antenna. The purpose of a lock is to insure that the ribs will not change position appreciably if the drum drive cable or a rib cable is damaged by a meteoroid.

2. Criteria

The original locks consisted basically of lock pins pressed into each of the twelve quadrants and cantilevered springs fastened to the hub rim. As the quadrant was rotated to its deployed position, the pin entered a hole in the spring thereby locking the rib in place. However, when the rib cable length was varied to adjust the screen tension, the quadrant did not retain its original deployed position. Then either the pin or spring had to be relocated.

A method for achieving the desired locking results would be to make the lock independent of the rib position. Thus if the rib position is varied, the lock position will not be affected. This may be accomplished by locking some other component; for example, the drum; instead of each individual quadrant. In such a design, at least two locks shall be employed for reliability. Although this design will not eliminate screen contour degradation caused by rib cable breakage, it is believed that at least two adjacent cables would have to break before the

contour is appreciably affected.

3. Proposals

Among the ideas considered to meet the above criteria are the following:

(a) An obvious solution is to add an adjustment feature as noted above to the existing quadrant locks. These may later be replaced by permanent locks if desired.

(b) Another solution is to install a device which would lock the drum drive cable after deployment and prevent the drum from rotating backward. This solution has the advantage of being independent of the rib position. The device may be installed close to the drum to increase the locking effectiveness in case of drive cable failure. However, this is essentially a single lock and hence will not achieve the desired reliability.

(c) A third method is to lock the drum after deployment. This design also has the advantage of being independent of rib position and in addition, will not be affected by drive cable breakage. Two locks may be spaced diametrically opposite to improve the reliability.

4. Comments

The original lock was a single position lock. That is, the antenna had to be deployed to an exact pre-adjusted position before the locks would function. For

added reliability, it is desirable to incorporate a lock that would function if the antenna does not deploy to its exact predetermined position. Such a lock would employ friction as the locking method and thereby have an infinite number of locking positions. However, such a device would inherently be quite heavy because of the loads in the locking mechanism.

The ideal design incorporates the advantages of the friction and single position locks. That is; a positive lock which will function even if the antenna is not deployed to its exact position. This can be accomplished to a degree by utilizing a pawl and ratchet with small spaced teeth. The teeth could be fine enough to limit the cable travel to a maximum of 0.06 inches. Such a lock can best be incorporated at the drum, as shown in Figure 21. The spring-loaded pawl engages the ratchet teeth when the drum is in the deployed position.

Incorporation of the lock required several modifications to the antenna. These include enlarging the existing drum clearance cutouts in the ribs, and revising the central roller bracket to permit passage of the ratchet. In addition, the structure in the pawl pivot area will have to be reinforced. The net weight change compared to the existing quadrant locks is negligible.

It should be borne in mind that the lock is essentially a safety or reliability feature. During normal operation, the drive cable will hold the drum in the deployed position. Only when the drive cable system is damaged will the drum

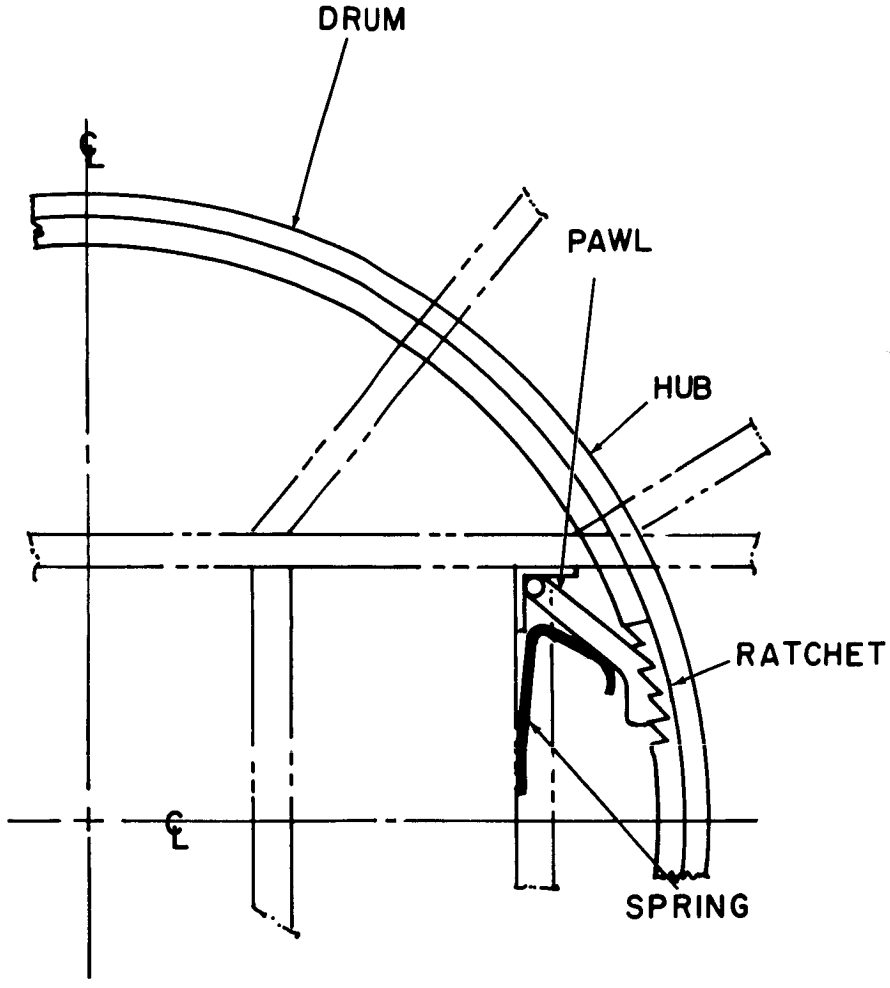

Figure 21. Drum Lock

rotate backward and cause a decrease in screen tension. By adding a lock, this backward travel is limited to a maximum of 0.06 inch at the drum, or a maximum of 0.50 inch at the rib tips. The effect on screen and rib contour causes deviations from the fully-deployed contour as shown in Figures 22 through 26.

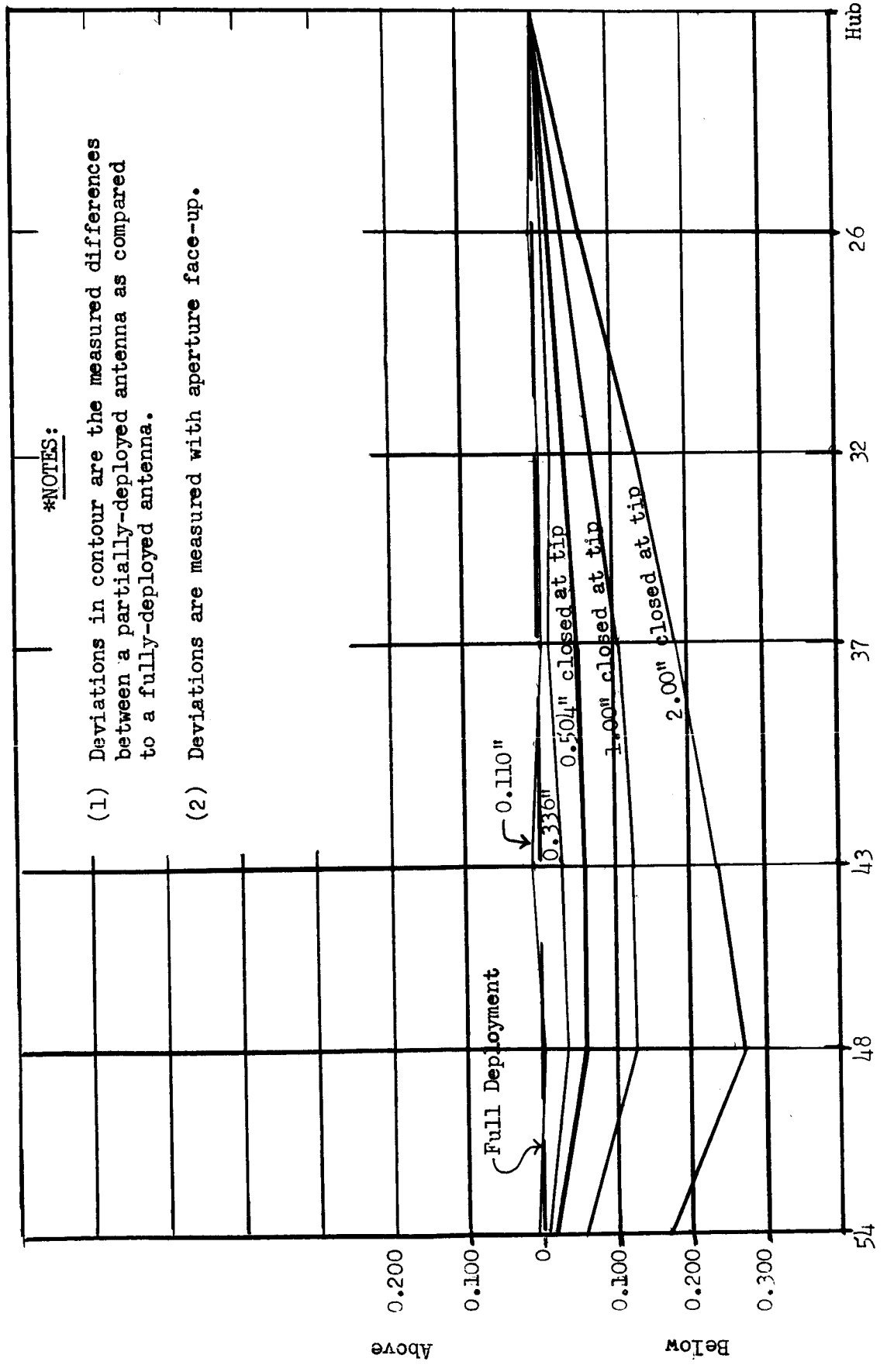

Figure 22. Contour Vs. Drum Backward Movement At Rib #1

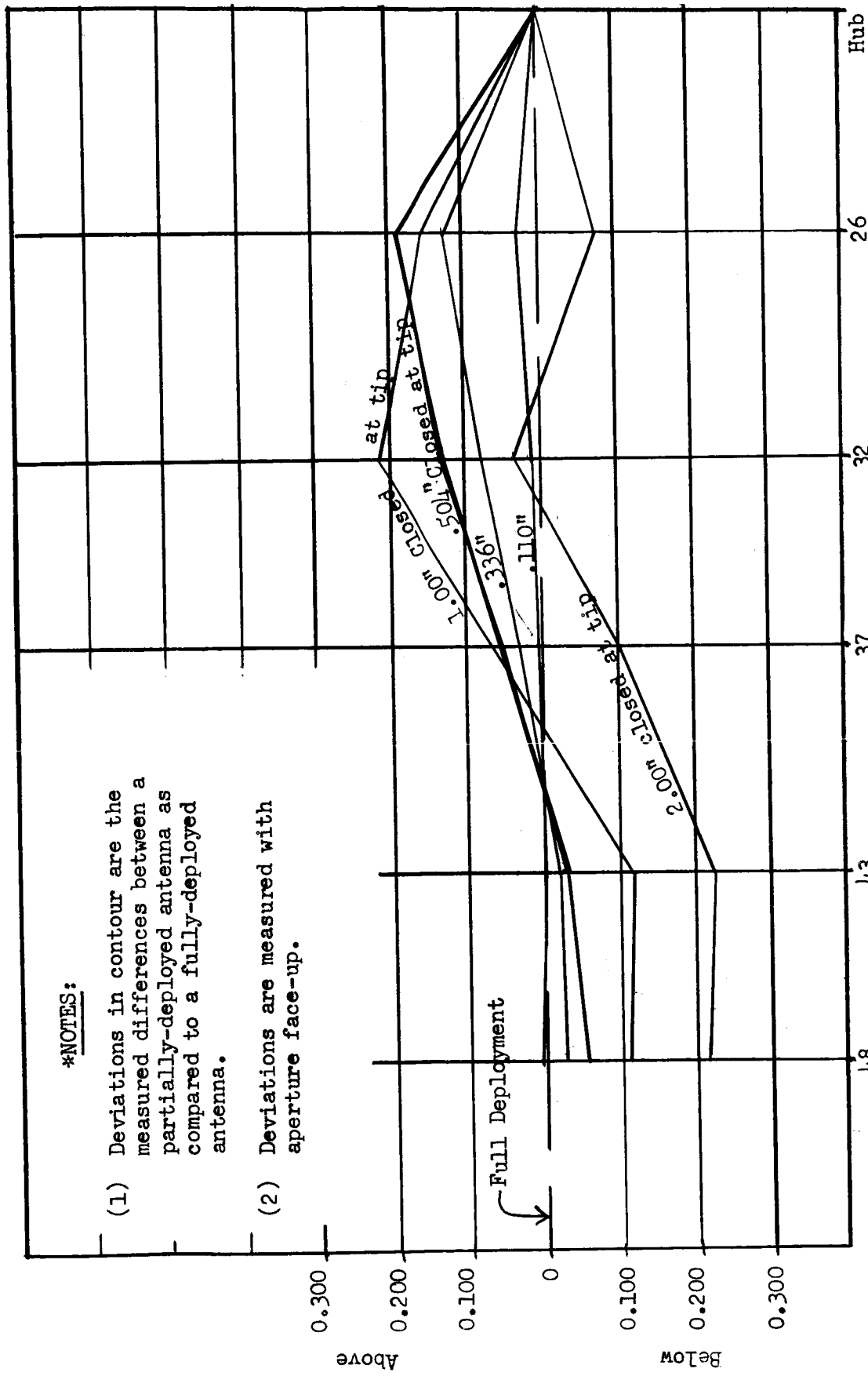

Figure 23. Contour Vs. Drum Backward Movement At One-Quarter Screen Distance From Rib #1

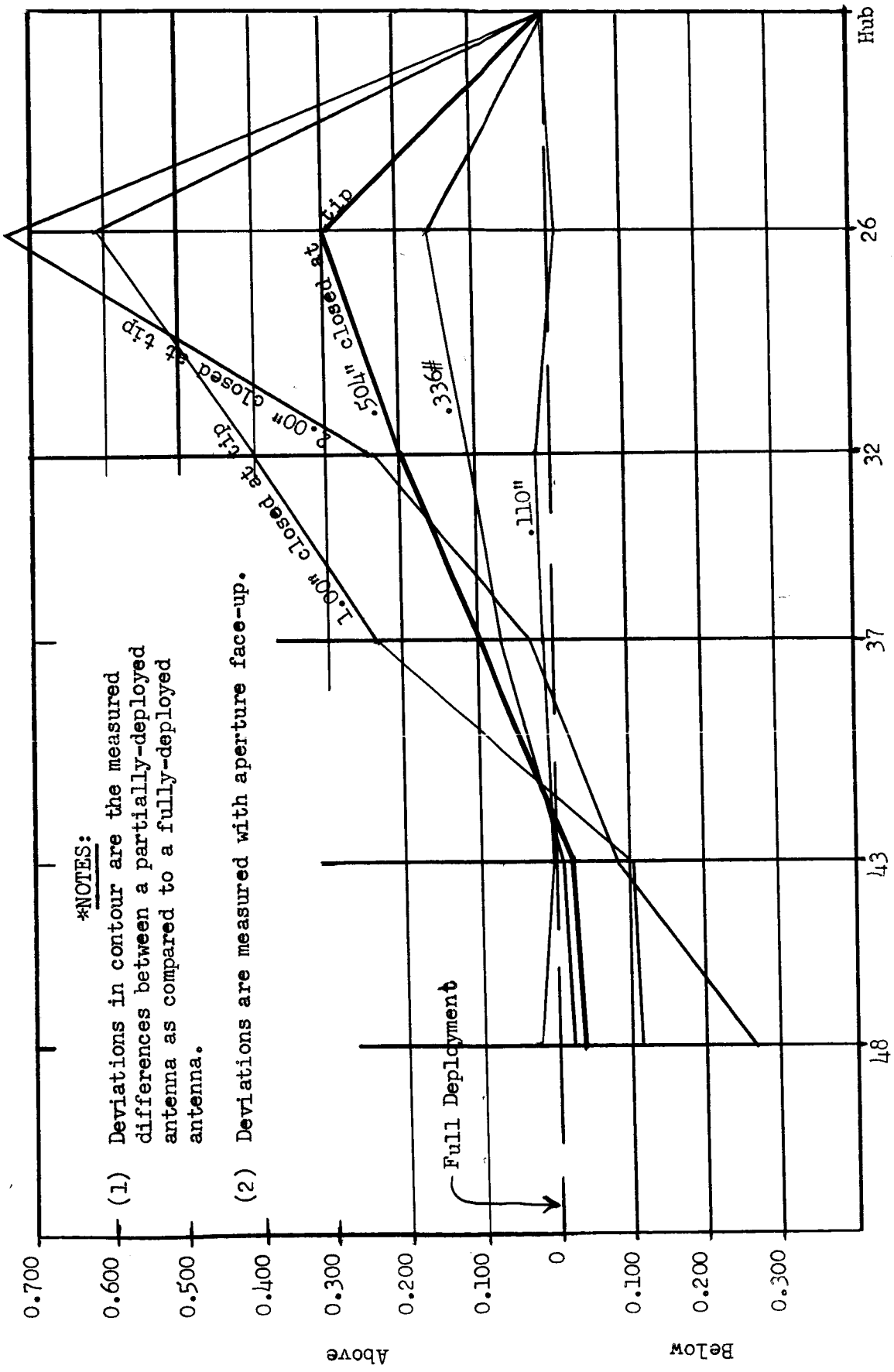

Figure 24. Contour Vs. Drum Backward Movement At Mid-Screen Position Between Rib #1 And Rib #2

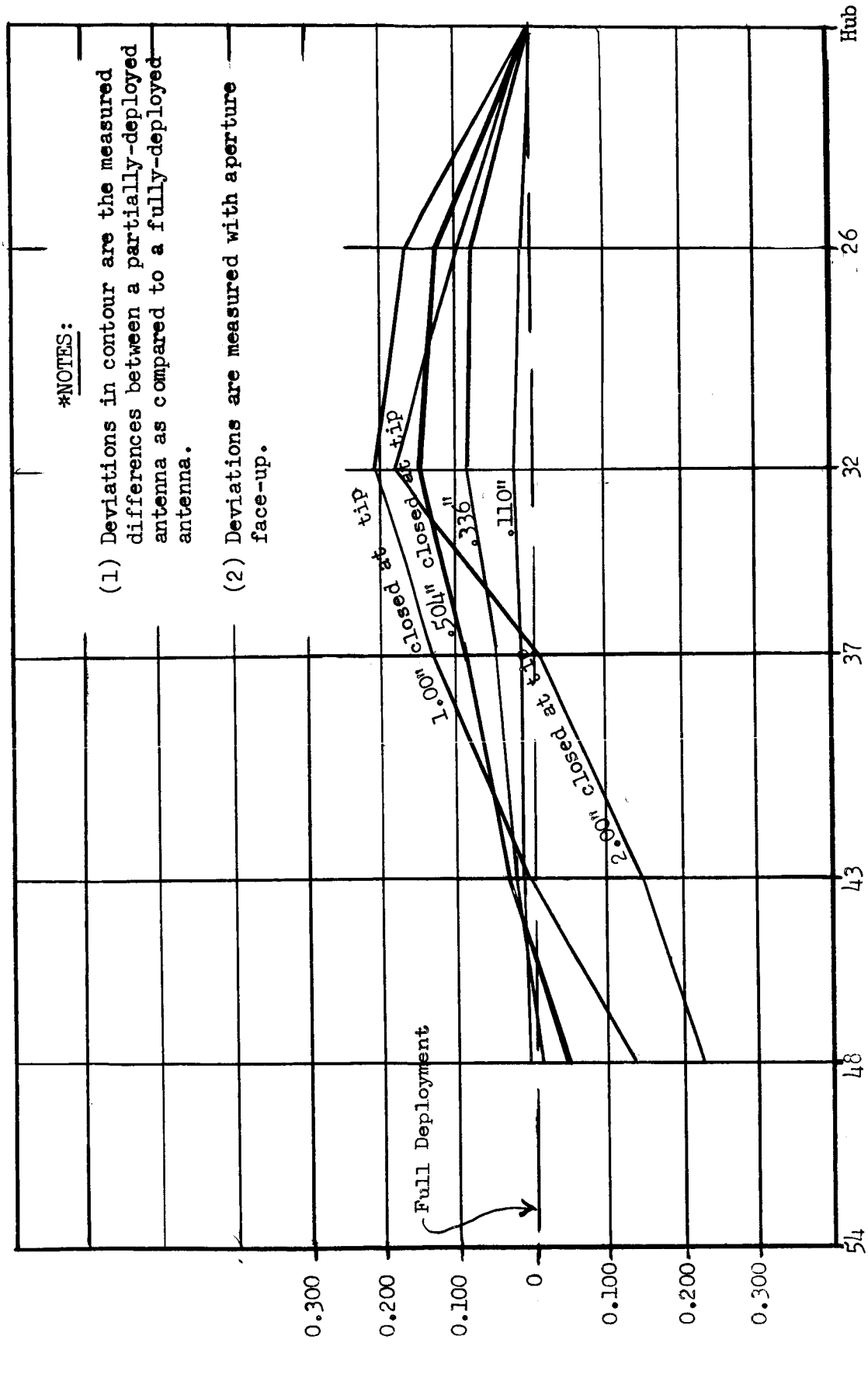

Figure 25. Contour Vs. Drum Backward Movement At Three-Quarter Screen Distance From Rib #1

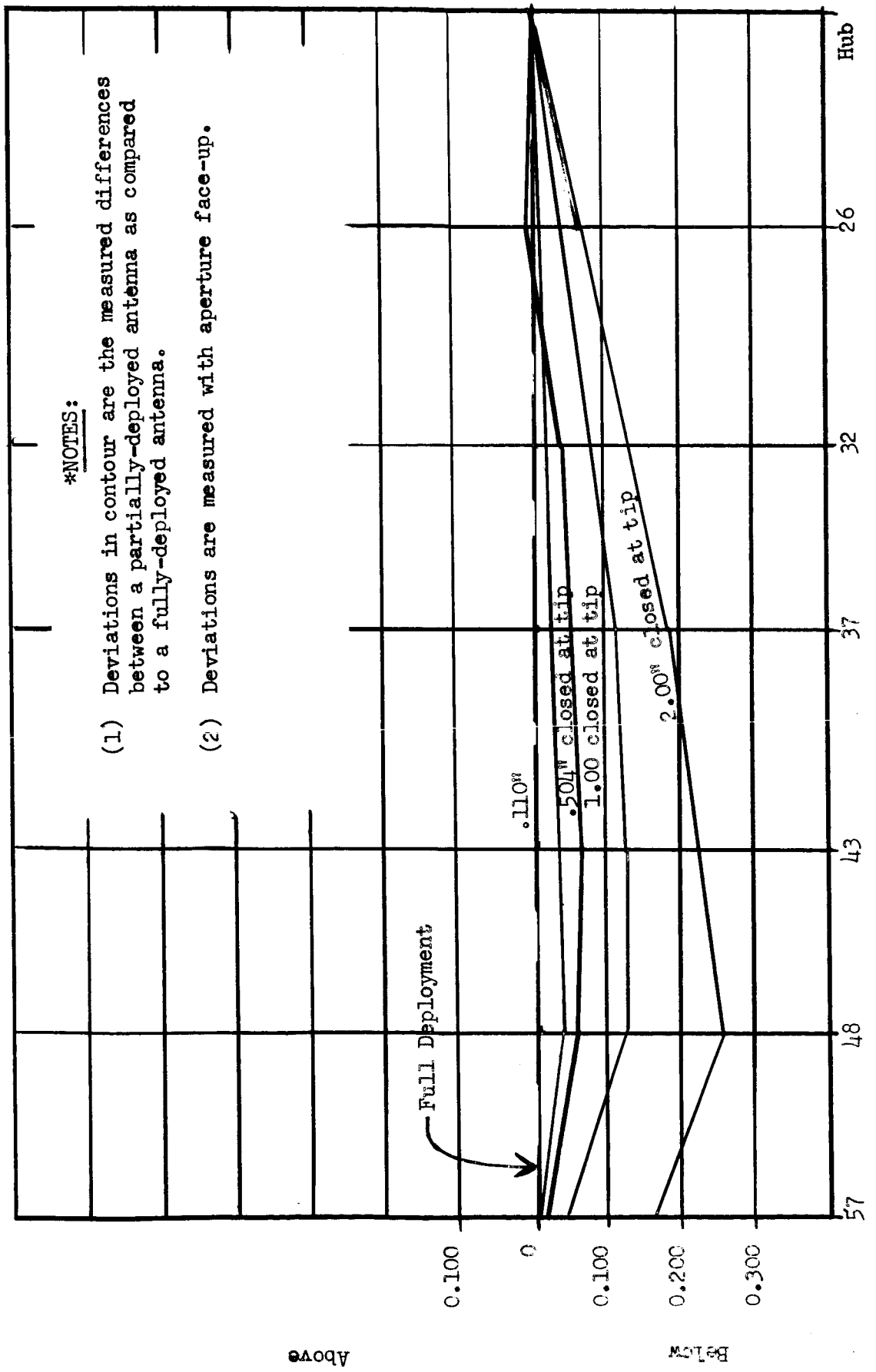

Figure 26. Contour Vs. Drum Backward Movement At Rib #2

K. ELECTRICAL BLOCKAGE IN THE PACKAGED CONFIGURATION

1. General

In accordance with item #10 of JPL Contract No. 950905, GAC conducted a study to minimize the electrical blockage of the antenna in the packaged condition.

2. Blockage Area

The area concerned is the screened hub (see Figure 13). The hub has approximately 1200 square inches of screened surface that remains coincident with the true paraboloid after closing the ribs to the packaged condition. However, the pulldown wires become a factor because these wires form a limiting circumference of unobstructed area which contains only 1068 square inches. This latter area is the maximum screened surface of the true paraboloid that is functional when the antenna is in the packaged condition.

3. Screen Packaging Study

As the antenna was being slowly closed from its deployed configuration, the screen was delicately maneuvered so that the natural folds would lie outside of the ribs. This action was taken to prevent encroachment upon the 1068 square inches of surface area. However, the spring action of the eight pulldown wires between each pair of ribs causes the screen to unfold in an unpredictable manner during deployment. The screen folds consistantly looped themselves over the rib packaging

supports. After numerous attempts, the decision was made to leave the folds inside the ribs in the interest of reliability. This decision means that the 1068 square inches of surface area must be reduced by approximately 12 percent.

L. RECOMMENDED CONFIGURATION

1. General

Table XI tabulates the configuration of the modified Hi-Gain Spacecraft Antenna delivered under JPL Contract No. 950905, and a recommended configuration for future antennas.

Table XI. Configuration Summary For Section II

Hardware Item	Item Description (Discussed in paragraph indicated)	Modified Antenna	Future Antenna
Rib	Tapered aluminum tube - Root O.D. 1.00 inch, Tip O.D. 0.50 inch, Constant wall thickness 0.020 inch (Par. B-3)	x	x
Rib Supports	Silicone rubber bumper and a tubular aluminum spacer (Par. H-2)	x	x
Hub Deployment	Deploy hub along boom with an electrically actuated screw drive (Par. I-2-a)		x
Hub Hardware	Change nuts, bolts and screws from steel to aluminum material (Par. I-3-c)		x
Boom	Replace welded, tubular-member truss with a riveted, aluminum web truss (Par. G-1)		x
Locks	Remove rib quadrant deployment locks and add deployment locks at main drum (Par. J-1)	x	x

(Table continued on next page.)

Table XI. (Continued)

Hardware Item	Item Description (Discussed in paragraph indicated)	Modified Antenna	Future Antenna
Shims	Add captive shims to screen in those areas which fold between ribs and rib supports in antenna packaged configuration (Par. H-3)	x	x
Screen Pull-down Wires	Install wires between ribs (or hub) which will pass through and pull mid-screen closer to paraboloid contour (Par. E-4)	x	x
Screen Material	Install tin-plated copper screen on reflector surface in lieu of Invar screen (Par. E-6)	x	x
Hub Material	Change hub structure from Invar to Aluminum material (Par. I-3-b)		x

SECTION III

MODEL RE-DESIGN AND FABRICATION

A. GENERAL

The model re-design and fabrication phase of the program consisted of modifying the original antenna to incorporate the selected changes shown in Table XI. The re-design and fabrication task is discussed under eight major paragraph headings, as follows:

B. REFURBISHING

C. RIB FABRICATION AND ASSEMBLY

D. ASSEMBLY OF RIBS ON HUB

E. INSTALLING HINGE BRACKET STIFFENERS

F. INSTALLING SCREEN

G. RIB PACKAGING SUPPORTS

H. DRUM LOCK

I. FEED MODIFICATION

B. REFURBISHING

The initial task was the refurbishing of the original antenna. Refurbishing tasks included the following:

(1) Removal of all parts that were to be replaced.

(2) Detailed inspection of the remaining parts.

(3) Minor repairs to restore many areas of the antenna to a satisfactory condition.

(4) Straighten bent pulley brackets.

(5) Remove rust from hub.

Items (4) and (5) could not be completely corrected. The bent brackets were straightened to approach their original configuration as closely as practicable without complete disassembly, but it was impossible to return the brackets to their exact original configuration (and therefore, to their original strength). Trial operation after straightening indicated that the antenna would operate properly for the limited function intended.

The rusted hub was cleaned and a water-soluable coating was applied. Due to the excellent penetration resistance of Invar, the rust did not affect the hub strength. However, the slight marring of the surface degrades the overall appearance of the antenna.

C. RIB FABRICATION AND ASSEMBLY

1. General

The ribs selected for installation on the antenna have a diameter which tapers from 1.00 inch O.D. at the root to 0.5 inch at the tip. The ribs have a constant wall thickness of .020 inch and are fabricated of 2014-T6 aluminum alloy material. The ribs meet all requirements established in Paragraph B of Section II (Preliminary Design and Analysis). They were fabricated and assembled to GAC Drawing 528A-055 which is included in the Appendix to this report.

2. Fabrication And Assembly Procedures

The procedure for tube fabrication is as follows:

a. Procure aluminum alloy 2014-T6 tubes 70 inches long with diameter which tapers uniformly from 1.10 inch O.D. to 0.40 inch O.D. The tubes must have a constant wall-thickness of 0.020 inch. Procurement tolerances are:

(1) Wall ± 0.0025 inch

(2) O.D. ± 0.005 inch

(3) Ovality ± 0.005 inch

(4) Flatness ± 0.06 inch maximum

b. Install one tapered tube inside a constant diameter tube 1.25 inch O.D. and fill the nested tubes with melted Cerrobend.

c. Conduct a trial contouring bend on the nested tubes, using bending rolls. Determine the spring-back characteristics of the tapered tube; then adjust the roll template to compensate for spring-back.

d. Using preceding steps "b" and "c" as a guide, roll all tapered tubes to the required rib contour.

e. Remove the tapered tubes from the constant diameter tubes.

f. Trim the tapered tubes to installation lengths.

g. Fill all tapered tubes with melted Cerrobend.

h. Hand form the ribs to exact contour, utilizing the antenna mold with hub and hinges installed, as a pattern.

i. Remove the Cerrobend filling from the tapered tubes.

j. Align and install the rib mounting flange welding fixture, utilizing the antenna mold with hub and hinges installed as a pattern.

k. Weld the mounting bracket to all ribs.

l. Re-check rib contour and hand form the rib as required.

m. Identify the ribs to match the specific hinges on which they will be mounted.

D. ASSEMBLY OF RIBS ON HUB

The assembly of ribs on the hub requires the precise positioning of the hinge pin prior to the attachment of each rib. Correct hinge pin location achieves correct spacing between ribs in the packaged configuration, controls the deployed position of the ribs, and prevents interference when the rib tips cross each other during deployment. To meet these three requirements, each hinge pin is canted to an angle of 7 degrees, 38 minutes and 31 seconds in the radial direction and to an angle of 2 degrees, 8 minutes and 43 seconds in the circumferential direction.

These hinge pin angles and pin positions were set by locating the hub on a surface

table and rotating each pin to one alignment fixture for adjustment. The pins were therefore located independent of any manufacturing tolerance which may have been present in the hub.

The ribs were attached to the hinges with the hub installed on the mold. The relative positions of the hub and ribs were checked against the mold and adjusted as required.

E. INSTALLING HINGE BRACKET STIFFENERS

A certain degree of deflection in the hub outer web was noted at the lower end of the rib hinge-to-hub interface. This deflection was eliminated by installing an aluminum stiffener from the bottom of the hinge bracket to the bottom flange of the hub as shown in Figure 27. The stiffener is fabricated of 6061-T6 aluminum alloy 0.032 inch thick. The stiffener design is shown on GAC drawing 528A-060, included in the Appendix to this report.

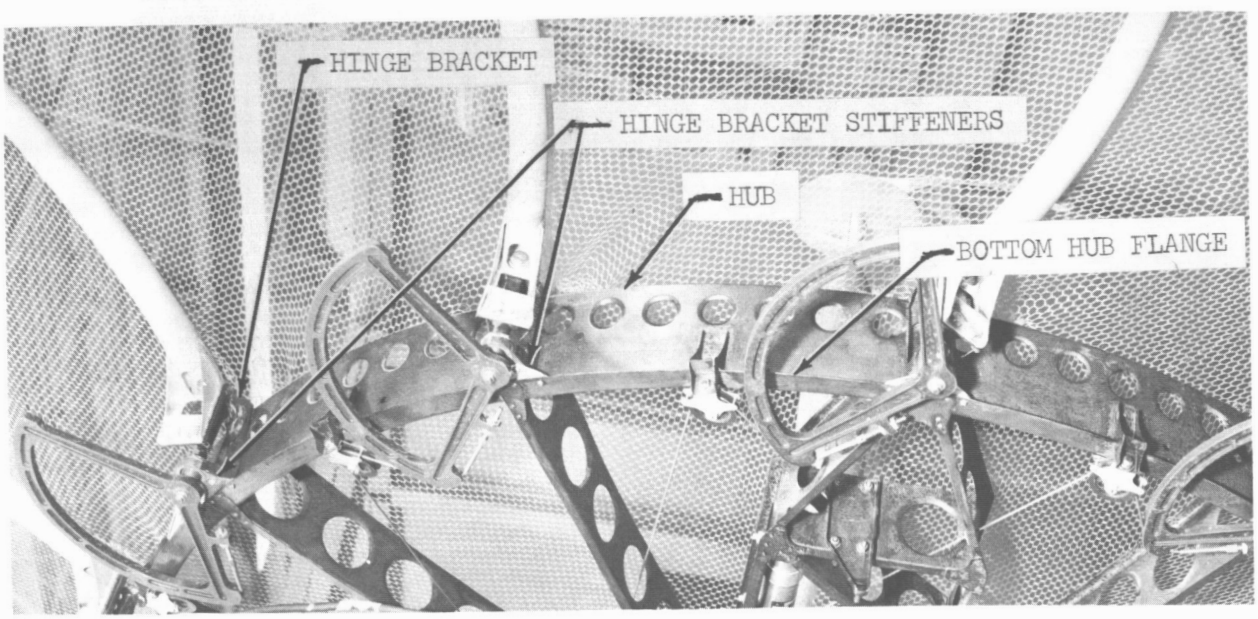

Figure 27. Hinge Bracket Stiffener

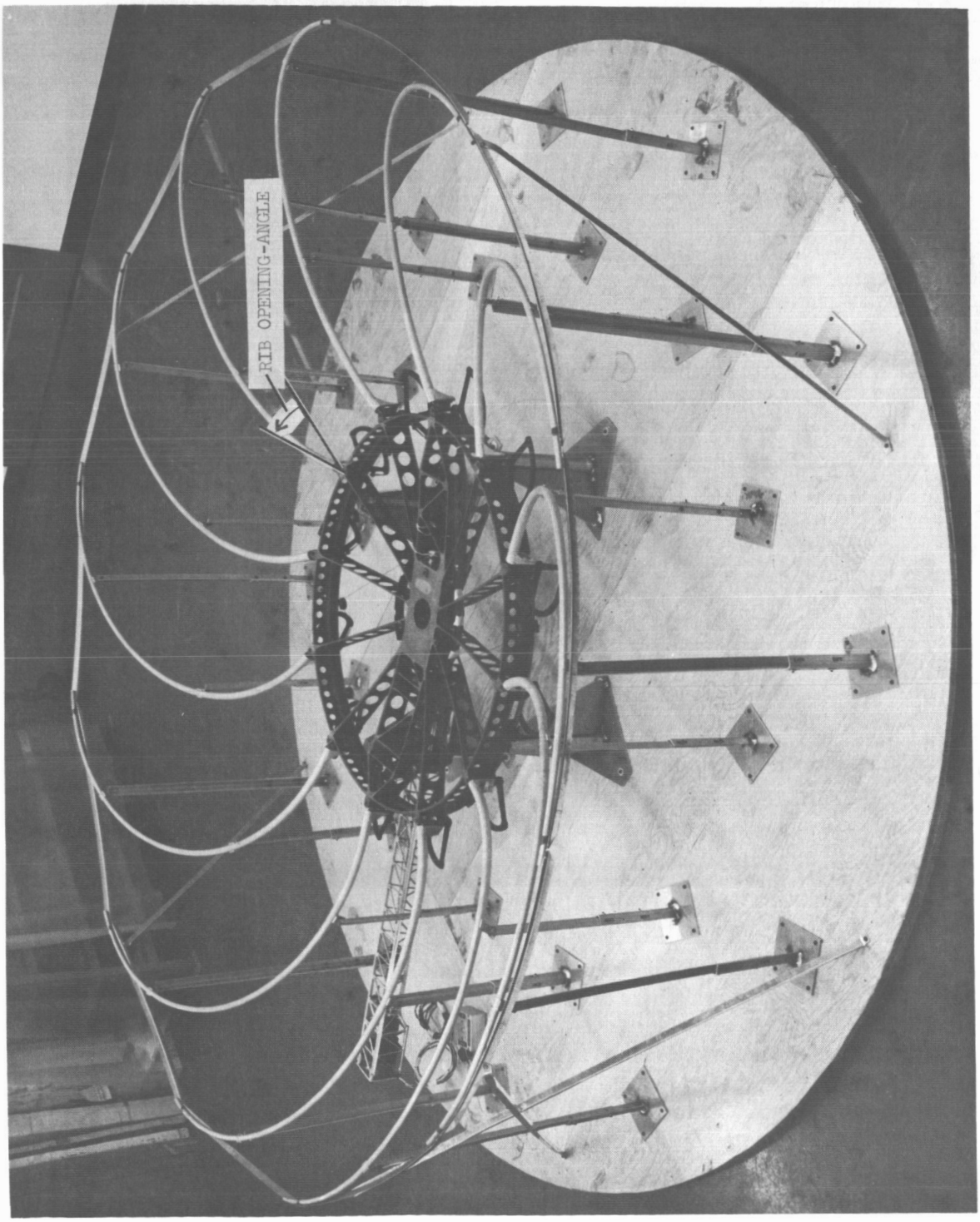

Figure 28. Screening Fixture

F. INSTALLING SCREEN

1. Counter-Stressing The Ribs

The 12 ribs and hub were placed in the Screening Fixture as shown in Figure 28. The ribs were initially opened to an angle of 28 degrees, 30 minutes. This angle placed the ribs on the required paraboloid contour.

To compensate for rib deflection caused by screen tension, the ribs were counter-stressed in the screening fixture. The required counter-stressed position had been established by previous load tests on the ribs. Counter-stressing was accomplished by rotating the rib an additional 4 degrees 40 minutes at the hinge and then applying a load at the rib tip to return the tip to the initial on-contour position. The rib tip was then attached to the screening fixture to maintain the pre-stressed position during the screening process.

2. Pre-Stretching and Installing the Screen

Prior to installation, the screen wire for each bay was pre-stretched on the rig shown in Figure 29, to ensure a uniform tension on the screen, and to ensure uniform rectangular wire spacings approximately 0.25 by 0.12 inches. The stretched screen was transferred to the Screen Transfer Frame shown in Figure 29, then positioned and cemented to two adjacent ribs. Epoxy compound consisting of EPON 828 (55%) and VERSAMID 115 (45%) was used to cement the screen to the ribs.

Figure 30 shows the screened antenna immediately after removal from the screening fixture.

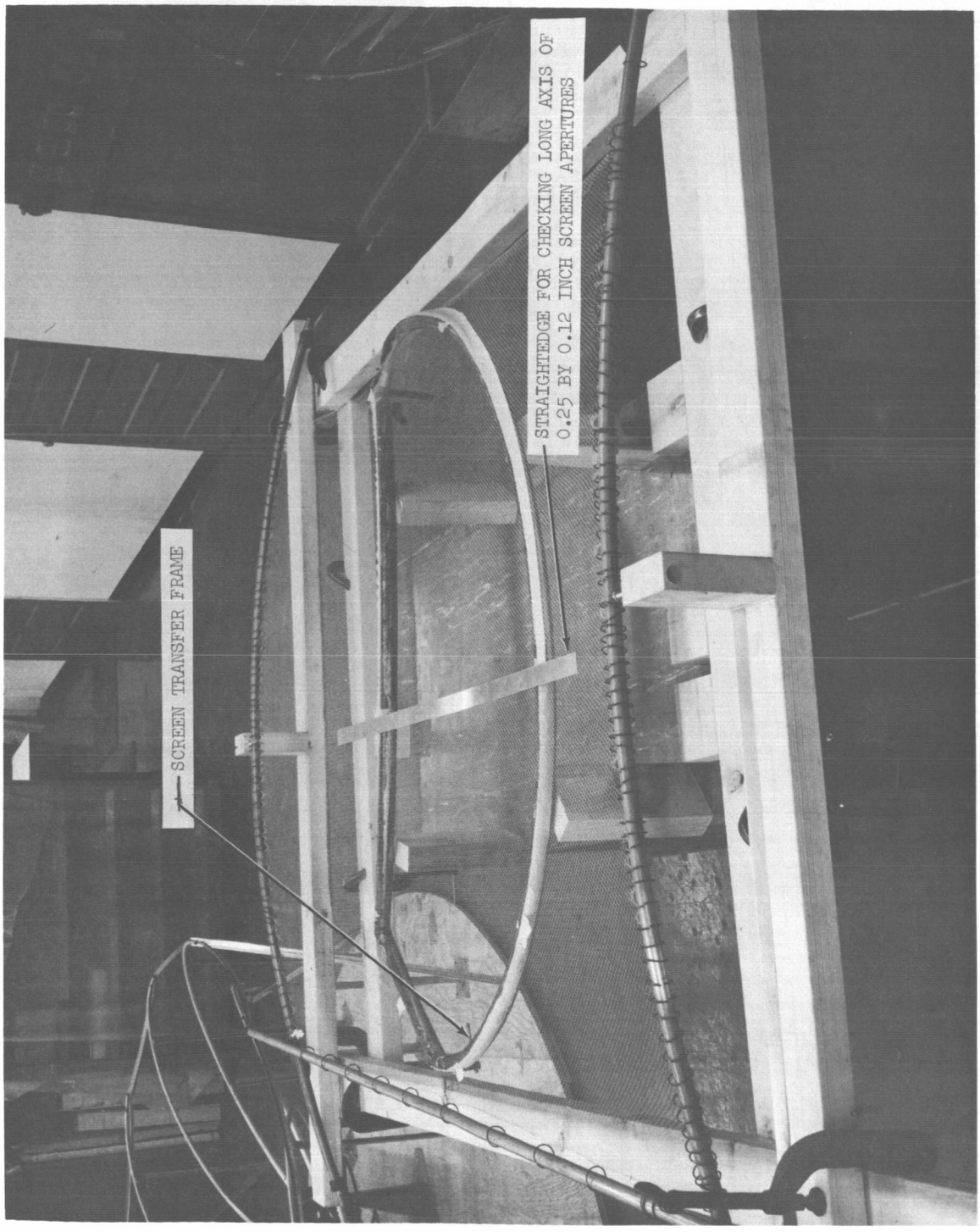

Figure 29. Pre-Stretching Rig for Wire Screen

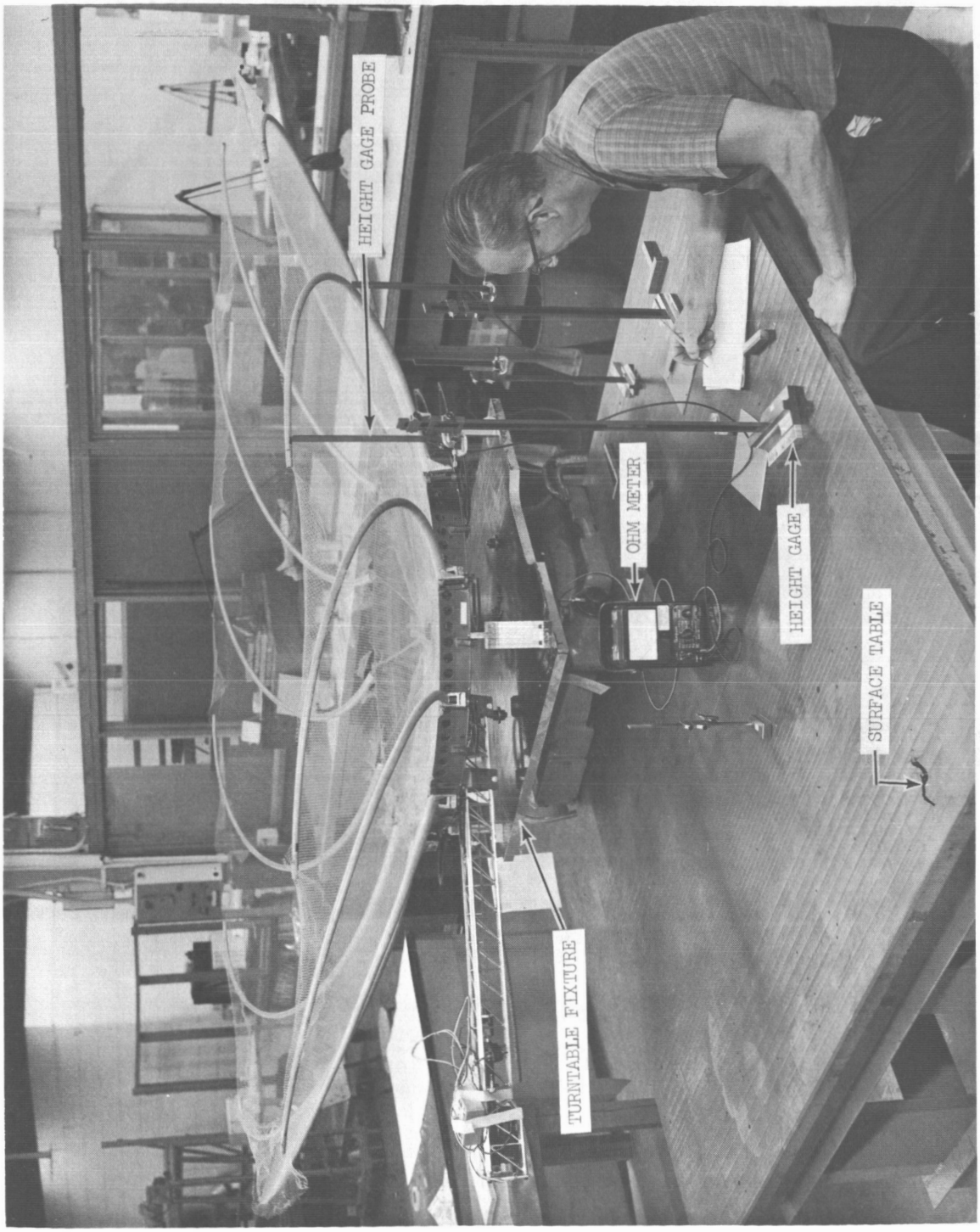

Figure 30. Contour Measurement Setup

3. Pull-Down Wires

a. Design Phase. The study and tests conducted during the preliminary analysis (Described in Paragraph C of Section II) proved the feasibility of using pull-down wires to reduce the deviations in screen contour. The pull-down wire scheme used in the preliminary analysis required wires spaced at two inch intervals along the rib radius, requiring a total of 19 wires for each bay (the screen section between two ribs). The short spacing between pull-down wires was designed to compensate for the orthotropic characteristics of the screen (elongation in the radial direction). Thus if there was large spacing between tie wires, the screen would elongate and return to its normal out-of-tolerance position at the midpoint between the pull-down wires.

The design phase for wire installation was initiated with a test program to establish a reasonable compromise between the required orthotropic characteristics of the screen and the multitude of pull-down wires required to hold contour. This program resulted in the establishment of the eight-wire configuration shown in Figure 31. In this configuration, the two radial wires (7 and 8) are interwoven with the screen and act as catenary elements between the rib-to-rib pull-down wires (1 through 6), thus holding the screen within contour tolerance. The position of wires 7 and 8 was selected to permit the screen to react orthotropically as required during packaging and deployment, and also to permit the antenna to be packaged and deployed without stretching the radial pull-down wires.

b. Test Phase. A test program was conducted on a simulated antenna bay

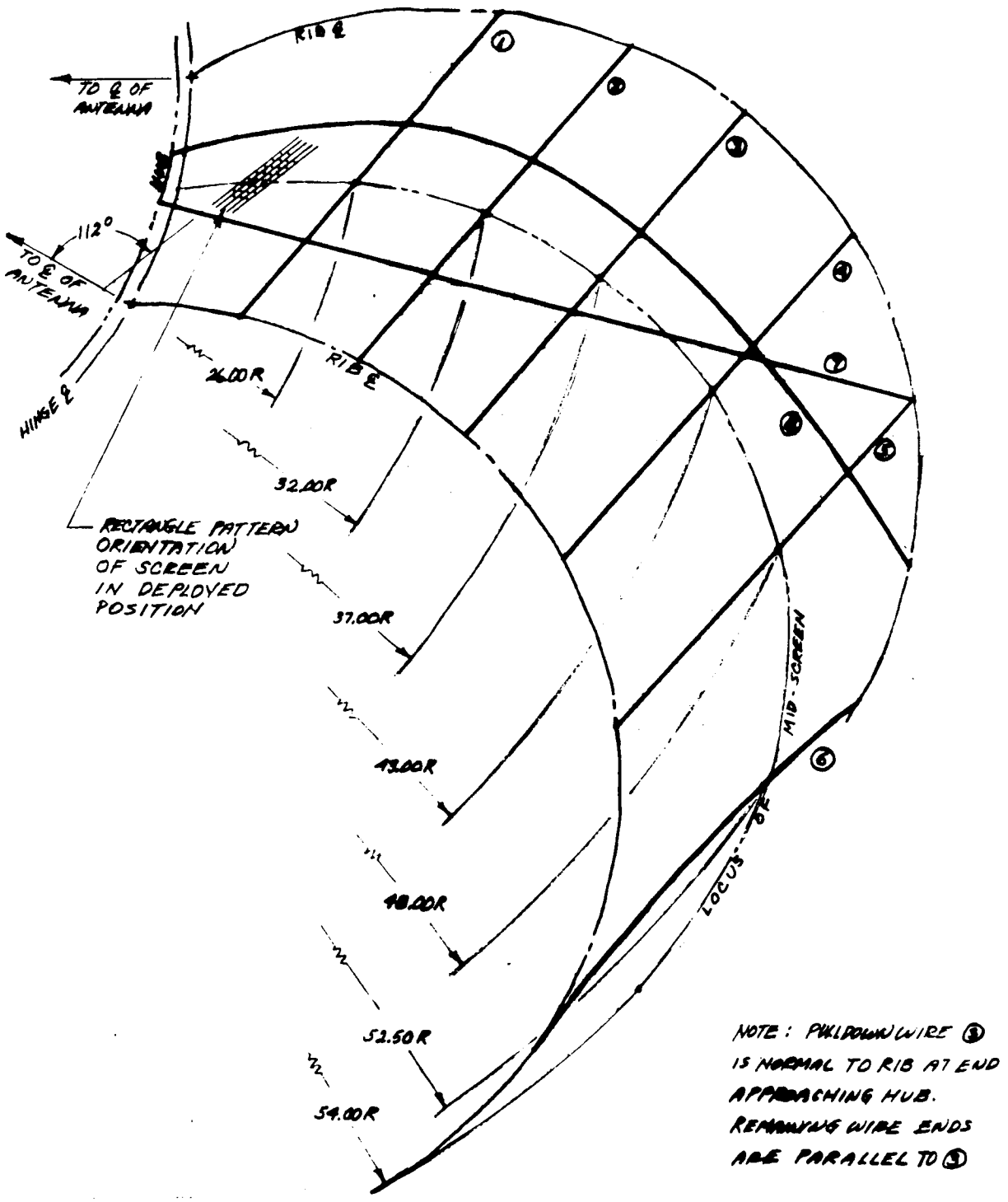

Figure 31. Mid-Screen Pull-Down Wire Geometry

consisting of two ribs with interconnecting screening. The test results indicated that the pull-down wire configuration shown in Figure 31 would maintain contour tolerances equivalent to those obtained from the system having pull-down wires spaced every two inches radially.

c. Installation. As shown in Figure 31, the center section of pull-down wires 1, 2 and 3 were interwoven in the screen. After passing over wires 7 and 8, the three wires exit from the screen and continue to a point of tangency at the ribs as shown in Figure 32. Wires 4 and 5 were interwoven in the screen in the same manner as if two radial pull-down wires were to be crossed. Wires 4 and 5 exit from the screen at a point 6.3 inches from the left rib centerline, and also become tangent to the ribs as shown in Figure 32. Wires 7 and 8 begin at the hub and are interwoven in the screen. Wire 7 leaves the screen after crossing wire 8 and continues on to the rib tangency point. Wire 8, which never leaves the screen, is positioned tangent to the top of the rib so that it cancels the rib torsion imposed by wire 7. Wire 6 is an approximate catenary curve used to tension the screen and produce a smooth contour in the outer screen bay.

All wires are wrapped 1-$\frac{1}{2}$ turns around the rib after becoming tangent, and are bonded to the ribs with epoxy. Obviously, the epoxy at the adjustment fixture end of the wires is not applied until the midscreen adjustments have been accomplished.

Wires 7 and 8 are terminated by a quarter-inch long hook at the hub end. The hooks

are formed by bending back the end quarter-inch of wire 180 degrees around a 0.030 inch diameter rod. The ends of wires 7 and 8 are hooked over the inner edge of the screened hub flange and are bonded in place on the hub at points 3.60 and 4.70 inches, respectively, from the rib hinge points.

Wire 8 terminates at the rib at a point midway between the wire 5 termination and the tip of the rib. Wire 8 crosses wire 1 midway between the rib and the intersection of wires 1 and 7, and crosses under wire 3 at a 90-degree angle 6.50 inches from the rib.

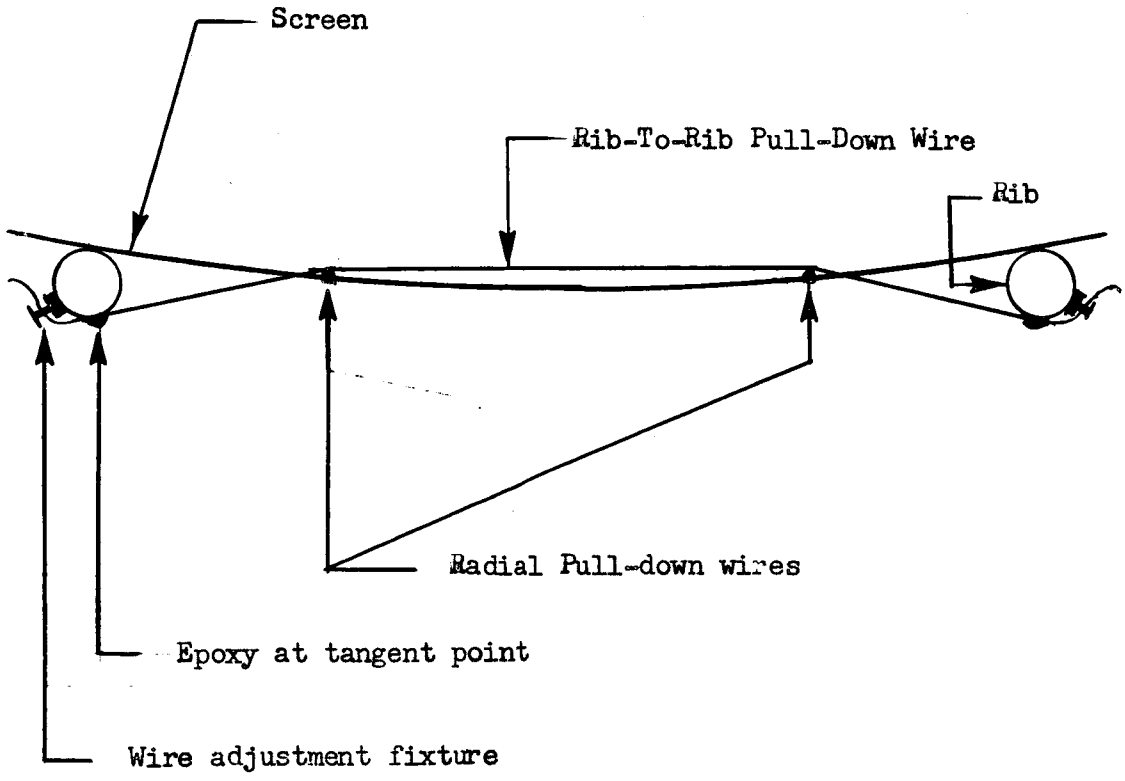

Figure 32. Rib-To-Rib Pull-Down Wire Fastening Details

During the adjustment period and throughout all contour measurements except the final measurement, the outboard ends of all pull-down wires terminate on wire adjustment fixtures. These fixtures consist of an Esna 22 NA7-68-82 nut plate with an AN 515 8R10 screw. The plate is attached to the rib with Caulk Grip Cement. Upon completion of the final adjustment, the pull-down wire is cemented to the rib and the adjustment fixture is removed.

G. RIB PACKAGING SUPPORTS

1. Design

The rib packaging supports consist of two parts: a molded silicone rubber bumper (Compound RTV No. 11); and a spacer fabricated from a short length of 0.50 inch diameter 6061-T6 aluminum tube. The design is shown on GAC Drawings 528A-059 (Bumper) and 528A-058 (Spacer) included in the Appendix of this report.

2. Installation

For installation of the rib packaging supports, the antenna was closed to the packaged configuration. All rib tips were then deflected downward in the hub direction, and held in that position. The rubber bumpers were placed on the tip of each rib at even-numbered hinge points as shown for Hinge No. 10 in Figure 13. The aluminum tube spacers were then sized to proper length and inserted between the bumper and the bottom of the next higher rib. The spacer was bonded to the rib with epoxy and to the silicone rubber bumper with DOW CORNING No. 1200 primer and No. 90092 adhesive.

H. DRUM LOCK

1. Design

The study conducted during the preliminary design (Discussed in Paragraph J of Section II) indicated the feasibility of maintaining the deployed antenna contour by locking the main drum in place with a pair of ratchet and pawl locks. The ratchets and pawls were machined from corrosion-resistant steel in order to provide high strength for locking engagement teeth. The mounting angles for the lock installation were fabricated from 6061-T6 aluminum alloy to provide minimum weight. The designs are shown in GAC Drawings 528A-056 (MODIFICATION-DRUM LOCK), 528A-057 (DETAILS-DRUM LOCK) and 528A-061 (MODIFICATION-DRUM LOCK DETAILS) included in the Appendix to this report.

2. Installation

The hub structure was modified to provide clearance for passage of the ratchet as the drum rotates from the packaged to the deployed position, as shown on drawing 528A-056. This was followed by the installation of the pawl and its mounting hardware on the hub, as shown on drawing 528A-056. With the antenna fully deployed, the ratchet was placed in position on the inner face of the drum. With the points of the ratchet and pawl teeth clearing each other by 0.002 inch, the ratchet was installed on the drum as shown in drawing 528A-056.

I. FEED MODIFICATION

1. Design

The feed designed by JPL (See JPL Drawing 126352) was modified to the configuration

shown on GAC Drawing SK-DW-33065. The major change was in the lengths of the JPL outer and inner conductors (Drawings 126354 and 126381, respectively) which were shortened by approximately 6.00 inches. This change placed the feed disconnect from the RG-11210 coaxial cable beyond the antenna feed support, so that assembly of the feed could be easily accomplished.

2. Fabrication

All detail parts, including the two modified conductors, were fabricated to the JPL specifications, except for minor deviations in materials and finish.

3. Installation

The GAC-designed parts which attach the feed to the feed deployment bellows assembly are shown on GAC Drawing SK-DW-33065, included in the Appendix to this report.

SECTION IV

MODEL TESTING

A. GENERAL

The model-testing phase of the program included performance of all contractually required tests on the modified antenna. The model-testing phase is described under five major paragraph headings, as follows:

B. CONTOUR ADJUSTMENT

C. CONTOUR REPEATABILITY TEST

D. CONTOUR MEASUREMENTS

E. RF TESTING AND EVALUATION

F. VIBRATION SURVEY

B. CONTOUR ADJUSTMENT

1. General

The contract requires the surface of the antenna to be adjusted to a true paraboloid contour within $\pm$ 0.25 of an inch with $\pm$ 1 g loading. This total tolerance includes all tolerances such as gravitational deflections, repeatability gaging and localized bowing of the screen.

The initial effort in making the antenna adjustments was concentrated on isolating each tolerance and establishing its limit. The combining of these tolerances dictated the position limits for the screen and the ribs with the antenna in the face-up position and the face-down position. The following paragraphs describe

the method used to obtain these limits.

2. Contour Measurement Procedure

The contour measuring set-up (shown in Figure 30) includes a surface table, a rotating fixture, a height gage and an electrical continuity meter. The antenna is shown in the position used for face-up measurements. The face-down measurements are accomplished in the same manner with the antenna inverted on the rotating fixture.

The measuring procedure is as follows:

(1) Deploy the antenna.

(2) Install antenna on the rotating fixture and level the hub.

(3) Vibrate antenna rib tips to normalize the rib position.

(4) Delay one day, then vibrate the rib tips again, to normalize the rib and screen position.

(5) Precisely locate the required radius for the height gage measurement.

(6) Adjust the height gage until contact is made with the antenna, as indicated by the electrical meter. Use care to avoid deflection of the antenna with the height gage.

(7) Record the height gage measurement.

(8) Rotate the antenna to the next measuring point and repeat steps (6) and (7).

The positive and negative nomenclature established for contour deviations reported in this section are defined as follows:

Positive:

A measurement along a line which is parallel to the antenna axis and is in the direction away from the concave surface of the antenna.

Negative:

A measurement along a line which is parallel to the antenna axis and is in the direction away from the convex surface of the antenna.

3. Repeatability Tolerance Tests

a. Procedure. The following procedure was used to establish the repeatability tolerance of the antenna:

(1) With the antenna installed face-up on the surface table, the rib tips were set at maximum negative tolerance.

(2) The pull down wires were adjusted to limit the mid screen deviation from the rib to +0.166 inches.

(3) Steps (1) and (2) were repeated until two successive measurements were consistent without adjusting the pull-down wires or the rib-tip position.

(4) The antenna was closed and opened several times. After each opening, the rib and mid-screen positions were measured at screen radii of 26, 32, 37, 43, 48 and 52 inches and at rib radii of 32, 43, 48 and 54 inches.

b. Results. The deviations from the initial setting at each radius were averaged to find the deviation of the rib in the negative direction (0.025 inches) and the deviation of the screen in the positive direction (0.075 inches). Deviations in the opposite directions are not important as they are always within the overall tolerance limitations.

4. Screen Bow Tolerance

a. Procedure. The screen bow tolerance adjustments were made as follows:

(1) With the antenna installed face-up on the surface table, the rib tips were set at maximum negative tolerance.

(2) The pull-down wires were adjusted to limit the mid screen deviation from the rib to +0.166 inches.

(3) The antenna was rotated slowly and the screen position was measured at small intervals at several radii.

(4) The antenna was inverted to the face down position and step (3) was repeated.

b. Results. The limiting deviation of the screen mid-screen measurements was found to be 0.060 inch in the positive direction. The negative deviations were always within the overall tolerance limitations.

5. Gaging Tolerance

The height gage probe was designed to measure, as nearly as practicable, a point on the antenna. However, since the screen has openings, the probe tip

must have a flat section that is large enough to detect screen contact with the naked eye. This eliminates probe penetration of the screen prior to electrical contact. The flat section of the probe introduces a small gaging error (approximately 0.005 inch) if the screen contact is at the edge of the probe instead of at the center. This relationship is shown in Figure 33.

Extraneous vibrations were noted in the vicinity of the antenna setup. These vibrations caused movements (approximately 0.012 inch) of the screen.

To insure conservative readings, the 0.005 inch gaging error and the 0.012 were added to give a maximum possible gaging error of 0.017 inches.

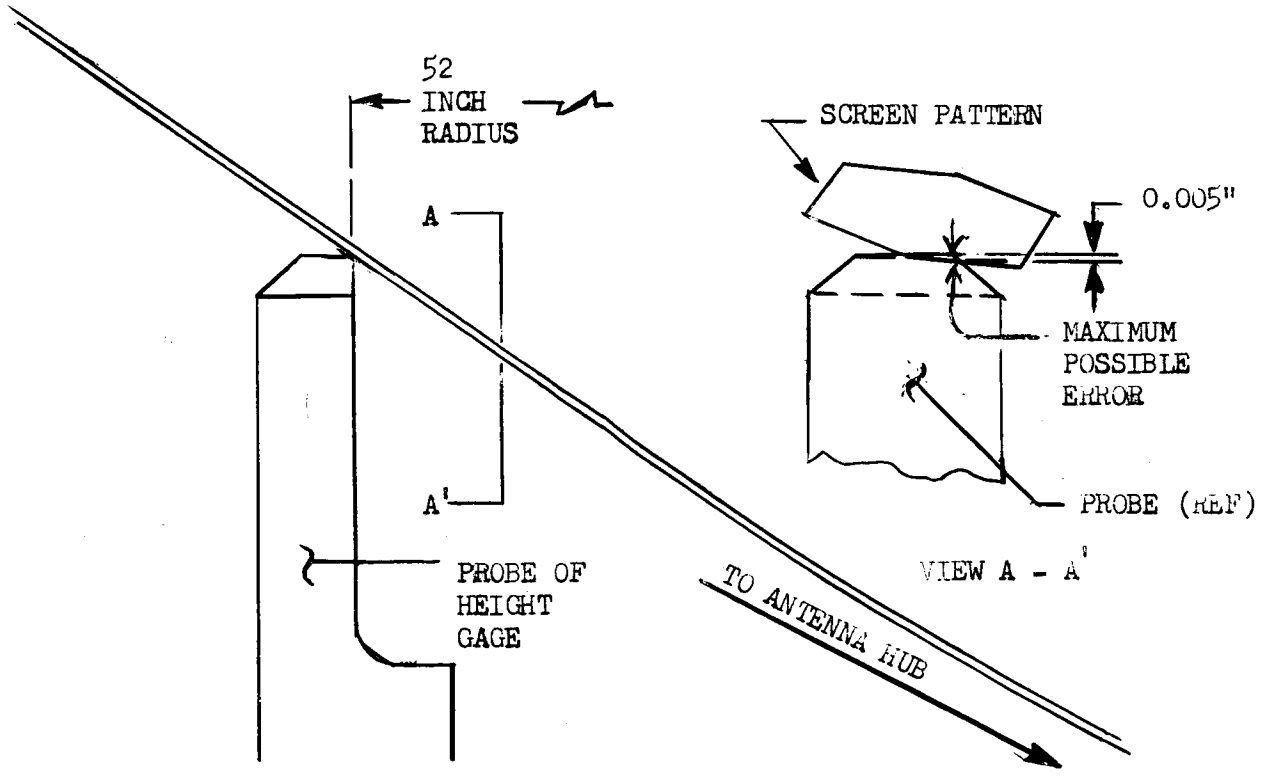

Figure 33. Probe Tolerance

6. Rib and Screen Gravitational Tolerance

a. General. The rib and screen gravitational tolerance adjustment consisted of two parts: (1) measuring the gravitational deflection with the pull-down fixtures installed on the ribs, and (2), measuring the gravitational deflections with the pull-down fixtures removed. The difference between these two sets of gravitational deflection measurements established the magnitude of extra contour deviation permitted for all contour measurements with the fixtures installed. These values also were used to establish the initial rib and screen settings so that the final settings were within the established tolerance settings when the pull-down fixtures were removed.

b. Procedure. The gravitational deflections with pull-down fixtures installed were measured in the following manner:

(1) The antenna was installed face-up on the surface table, and the pull-down wires were adjusted with the pull down fixtures.

(2) Rib and screen positions were measured and recorded.

(3) The antenna was installed face-down on the surface table, but no adjustments were made in the pull-down wires.

(4) Rib and screen positions were measured and recorded.

The measurement of gravitational deflections with the pull-down fixtures removed could not be measured directly, because the fixtures were needed to hold the required tension in the pull-down wires. The deflection force was simulated by adding weights (equivalent to the weights of the pull-down fixtures)

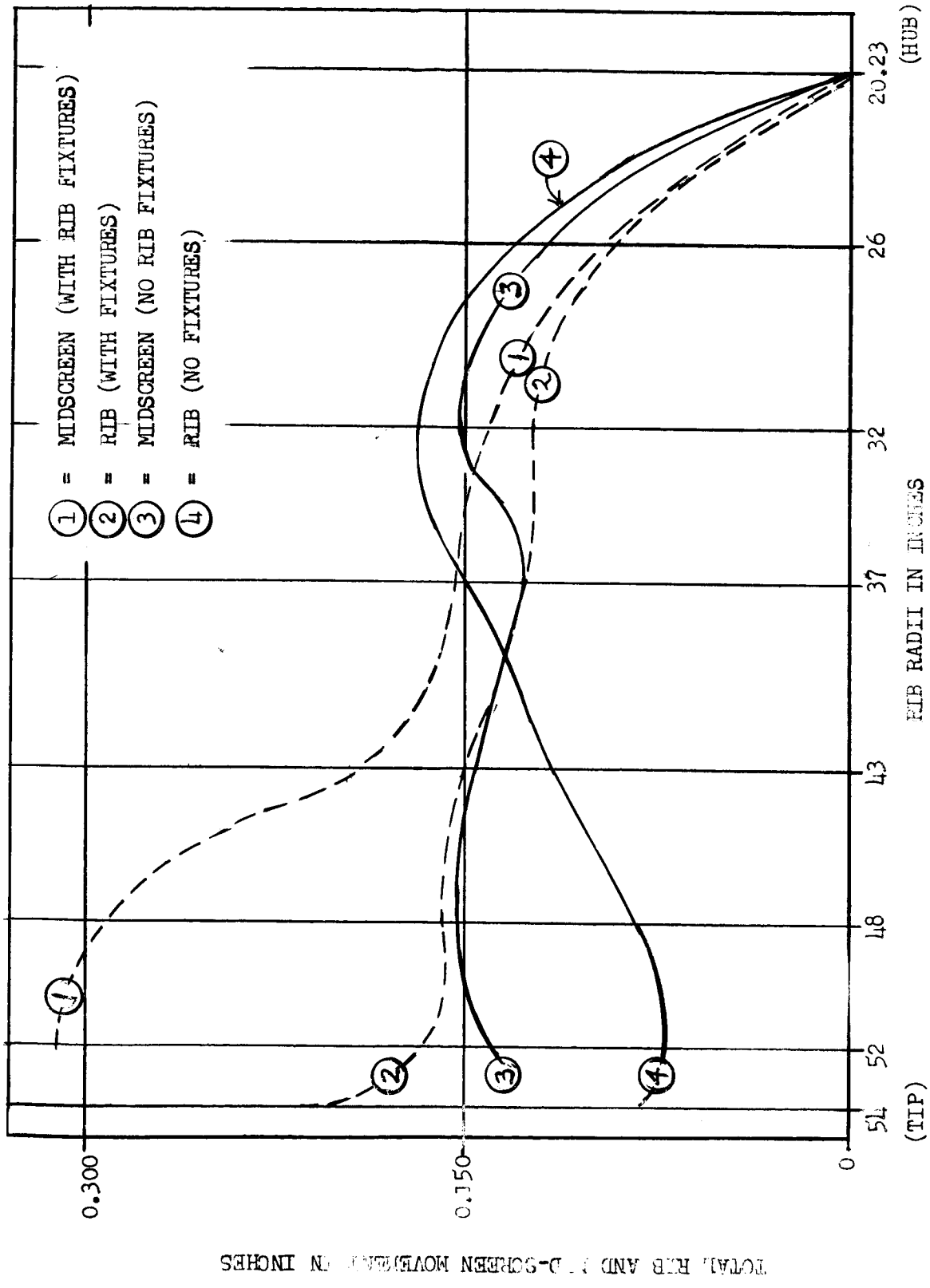

Figure 34. Gravitational Tolerances With and Without Pull-Down Wire Fixtures

to the ribs and determining the added deflection. This added deflection was then subtracted from the initial deflection, to determine the approximate rib and screen positions when the fixtures were removed. The measurements were accomplished in the same manner as shown in steps (1) through (4) above.

c. Results. The gravitational tolerances measured during the initial calibration for each of the two conditions are shown in Figure 34. These measurements were considered tentative, because the final pull-down wire tension had not been established and because the deflection measurements with no fixtures were obtained under simulated conditions. However, the final measurements proved that the approximations were sufficiently accurate to result in an accurately contoured antenna with the fixtures removed.

7. Composite Tolerance

Figure 35 shows the initial screen setting limits and rib tip setting limits for two conditions. Condition A shows the limits for the antenna face-up and face-down with no pull-down wire fixtures installed. Condition B shows the limits for the antenna face-up and face-down with the pull down wire fixtures installed.

Since all calibrations and adjustments are made with the pull-down fixtures installed, the initial settings were made to Condition B. The tests indicated that the rib and screen will return to the required specification limits of Condition A when the pull-down fixtures are removed.

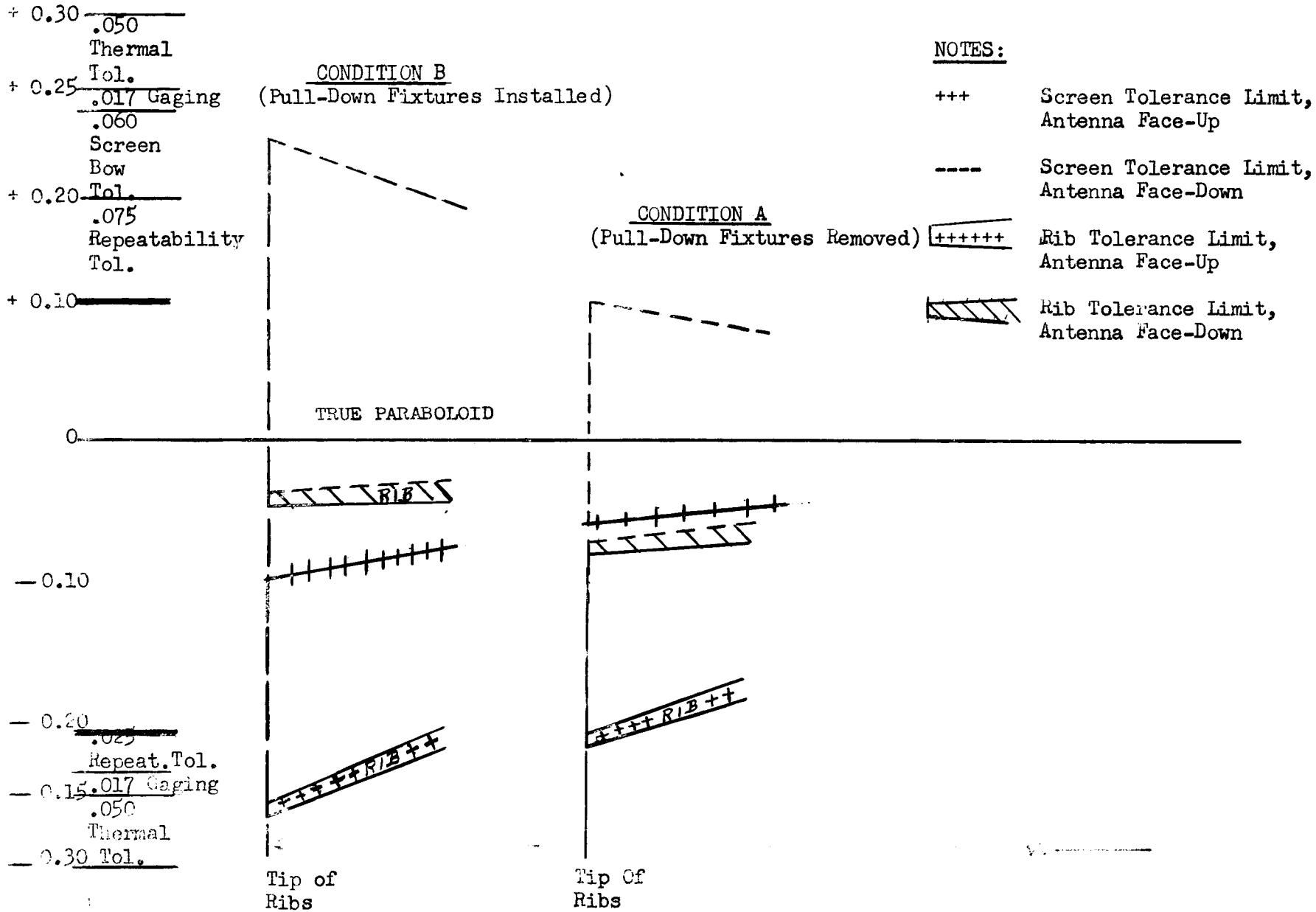

Figure 35. Initial Setting Tolerance Limits

The initial setting limits for the full length of the rib and the screen with the antenna aperture face-up is shown in Figure 36. The rib was set as near to the lower rib limit line as practicable at the tip, with gradually decreasing tolerances toward the hub.

The screen was set as near to the screen upper-limit line as practicable for the full radius.

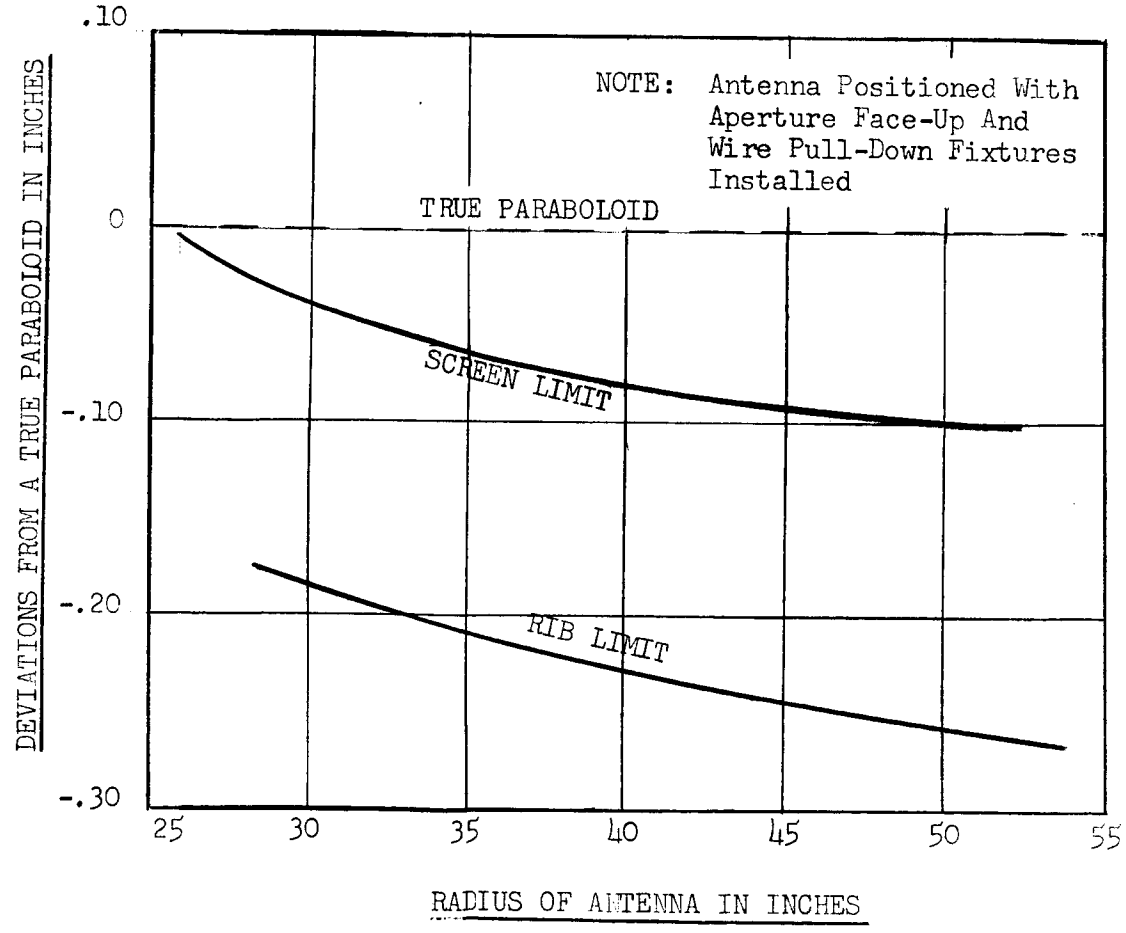

Figure 36. Initial Setting Limits For Rib and Screen

C. CONTOUR REPEATABILITY TEST

Contour repeatability tests were conducted with the antenna mounted face-up on the surface table. The measurements were made in the manner described in Paragraph B-2. The initial (or standard) measurement was made immediately prior to the first closing and reopening of the antenna. The subsequent measurements were made approximately 12 hours after each closing and reopening operation had been completed. The 12 hour delay was scheduled into the program to allow the antenna to stabilize.

The data on the average deviation during the repeatability tests for each rib and screen measuring radius are given in Table XII. Rib deviation data is plotted in Figure 37 and screen deviation data is plotted in Figure 38.

Note that, except for one point on the screen and one point on the rib, all tolerances were well within the allotted values of 0.075 inches for the screen and 0.025 inches for the rib. It should also be noted that the majority of the deviations occurred on the initial deployment, and that the deviations on subsequent deployments were nearly identical to those on initial deployment. It is believed that this is due to the relaxation characteristics of the screen and that any further delay (beyond the 12 hours) in recording the data would have resulted in even lower tolerance values. It is also believed that, in a long term space flight, the antenna would nearly duplicate the zero-gravity positions determined by ground tests.

Table XII. Repeatability Test Data

	AVERAGE DEVIATION FROM ORIGINAL SETTING (INCHES)									
Repeatability Test	Rib R=54"	Mid-Screen R=52"	Rib R=48"	Mid-Screen R=48"	Rib R=43"	Mid-Screen R=43"	Mid-Screen R=37"	Rib R=32"	Mid-Screen R=32"	Mid-Screen R=26"
First	-0.025	-0.004	-0.012	+0.058	-0.005	+0.064	+0.049	+0.001	+0.031	+0.037
Second	-0.039	-0.003	-0.012	+0.077	-0.006	+0.058	+0.058	-0.003	+0.046	+0.053
Third	-0.031	+0.001	-0.006	+0.102	-0.002	+0.072	+0.060	-0.026	+0.037	+0.033
Fourth	-0.035	-0.002	-0.010	+0.107	0.000	+0.072	+0.067	-0.000	+0.050	+0.054

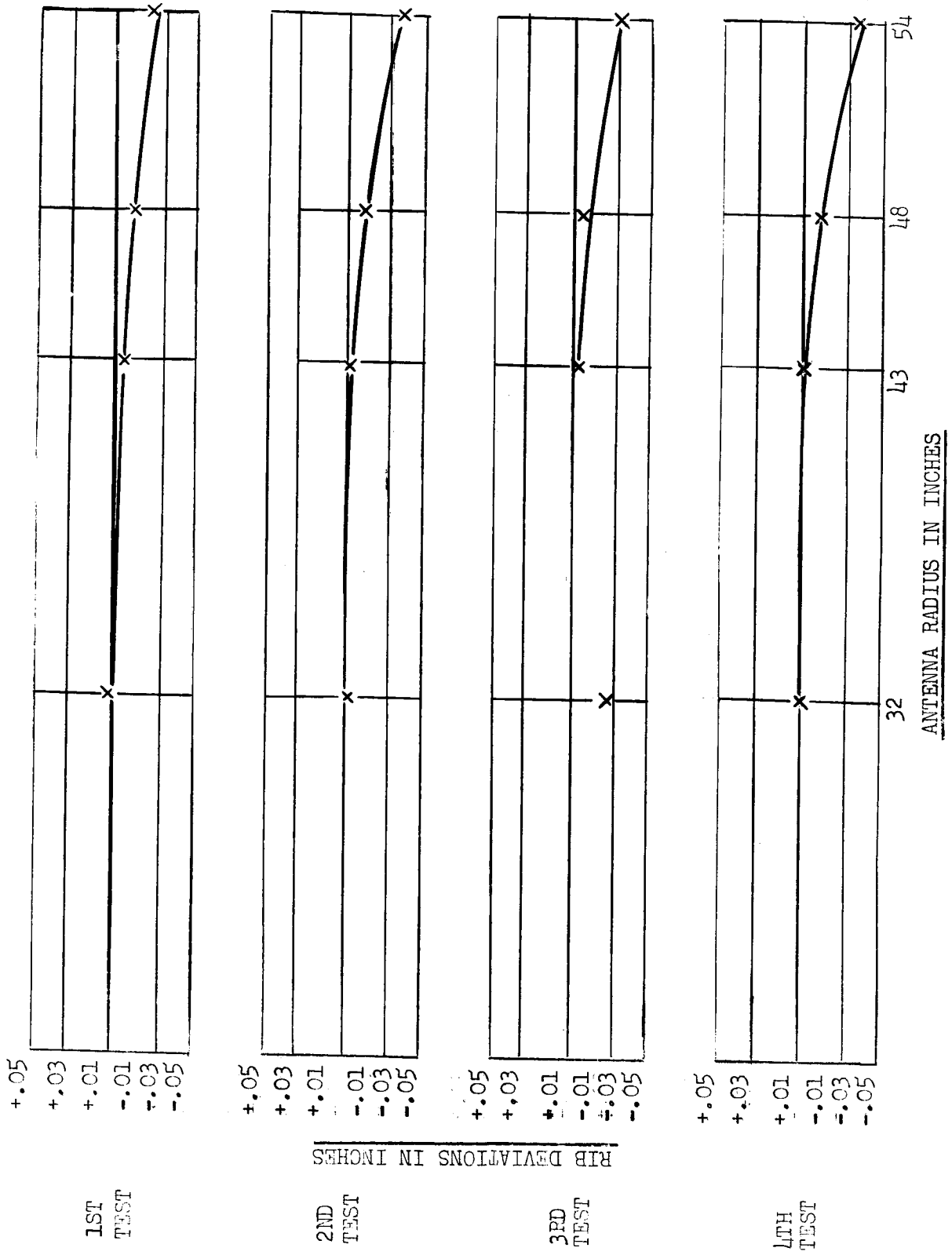

Figure 37. Rib Repeatability Test Data Graph

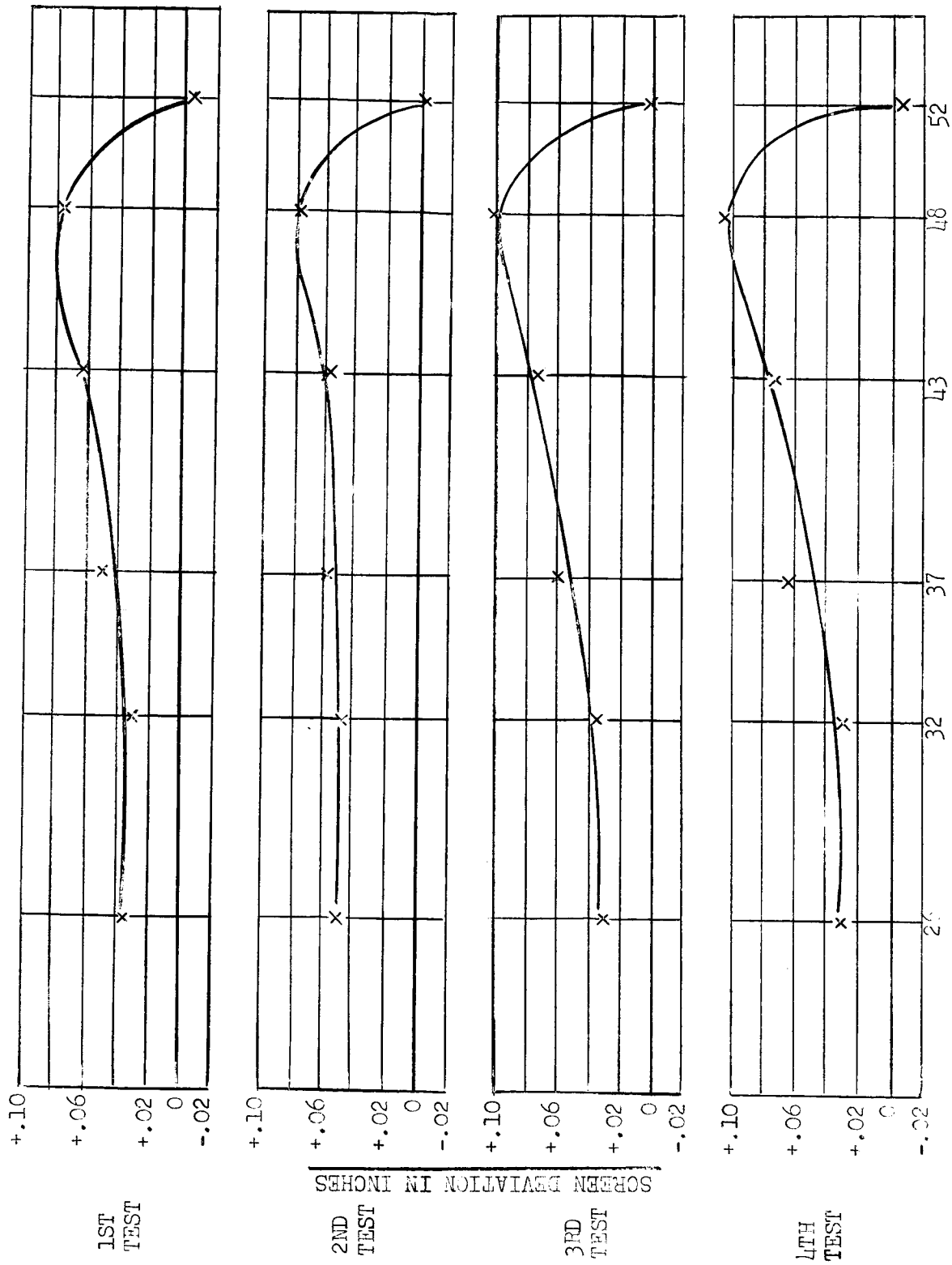

Figure 38. Screen Repeatability Test Data Graph

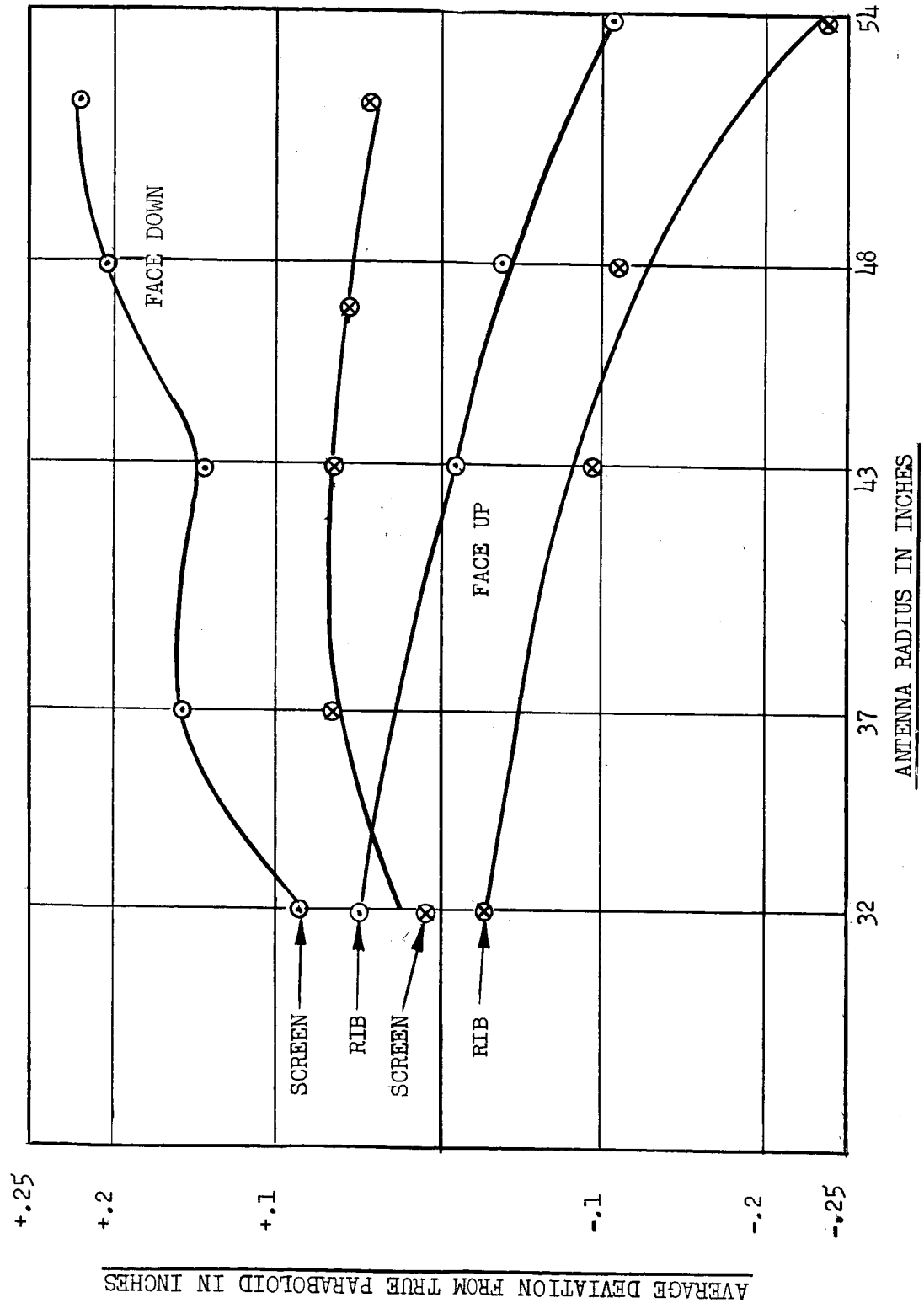

Figure 39. Graph Showing Average Values of Screen And Rib Deviations After 18 Deployments

D. CONTOUR MEASUREMENTS

The contour test was conducted with the antenna mounted face-up and face-down on the surface table. The measurements were made in the manner described in preceding paragraph B-2.

The antenna had been previously set at the established contour position, with the pull-down wire fixtures installed on the ribs. No contour adjustments were required as the antenna was subjected to the various physical repeatability tests, electronic tests, and vibration tests, or during the final assembly of the canister and supports or the removal of the pull-down wire fixtures. These operations required opening and closing of the antenna 18 times from the initial setting to the final contour measurements. The average value of final contour measurements with ± 1g loading are well within the required ± 0.25 inch tolerance, as shown in Figure 39.

There were some small localized areas which deviated beyond the ± 0.25 inch tolerance. These deviations have no significant effect on the overall antenna gain. It is also believed that they probably would not exist on an actual flight model which would be manufactured with more refined tooling and which would be tested less severely. The deviations for all measured points for the antenna face-up and face-down are listed in Tables XIII and XIV.

Table XIII. Face-up Deviations After 18 Deployments

Rib No.	Rib R=54"	Mid-Screen R=52"	Rib R=48"	Mid-Screen R=48"	Rib R=43"	Mid-Screen R=43"	Mid-Screen R=37"	Rib R=32"	Mid-Screen R=32"	Mid-Screen R=26"
1	-0.194		-0.045		-0.009			-		
		+0.061		+0.060		+0.141	+0.045		+0.006	-0.005
2	-0.233		-0.089		-0.044			+0.024		
		+0.119		+0.149		+0.056	+0.027		-0.029	-0.014
3	-0.273		-0.094		-0.068			-		
		+0.052		+0.087		+0.026	+0.041		-0.026	-0.032
4	-0.291		-0.141		-0.218			-0.121		
		+0.002		+0.045		+0.054	+0.056		-0.030	-0.149
5	-0.247		-0.104		-0.079			-		
		+0.021		+0.083		+0.048	+0.103		+0.048	-0.002
6	-0.239		-0.125		-0.079			-0.012		
		+0.072		+0.151		+0.046	+0.076		+0.035	-0.019
7	-0.200		-0.088		Boom			-		
		+0.024		+0.108		+0.029	+0.048		+0.021	+0.019
8	-0.232		-0.169		-0.148			-0.019		
		+0.012		+0.065		0.000	+0.053		-0.016	-0.029
9	-0.225		-0.086		-0.094			-		
		+0.049		+0.001		+0.053	+0.072		+0.025	+0.008
10	-0.244		-0.137		-0.107			-0.008		
		+0.029		+0.137		+0.049	+0.093		+0.033	+0.021
11	-0.236		-0.096		-0.091			-		
		+0.012		-0.273		+0.113	+0.078		-0.008	-0.003
12	-0.287		-0.141		-0.105			-0.035		
		+0.085		+0.044		+0.162	+0.125		-0.040	-0.064

Table XIV. Face-Down Deviations After 18 Deployments

Rib No.	Rib R=54"	Mid-Screen R=52"	Rib R=48"	Mid-Screen R=48"	Rib R=43"	Mid-Screen R=43"	Mid-Screen R=37"	Rib R=32"	Mid-Screen R=32"	Mid-Screen R=26"
1	-0.042		+0.040		+0.066			+0.100		
		+0.255		+0.207		+0.221	+0.136		+0.070	+0.081
2	-0.075		-0.012		-0.006			+0.053		
		+0.277		+0.249		+0.097	+0.088		+0.063	+0.032
3	-0.144		-0.056		-0.049			+0.044		
		+0.174		+0.166		+0.150	+0.094		+0.034	+0.002
4	-0.168		-0.150		-0.143			-0.059		
		+0.174		+0.151		+0.113	+0.157		+0.069	-0.103
5	-0.105		-0.012		-0.007			+0.087		
		+0.207		+0.242		+0.181	+0.207		+0.136	+0.068
6	-0.079		-0.021		+0.105			+0.075		
		+0.237		+0.261		+0.103	+0.164		+0.087	+0.027
7	-0.113		-0.061		-0.010			+0.028		
		+0.199		+0.236		+0.111	+0.142		+0.118	+0.123
8	-0.058		-0.008		-0.029			+0.078		
		+0.275		+0.227		+0.100	+0.165		+0.083	+0.002
9	-0.066		-0.000		-0.040			+0.015		
		+0.220		+0.093		+0.093	+0.153		+0.109	+0.045
10	-0.146		-0.089		-0.047			+0.041		
		+0.174		+0.203		+0.091	+0.187		+0.129	+0.089
11	-0.120		-0.051		-0.005			+0.034		
		+0.176		-		+0.164	+0.167		+0.092	+0.050
12	-0.164		-0.051		-0.015			+0.039		
		+0.291		+0.178		+0.230	+0.232		+0.015	-0.001

E. RF TESTING AND EVALUATION

1. General

The RF testing portion of the program consisted of the following items:

(a) Primary feed evaluation

(b) Antenna pattern and gain measurements

(c) Antenna pattern and gain repeatability measurements after deployment

(d) Antenna pattern and gain measurements with antenna packaged and canister installed

(e) Antenna pattern and gain measurements with antenna packaged and canister installed, but with canister wires removed

(f) Antenna pattern and gain measurements with antenna packaged and canister not installed

The RF evaluation portion on the program consisted of relating the physical contour measurements to antenna gain, and comparing the calculated results with the test results.

The subsequent paragraphs describe the test methods and the test results obtained.

2. Primary Feed Evaluation

The feed was evaluated in the anechoic chamber for electrical performance characteristics. The VSWR of the feed from 2200 MHz through 2390 MHz was

measured and the results are shown in Figure 40. A rotating, linearly polarized transmitting antenna was used as the signal source for primary patterns. This allowed the axial ratio of the feed to be evaluated directly from the patterns. Patterns were taken for several angular orientations of the test feed and an axial ratio of 5 db was obtained. Since optimization of the feed was not part of the program, it was decided to withhold any action on feed modification to improve the axial ratio until after the range tests of the complete antenna. The equipment used in evaluating the primary test feed is shown in Figure 41.

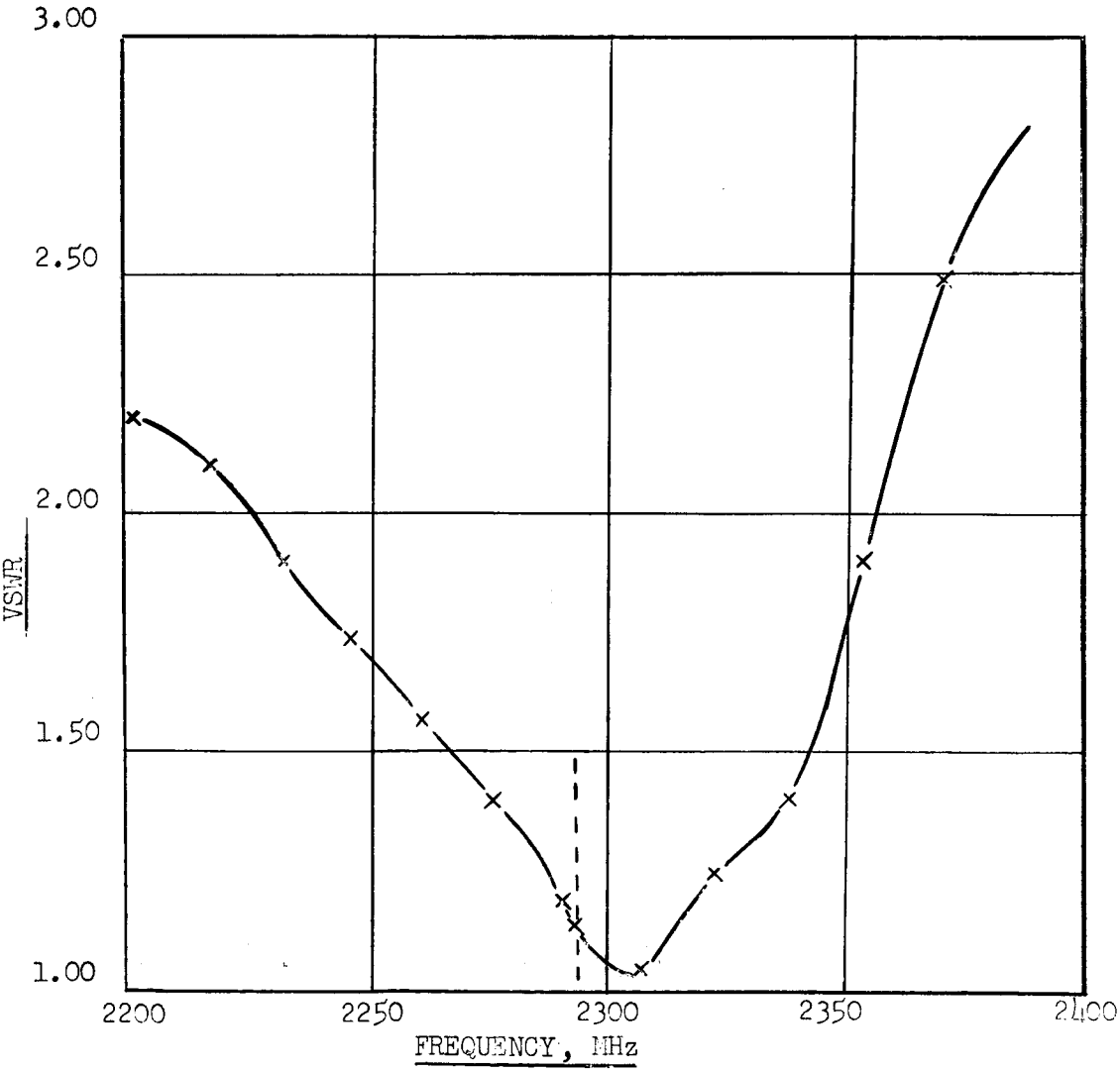

Figure 40. Feed VSWR Measurements

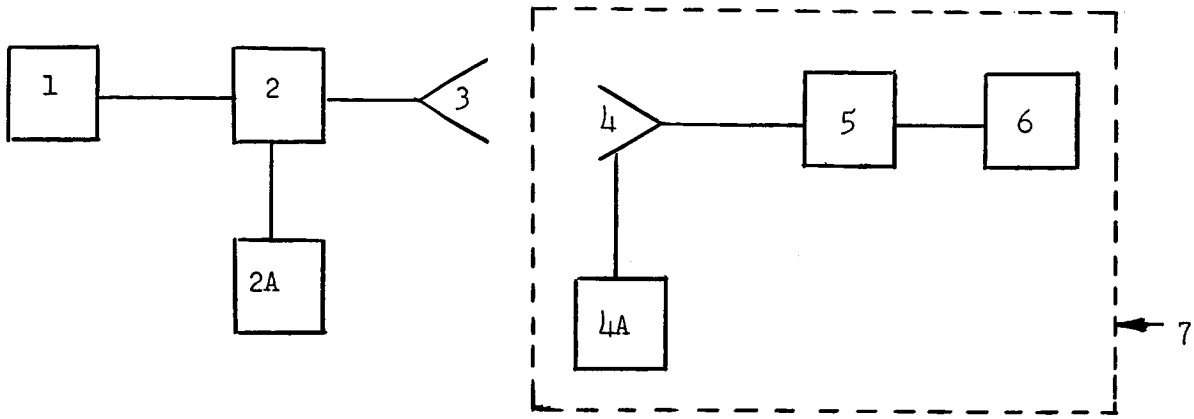

PRIMARY FEED PATTERN TEST INSTRUMENTATION

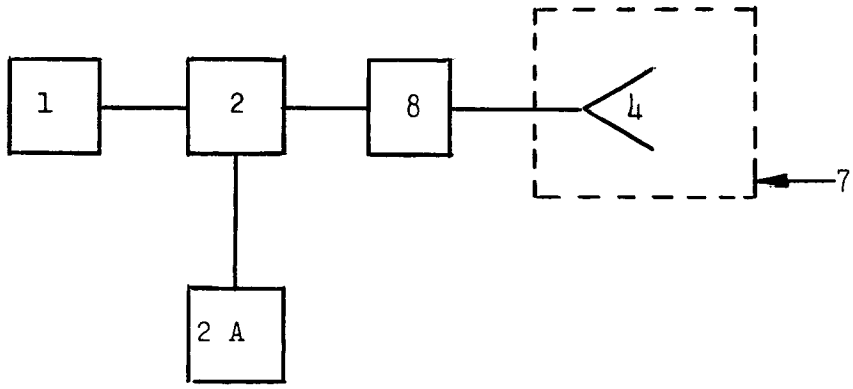

VSWR TEST INSTRUMENTATION

1. HP 616 A SIGNAL GENERATOR
2. TYPE N TEE
2A. SPERRY MICROLINE 124C FREQUENCY METER
3. ROTATING TRANSMIT ANTENNA
4. FEED UNDERGOING EVALUATION
4A. ROTATOR (GAC ITEM)
5. HP 420 DETECTOR
6. ANTLAB PATTERN RECORDER
7. ANECHOIC CHAMBER
8. HP SLOTTED SECTION AND PROBE.

Figure 41. Anechoic Chamber Instrumentation

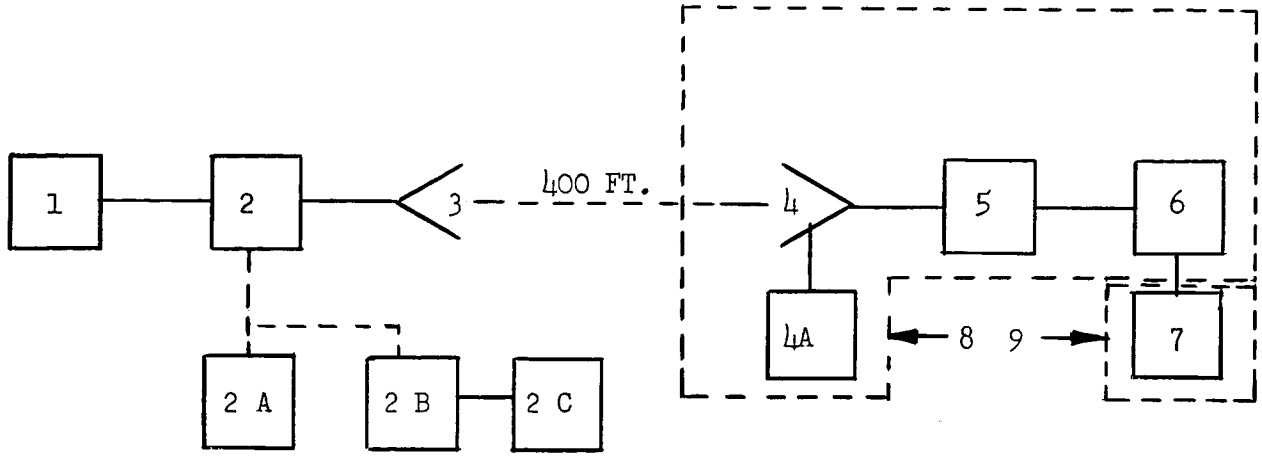

1. A&L 124C OSCILLATOR
2. COAX DIRECTIONAL COUPLER
2A. SPERRY MICROLINE 124C FREQUENCY METER
2B. HP 420 DETECTOR
2C. HP 415 B VSWR METER
3. TRANSMIT ANTENNA
4. ANTENNA UNDER EVALUATION
4A. ANTLAB ANTENNA POSITIONER
5. MICROLAB AT-46N CALIBRATED ANTTENUATOR
6. HP 420 DETECTOR
7. ANTLAB PATTERN RECORDER
8. WEATHER ENCLOSURE
9. REMOTE RECORDING AND CONTROL STATION

Figure 42. Transmit-Receive Antenna Range Instrumentation

Figure 43. Antenna Test Enclosure

3. Antenna Test Procedure

a. Range and Instrumentation. The antenna test range was 400 feet long, with the transmit and receive stations located approximately 40 feet above ground level. The space antenna was installed at the receive station. The receive station was enclosed by a shield which was transparent to RF energy, to protect the space antenna from inclement weather.

The transmit station was operated to produce horizontally-polarized 2295 MHz signals used to test the receiving capabilities of the space antenna.

Instrumentation for the transmit and receive stations is shown in Figure 42. Figure 43 is a photograph showing the receive station with the deployed space antenna installed for testing.

b. Procedure. The space antenna was tested in the following manner:

(1) A field probe was performed for two orthogonal polarizations of the transmit antenna. Results indicated both polarizations had a maximum variation of 1.2 db over the desired area.

(2) The space antenna was mounted on the rotator and deployed. The feed was focused and the axial circularity ratio was measured. Since the axial ratio was approximately 2 db, it was decided to continue the tests without modifying the feed. Modifying the feed to improve circularity would not be worth the resulting schedule delay and the additional effort required

to completely retest the primary feed.

(3) Patterns and gain for both maximum (0 Feed Position), and minimum (0 + 90 degree feed position) received-signal polarization positions of the feed were taken. This was considered the first deployment.

(4) The space antenna was re-packaged.

(5) Principal plane patterns and gain were taken.

(6) The wire supports on the canister feed cover were removed and procedure (5) repeated.

(7) The canister and wires were removed, and (with the antenna still in non-deployed condition), the procedure in preceding step (5) was repeated.

(8) The antenna was fully deployed for the second time and the procedure in preceding step (3) was repeated.

(9) The antenna was restored to the packaged configuration. No tests were performed.

(10) The antenna was fully deployed for the third time and the procedure in preceding step (3) was repeated.

4. Test Results

The summary of results for the RF test on the feed are listed in Table XV; and for the antenna in Table XVI. The patterns associated with these test results are given in Appendix B of this report.

Table XV. Primary Feed RF Test Results

Test	Results
VSWR From 2200 MHz through 2390 MHz (See Figure 40)	1.05 Minimum to 2.8 Maximum
VSWR at 2295 MHz (See Figure 40)	1.16
Axial Ratio	5 db

Table XVI. Antenna RF Test Results

Antenna Test Condition	Average Gain In db	Axial Ratio In db	Pattern Shown In Appendix B Figure No.
First Deployment	33.05	1.9	B-1, B-2, B-3 and B-4
Second Deployment	32.25	1.9	B-11, B-12, B-13 and B-14
Third Deployment	32.30	2.0	B-15, B-16, B-17 and B-18
Packaged, With Canister	6.2		B-5 and B-6
Packaged With Canister, But With Wires Removed	7.2		B-7 and B-8
Packaged, Without Canister	7.2		B-9 and B-10
NOTE: Test Frequency Was 2295 MHz			

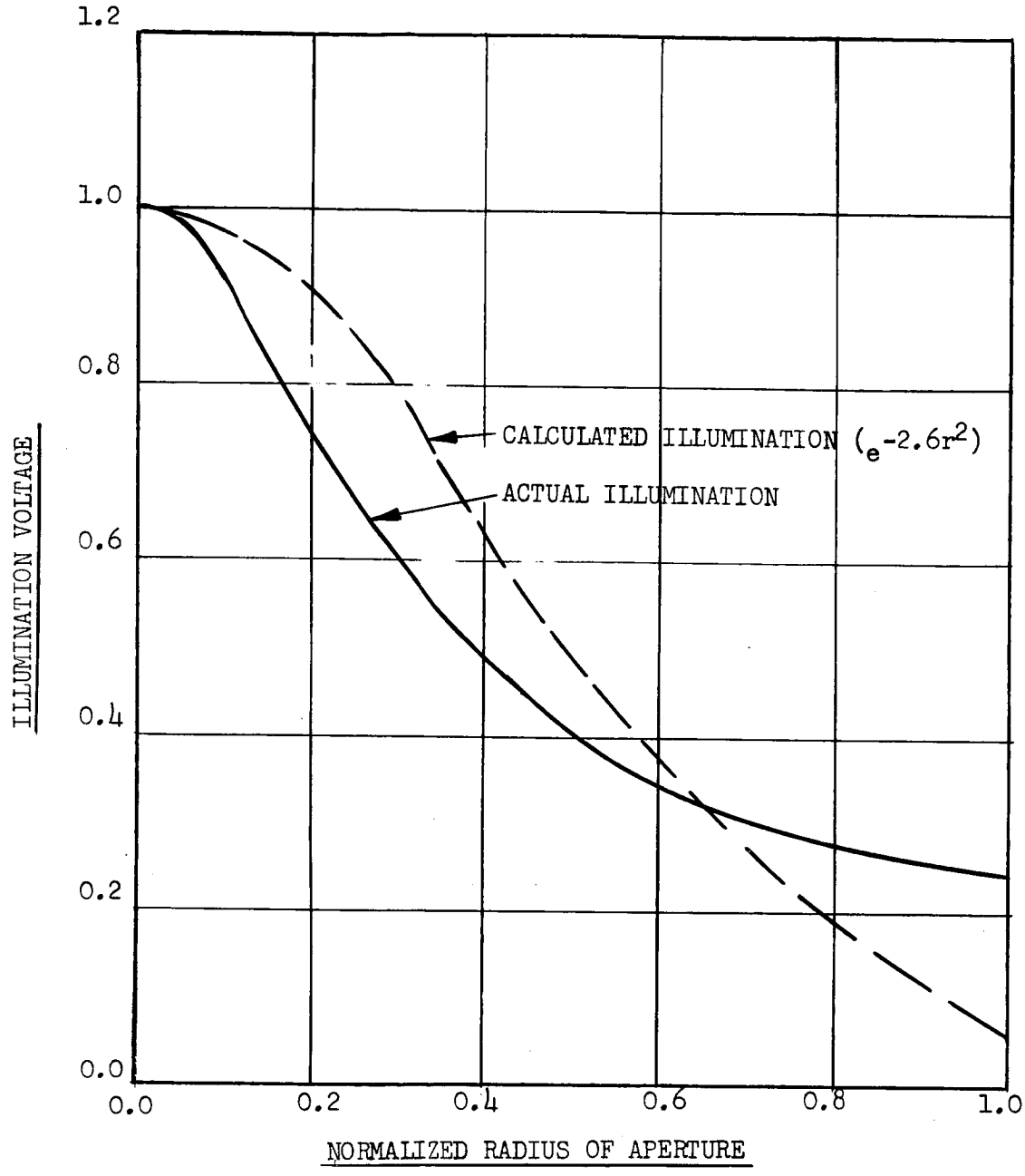

Figure 44. Average Pattern of Dipole-Disk Feed With Path Taper Compared To $e^{-2.6\ r^2}$

5. Test Results Evaluation

a. General. The evaluation of the test results consists of two parts: (1) calculating the expected gain reduction caused by the physical and RF characteristics of the reflector and feed; and (2) relating the expected gain reduction to the actual range test results.

b. Calculating the Losses Due To Imperfect Reflector Area. The antenna periphery is established by 12 equally-spaced rib tips, with taut screen forming a catinery line between rib tips. This periphery deviates from a truly circular periphery and causes a loss of about 9 percent in total projected area at the aperture of the antenna. Using the actual illumination function (shown in Figure 44) for the circularly-polarized dipole-disk feed, the total gain reduction due to lost area (as compared to an ideal circular paraboloidal surface) is 0.32 db.

c. Calculating the Losses Due To Contour Deviations. Certain contour errors exist in the surface of the antenna because the surface deviates from a paraboloidal form. These deviations errors are due to the use of bays, and to random errors inherent in manufacturing techniques and processes.

Measured deviations at particular points on the bay sections were averaged to determine the general curved surface the bays tend to follow. R.M.S. values of deviations about these mean values were determined. The gain reduction,

G/G_T, was calculated for the contour deviations in the hub and bay areas as follows:

$$\frac{G}{G_T} = \left[\text{Hub loss}\right] + \left[\text{Bay loss}\right] \qquad (1)$$

$$\frac{G}{G_T} = \left[\frac{a^2}{\eta}\left(e^{-\bar{\delta}_R^2} - 1\right)\right] + \left[e^{-\delta_R^2} K\right]$$

where:

$\frac{G}{G_T}$ = gain reduction

a = normalized radius of hub section

η = aperture efficiency

$\bar{\delta}^2$ = mean squared phase error in the center hub section

δ_R^2 = mean squared phase error in the bay sections

K = gain reduction due to use of bay sections in lieu of paraboloidal sections

Using the normalized radius of the hub section, the actual aperture efficiency of 56%, and r.m.s. errors of 0.020 inches for the hub of the antenna,

$$\frac{a^2}{\eta}\left(e^{-\bar{\delta}^2} - 1\right) < 0.001$$

which would correspond to a gain reduction of less than 0.01 db due to errors in the center hub.

For the construction and illumination used, K corresponded to a 0.37 db loss.

This loss was calculated using mean phase errors weighted by the feed taper. K also includes the effect of the lost area which by itself accounts for 0.32 db loss.

The r.m.s. surface error over the bay sections of antenna is 0.031 inches. Thus in the expression for loss in the bay sections,

$$\frac{G}{G_T} = e^{-\delta_R^2} K$$

$e^{-\delta_R^2}$ accounts for an additional 0.03 db for a total loss of 0.40 db due to construction and contour deviations. Since this includes the reduction due to lost area, the only loss attributed to contour deviations is

0.40	db total construction loss
-0.32	missing area loss
0.08	db contour loss

d. Calculating The Losses Due To A Lossy Reflector. Samples of the wire mesh used for the reflecting surface of the antenna were subjected to waveguide tests, to obtain an indication of the power reflected from this material. As shown in paragraph E of Section II, approximately 94% of the incident power was reflected from this material in free space at 2.295 gcs. This 94% reflected power represents a 0.27 db gain loss for the antenna.

e. Calculating Other Losses. In addition to the losses due to an imperfect reflector, other losses common to all paraboloidal antennas are also inherent in this antenna. These losses were calculated using the average feed pattern (Figure 44) and the physical properties of the antenna. The losses are itemized in the following list:

(1)	Loss due to illumination taper and spillover	- 2.52 db
(2)	Cross polarization loss	- 0.12 db
(3)	Feed blockage loss	- 0.01 db
(4)	Transmission line loss	- 0.12 db
	Total other losses	- 2.77 db

f. Calculating The Antenna Gain. The gain of the antenna with respect to circular-polarized isotrope was calculated as follows:

(1)	ANTENNA GAIN FOR UNIFORM ILLUMINATION	36.38 db
(2)	LESS:	
	(a) Other losses	- 2.77 db
	(b) Area loss	- 0.32 db
	(c) Contour loss	- 0.08 db
	(d) Lossy reflector	- 0.27 db
(3)	EQUALS CALCULATED GAIN	32.94 db

g. Summary. The calculated gain of 32.94 db and the average measured gain for three deployments of 32.6 compare favorably. It is therefore assumed

that the calculated losses for area, contour and lossy reflector are reasonably accurate. Since these losses are small, further optimization of these factors does not appear practicable.

F. VIBRATION SURVEY

1. Discussion

The antenna was subjected to a frequency sweep from 10-1500 cps with a 0.3 g input in both the packaged and the deployed configuration. Three axes of vibration were chosen: axis 1 is parallel to the axis of the boom; axis 3 is parallel to the axis of the feed; and axis 2 is orthogonal to axes 1 and 3.

The tests were performed on a model MB C-25 vibration shaker utilizing a slippery table.

The pickups used are the small (2.75 gram) Endevco model 2226 crystal accelerometers with their associated amplifiers (Endevco model 2713 and/or 2702). The recording oscillographs were Honeywell Visicorders.

An additional vibration test was performed, to determine the natural frequencies of one tapered tube. The end fixity for the tube is stiffer in one direction than it is in an orthogonal direction. This is due to the fact that the triangular tube-mounting plates are soft when loaded along an axis perpendicular to the plate. For this reason, the single tube has two cantilever natural frequencies when the loads are applied in axes perpendicular to each other.

Tests showed that the lowest natural frequency was 11 cps and the highest was 32 cps. When the tube is mounted on the antenna structure, the frequency drops to 10.5 cps because the support is softer than that used for the single-tube test.

In the deployed configuration, the single tubes vibrate in an aimless pattern having no constant phase relationship.

The original antenna design utilized single tubes of constant cross-section. These tubes had a natural frequency of 13 cps rather than the 32 cps measured in the re-designed antenna.

In general, the re-designed antenna is noticeably superior to the original design. The measured natural frequencies and mode-shape determined on the re-designed antenna are given in Table XVII.

2. Vibration Test Summary

Results of the engineering vibration test phase can be summarized as follows:

(a) During launch, some method of stabilizing the top of the boom structure attached to the spacecraft would considerably reduce dynamic response.

(b) Light pressure on the periphery of the packaged antenna is desirable, but not as imperative as stabilizing the boom.

Table XVII. Vibration Test Results

Condition	Axis	Position	Natural Frequency In CPS	Mode Shape
Packaged	1	Truss	16.5	Truss bending
	1	Tube	31.5	Single tube bending with stiff end restraint
Deployed	1	Truss	55	Truss higher bending mode
	1	Tube	23	
	1	Tube	31	Tube bending
	1	Tube	87	2nd bending of single tube
Packaged	2	Truss	13	Truss bending
	2	Truss	112	Higher mode of truss bending
	2	Tube	34	Single tube in bending about its stiff end restraint
Deployed	2	Truss	4.6	Truss bending
	2	Tube	13.5	Single tube bending about soft end fixity
	2	Tube	31	Single tube bending about stiff end fixity
Packaged	3	Truss	15	Truss bending - torsion mode
	3	Truss	47	2nd mode of truss in pitch - torsion
	3	Tube	27	Single tube bending about stiff axis
Deployed	3	Truss	5.5	Cantilever bending
	3	Truss	25	Complete antenna screen pitching
	3	Truss	105	Truss response
	3	Tube	10.5	Single tube bending about soft axis
	3	Tube	32	Single tube bending about stiff axis
	3	Tube	45	Single tube responding

NOTE: Modes were identified by means of pickups and/or strobe light.

SECTION V

CONCLUSIONS AND RECOMMENDATIONS

The Hi-Gain Spacecraft Antenna Development Program proved the feasibility and practicability of using large deployable antennas for planetary mission spacecraft. The following concepts were proven, either during the initial program or during the follow-on study and modification program:

(1) The deployment concept was suitable for either 1 g or 0 g.

(2) Contour accuracy tolerances of $\pm$ 0.25 inches can be maintained with $\pm$ 1 g loading.

(3) Thermal deflections of less than $\pm$ 0.05 inches can be maintained in space.

(4) Contour accuracy is maintained, even after multiple deployments.

(5) Actual per-unit aperture weight of 0.35 psf was attained for a deployable antenna and feed, and a per-unit weight of 0.30 psf was considered possible for future antennas.

(6) R.F. reflectivity of at least 94 percent was attained with a light weight orthotropic screen material.

(7) Gain of at least 32.6 db was attained for a 9 foot diameter deployable antenna at 2295 MHz.

(8) Natural vibration frequencies are in excess of 13 cps in the packaged condition and 4.6 cps in the deployed condition.

(9) Deployed-to-packaged size ratio of 2.4 was attained.

The antenna concept investigated on this program has been proven through full-scale model testing and analysis. Sufficient data has been generated to extrapolate to various size antenna with high confidence of success. Thus, except for constraints associated with a specific space program, the antenna is ready for a space communication application.

TABLE XVIII LIST OF REFERENCES

Ref. No.	Title
1	Timeshenko, Strength Of Materials, Part II, Second Edition, D. Van Nostrand Co., Inc.
2	Holm, Ragnar, Electrical Contacts Handbook, Springer-Verlag, Berlin Gottingen-Heidelberg, Chapter 23, 1947.
3	Frant, Martin S., Copper Oxides on the Surface of Gold Plate, December 1961.
4	Schreiber, O. P., Reliable Electrical Contact Theory Applied to RFI Control, paper presented at Fourth National Symposium on RFI, San Francisco, California, June 28-29, 1962.
5	Britton, S. C., and Clarke, M., Effects of Diffusion From Brass Substrates into Electrodeposited Tin Coatings on Corrosion Resistance and Whisker Growth, Tin Research Institute Publication, No. 341, reprinted 1963.

APPENDIX A

REFLECTANCE TEST SETUP AND CALCULATION PROCEDURE

A. TEST SETUP AND MEASUREMENT

A block diagram of the test equipment setup is shown in Figure A-1. Figure A-2 is a picture of the test equipment and several different material samples.

A signal generator operating at 2295 MHz provides the primary energy for the system. A slotted line and probe are used to determine the voltage standing wave ratio (VSWR) and position of a voltage minimum. Energy from the probe is coupled to one input of the coaxial mixer via a tuner. The other input terminal of the mixer is connected to a local oscillator operating at a

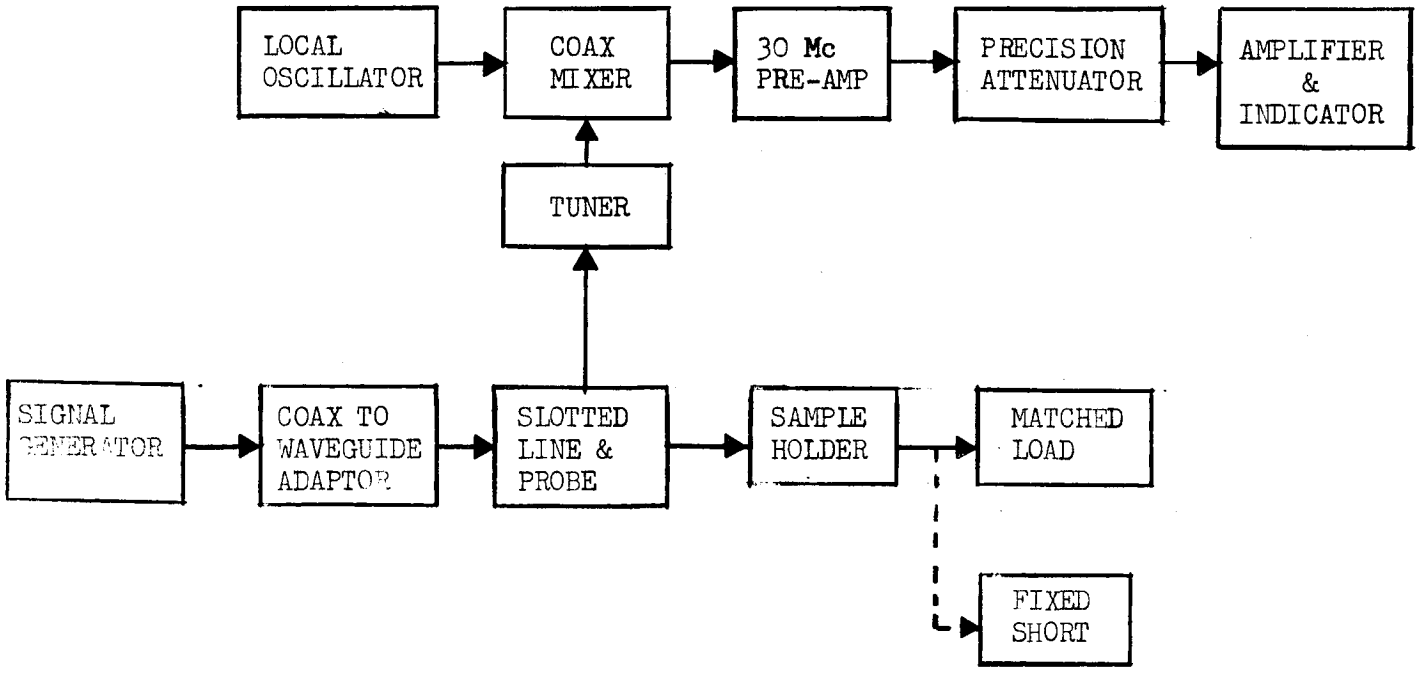

Figure A-1. Block Diagram of Test Equipment Setup

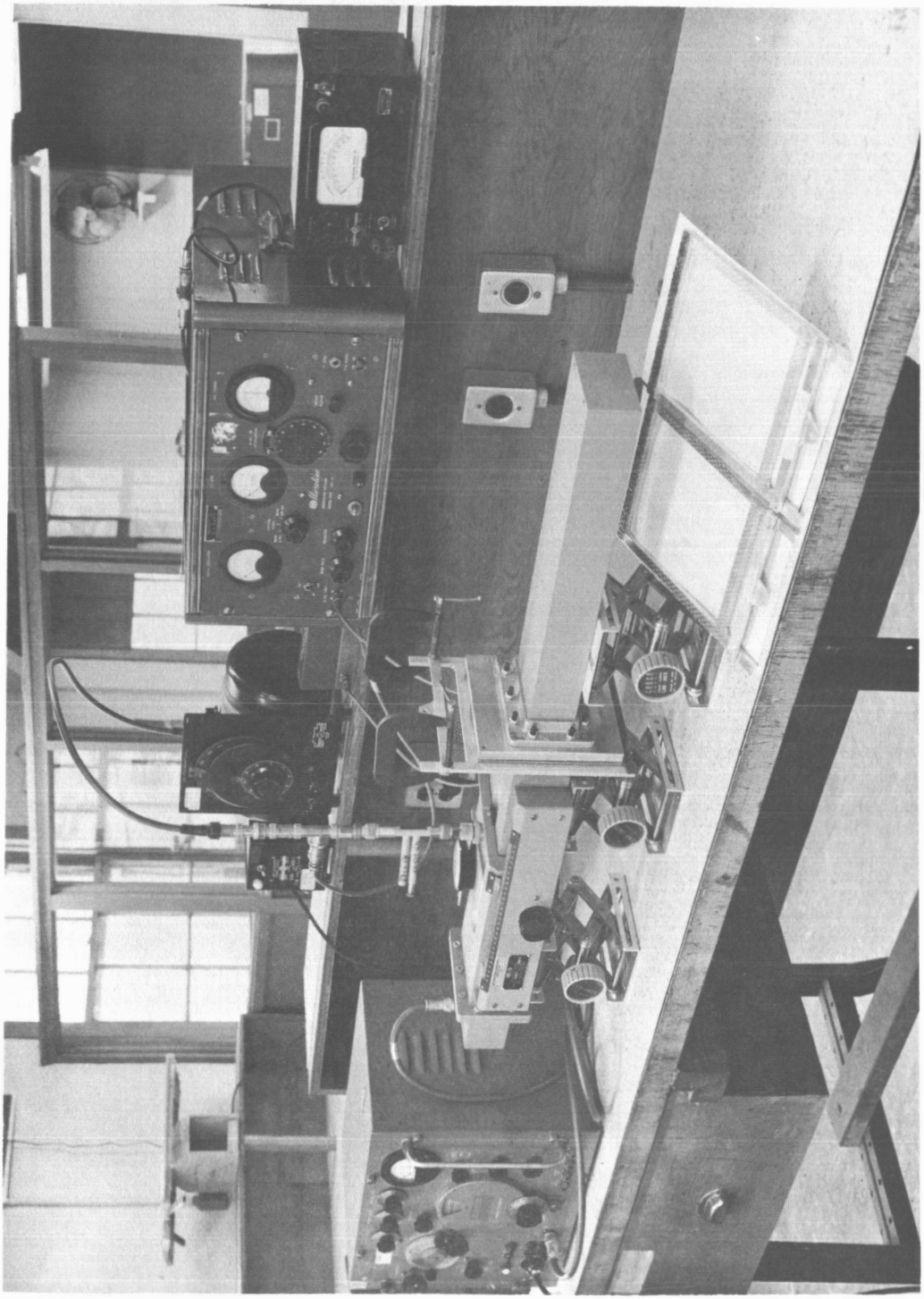

Figure A-2. Screen Test Sample Positioned Between Special Waveguide Flanges

frequency of 2295 MHz (± 30 MHz). The 30 MHz difference signal from the mixer is fed to a preamp. The output of the preamp is coupled to an amplifier and indicator, via a 30 MHz precision attenuator. The sample screen material is mounted on a special bracket that allows the application of an adjustable tension to the material, as shown in Figure A-2. After the sample is properly tensioned, it is clamped in place between two special waveguide flanges.

There are several methods that may be used to evaluate the reflection characteristics of screen material. For this study, the system was terminated in a matched load. Initial VSWR and position of voltage minimum conditions were determined by removing the matched load and placing a fixed short at the test sample location. The initial VSWR measurement insures that waveguide wall losses are not excessive. This reading may also be used to correct the readings taken with the sample in place. However, since the wall losses appeared to be low, this correction factor was not applied at this time. The reported test results are therefore slightly pessimistic. The initial position of voltage minimum reading with a fixed shorting plate is necessary in determining free space reflection coefficients.

The cells of the screen material are rectangular in shape when tensioned. The long dimension of the rectangles tend to form continuous parallel lines. The short dimension of the rectangles tend to form discontinuous parallel lines. Because of this non-symmetry in the cell structure, the tests were conducted

with the long dimension of the rectangle oriented in two different positions: (1) parallel to the electric field vector in the waveguide; and (2) perpendicular to the electric field vector in the waveguide.

B. FREE SPACE REFLECTANCE CALCULATIONS

The free space reflection characteristics of thin films and wire grid material may be determined from waveguide measurements if the material can be represented by a characteristic admittance shunting an equivalent transmission line as shown in Figure A-3.

One test method is to measure the voltage standing wave ratio (VSWR) and the shift of voltage minimum in a slotted line when the test sample is terminated in a matched load. The amplitude of the reflection coefficient $\overline{\Gamma}_w$ as measured in a waveguide is given by

$$\left|\overline{\Gamma}_w\right| = \frac{(\text{antilog}_{10}\ \text{VSWR}) - 1}{(\text{antilog}_{10}\ \text{VSWR}) + 1} \qquad (1)$$

where the VSWR is measured in decibals (db).

The phase angle, θ, of the complex reflection coefficient, $\overline{\Gamma}_w$ is given by

$$\theta = \frac{720}{g}\ D_2 - D_1 - \frac{g}{4} \qquad (2)$$

where: λ_g is the waveguide wavelength; D_2 is the position of a voltage

minimum with the test sample terminated by a matched load; and D_1 is the position of a voltage minimum when the test sample is replaced by a shorting plate.

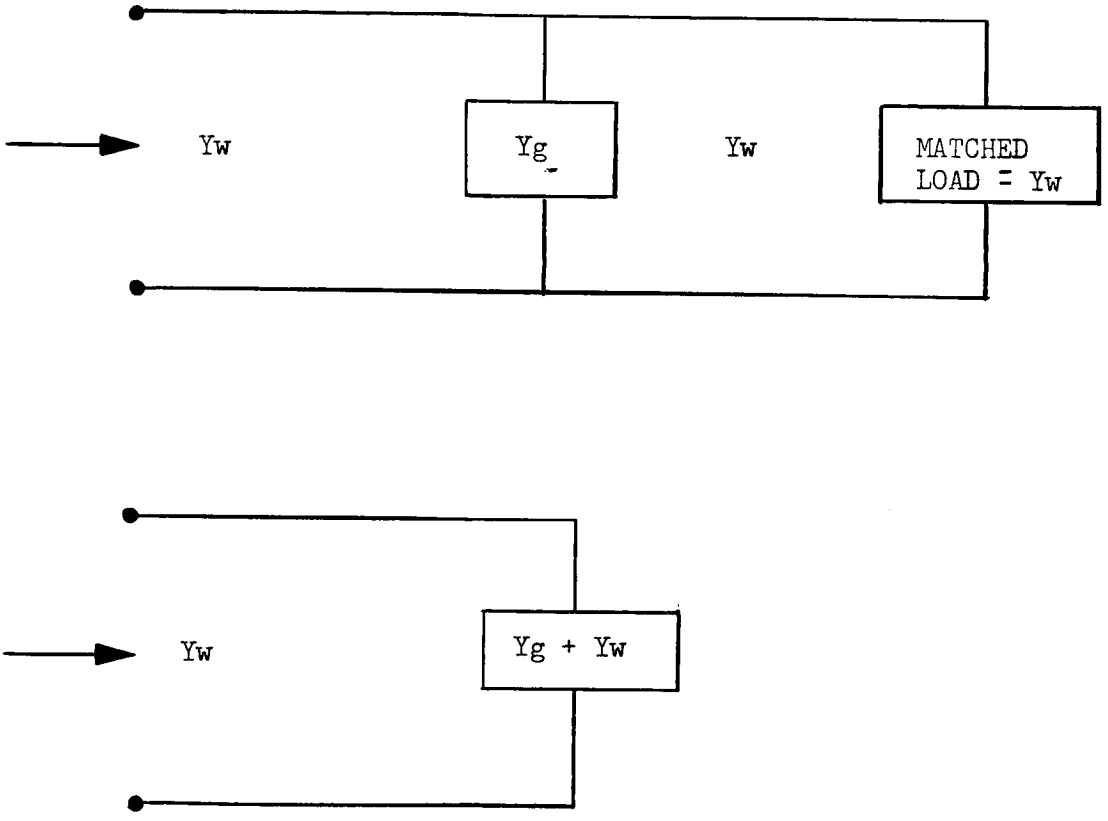

Figure A-3. Transmission Line Analogy, And Equivalent Circuit

The reflection coefficient measured in a waveguide is related to the characteristic admittance of the waveguide and the test sample by:

$$\overline{\Gamma}_w = \frac{Y_w - Y_L}{Y_w + Y_L} \tag{3}$$

$$Y_L = Y_w + Y_g \tag{4}$$

where Y_w is the characteristic admittance of the waveguide, and Y_g is the characteristic shunt admittance of the wire grid material. Equation (3) may then be rewritten as:

$$\overline{\Gamma}_w = \frac{-Y_g/Y_w}{2 + Y_g/Y_w} \tag{5}$$

and

$$\frac{Y_g}{Y_w} \quad \frac{-2\,\overline{\Gamma}_w}{1 + \overline{\Gamma}_w} \tag{6}$$

For tests conducted in waveguide using a TE mode, the shunt admittance of the grid material may be normalized to free space by:

$$\frac{Y_g}{Y_o} = \frac{Y_g}{Y_w} \cdot \frac{Y_w}{Y_o} = \frac{Y_g}{Y_w} \cdot \frac{\lambda_o}{\lambda_g} \tag{7}$$

where Y_o is the characteristic admittance of free space, and λ_o is the

free space wavelength. The reflection coefficient, $\overline{\Gamma}_o$, of the grid material in free space at normal incidence is then given by

$$\overline{\Gamma}_o = \frac{-Y_g/Y_o}{2 + Y_g/Y_o} \tag{8}$$

The power reflection coefficient in free space is $\left|\overline{\Gamma}_o^{\,2}\right|$.

APPENDIX B

RF TEST PATTERNS

(Figures B-1 through B-18)

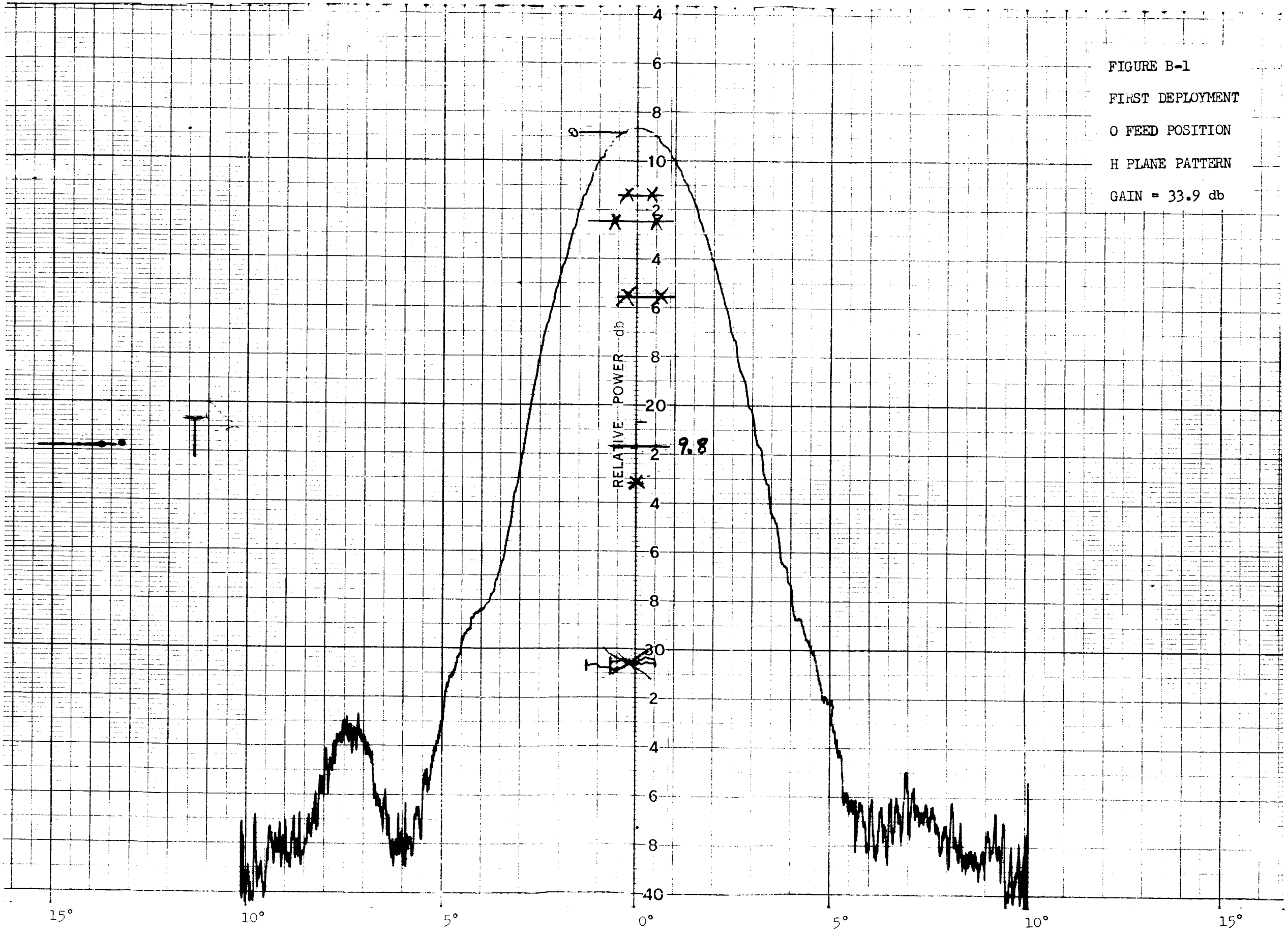

FIGURE B-1

FIRST DEPLOYMENT

0 FEED POSITION

H PLANE PATTERN

GAIN = 33.9 db

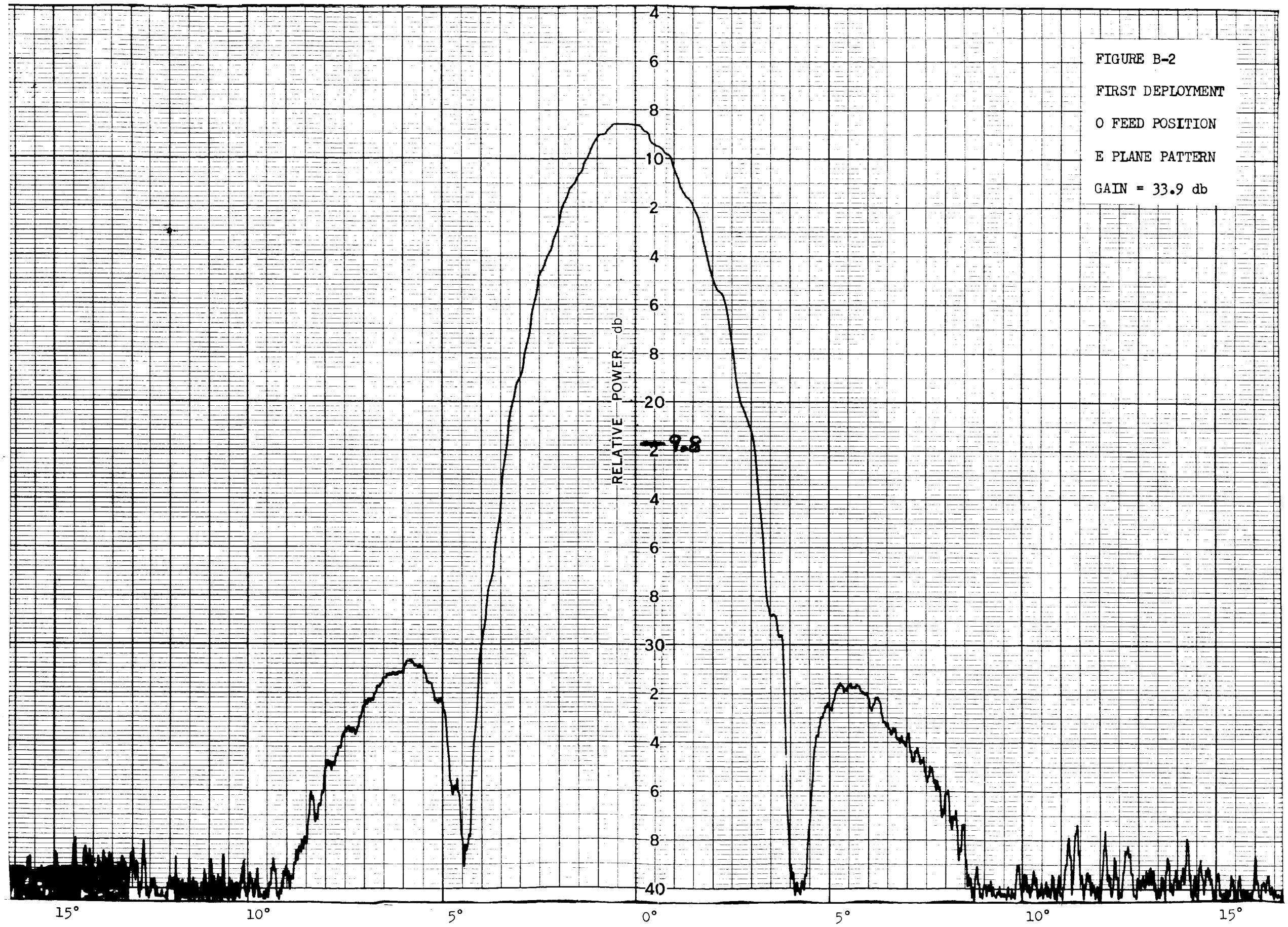

FIGURE B-2

FIRST DEPLOYMENT

O FEED POSITION

E PLANE PATTERN

GAIN = 33.9 db

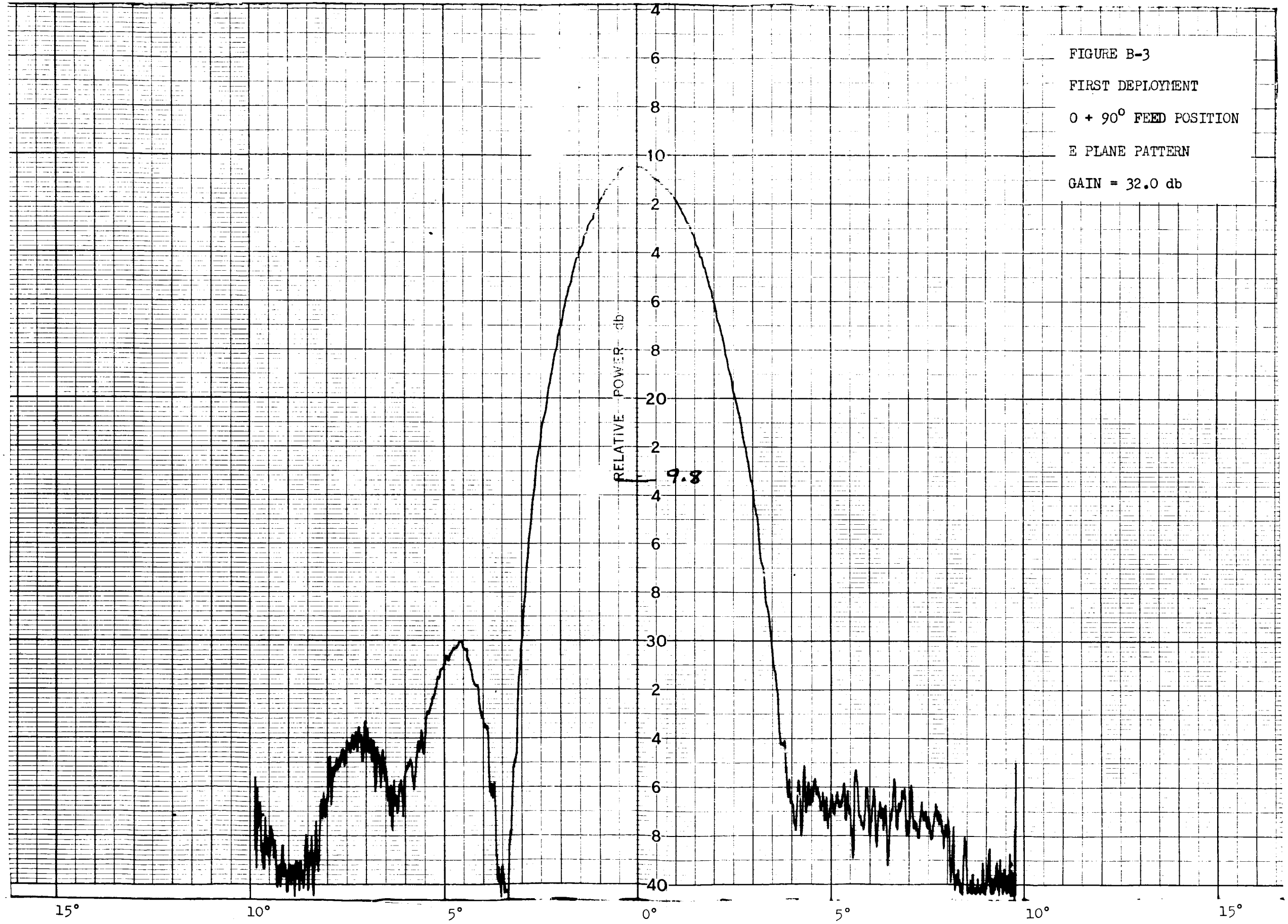
FIGURE B-3
FIRST DEPLOYMENT
0 + 90° FEED POSITION
E PLANE PATTERN
GAIN = 32.0 db
RELATIVE POWER db
9.8
4
6
8
10
2
4
6
8
20
2
4
6
8
30
2
4
6
8
40
15°
10°
5°
0°
5°
10°
15°

FIGURE B-4

FIRST DEPLOYMENT

0 + 90° FEED POSITION

E PLANE PATTERN

GAIN = 32.0 db

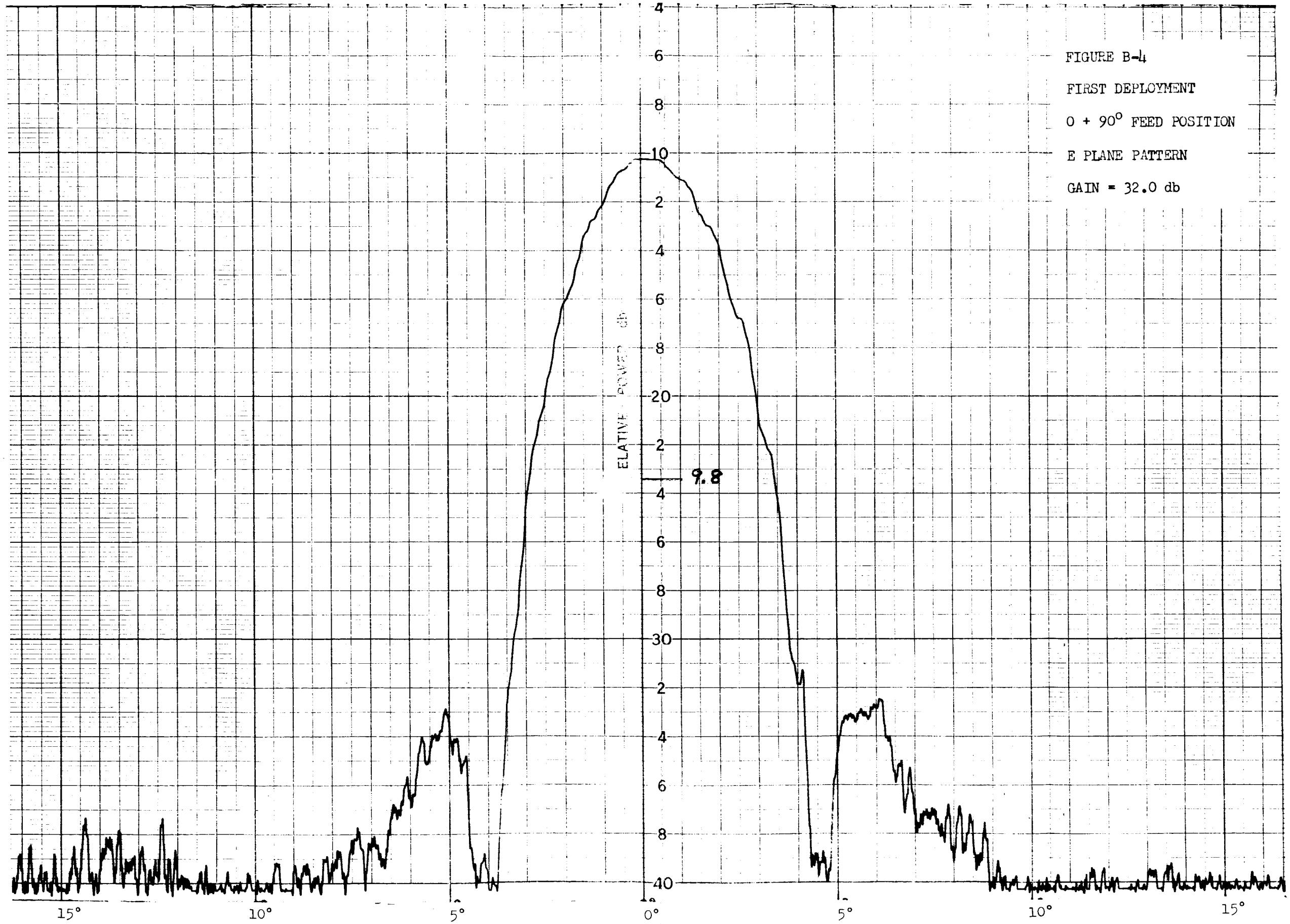

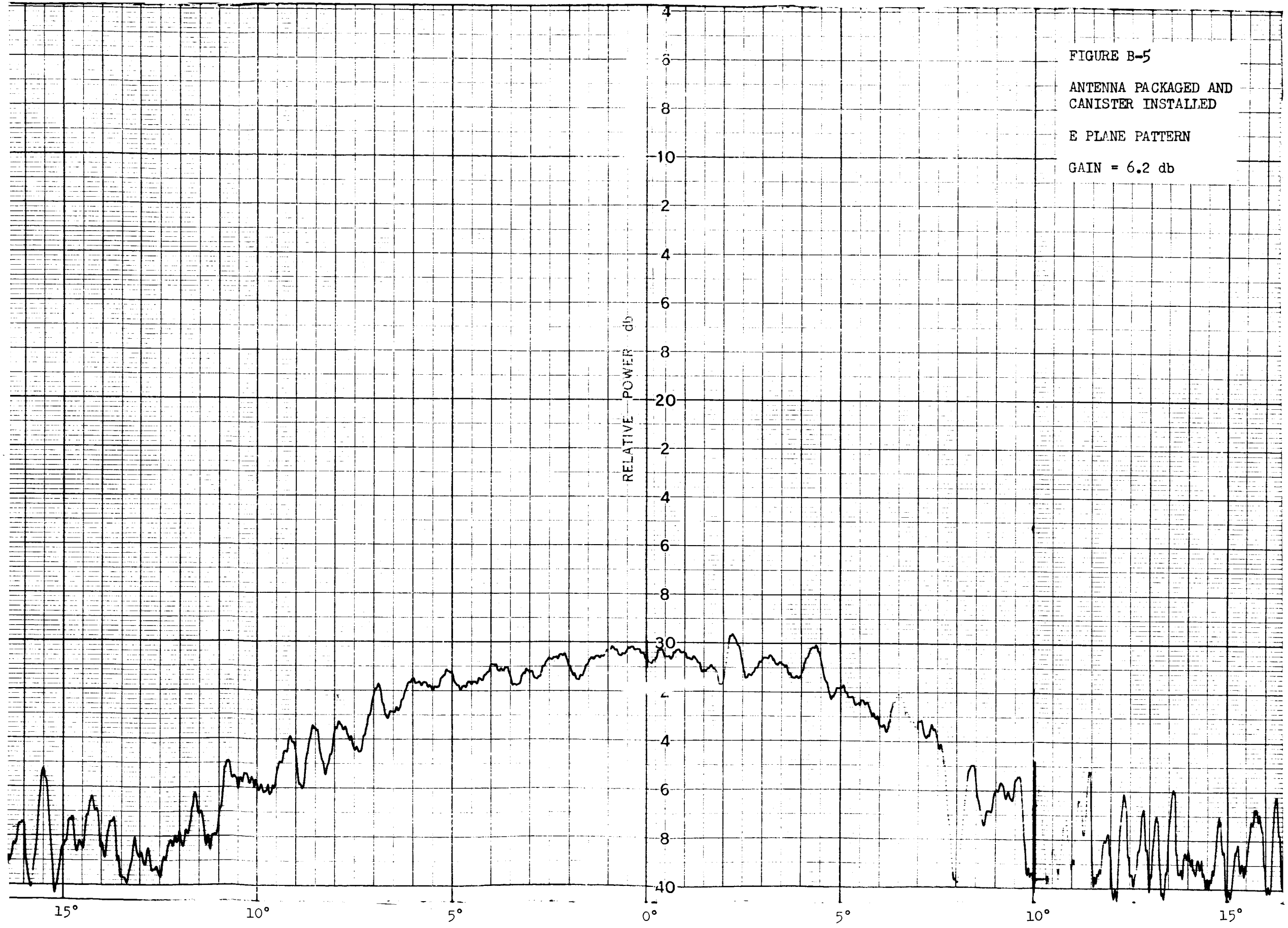

FIGURE B-5

ANTENNA PACKAGED AND CANISTER INSTALLED

E PLANE PATTERN

GAIN = 6.2 db

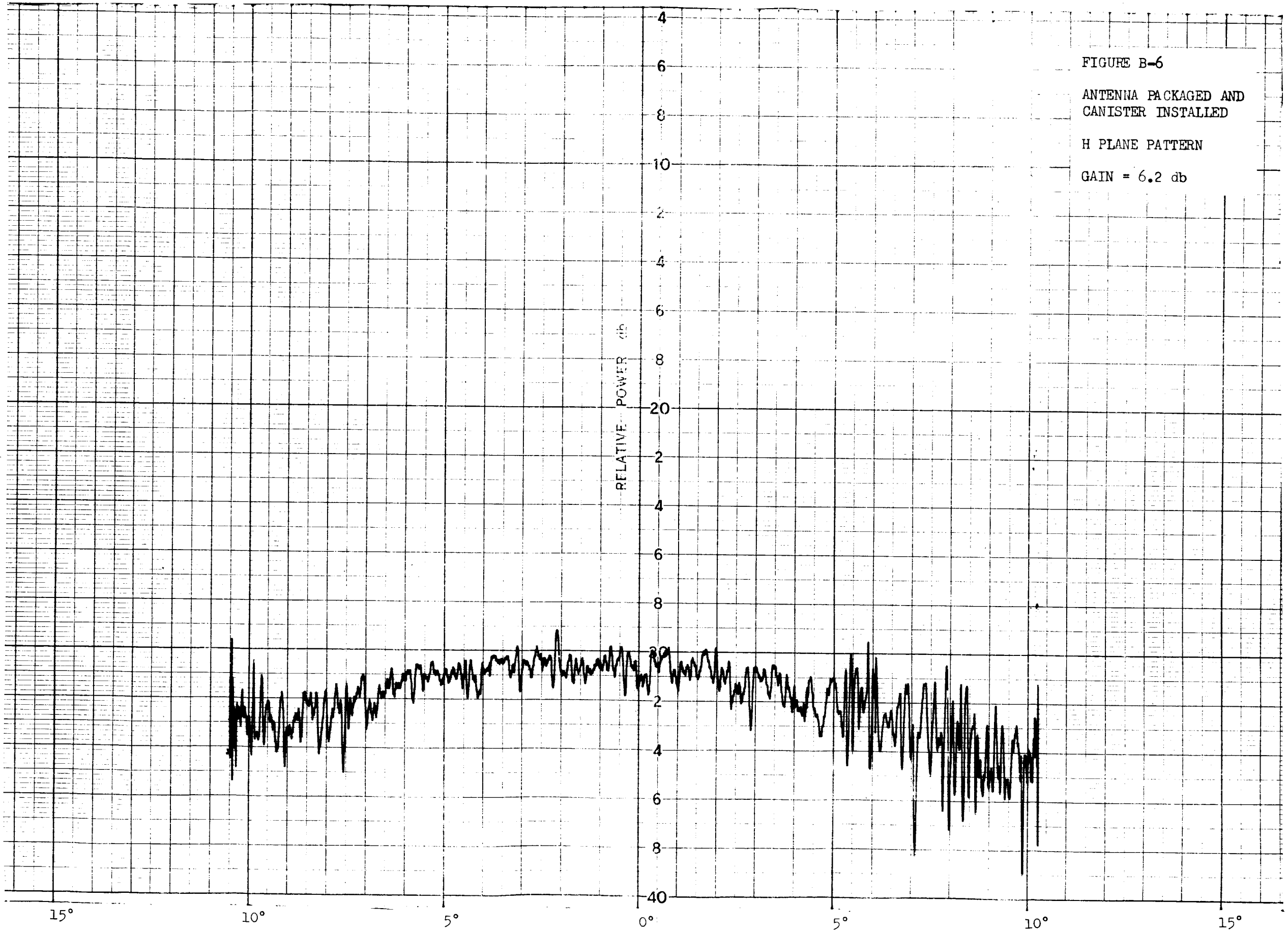

FIGURE B-6

ANTENNA PACKAGED AND CANISTER INSTALLED

H PLANE PATTERN

GAIN = 6.2 db

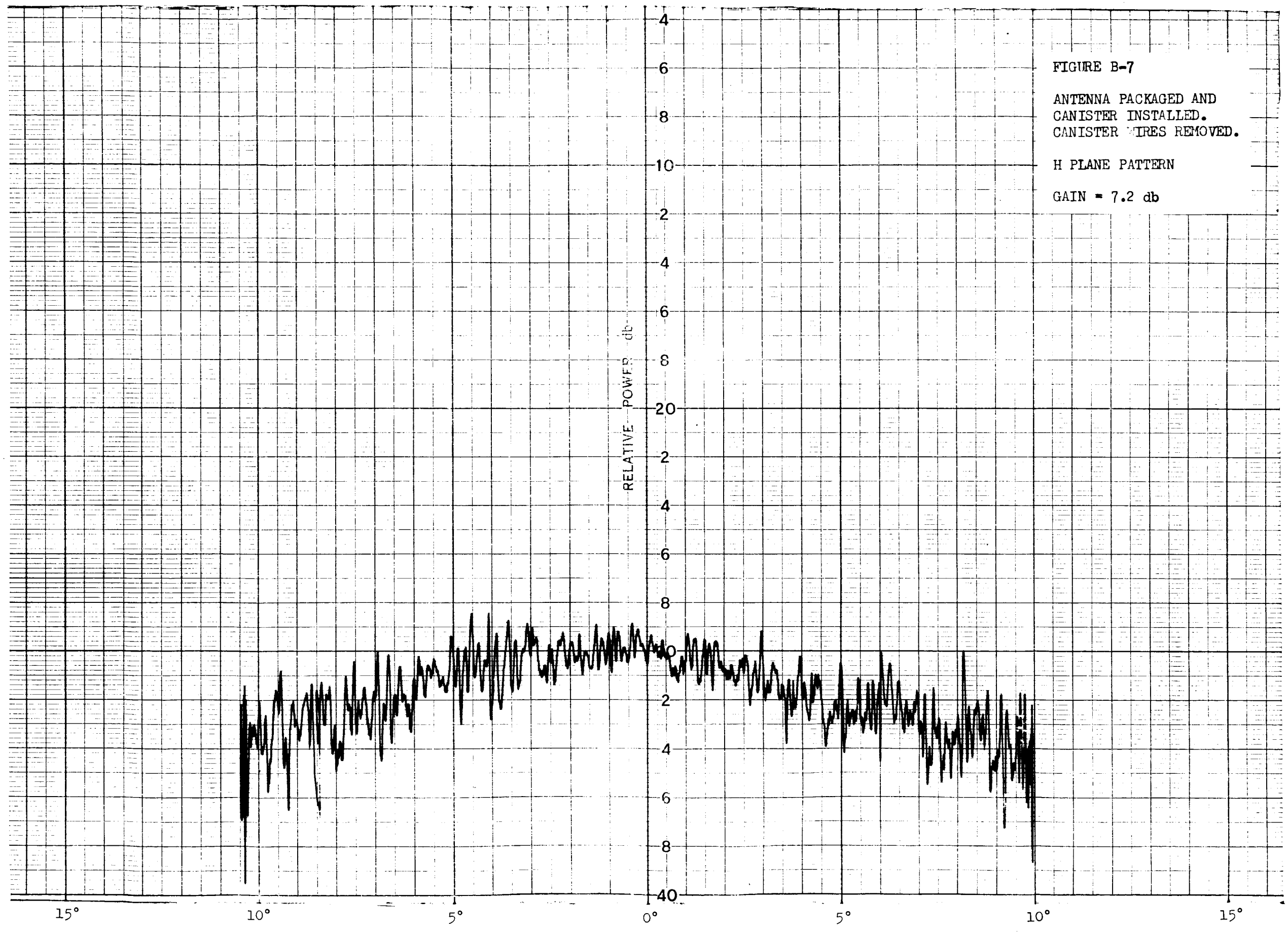

FIGURE B-7

ANTENNA PACKAGED AND
CANISTER INSTALLED.
CANISTER WIRES REMOVED.

H PLANE PATTERN

GAIN = 7.2 db

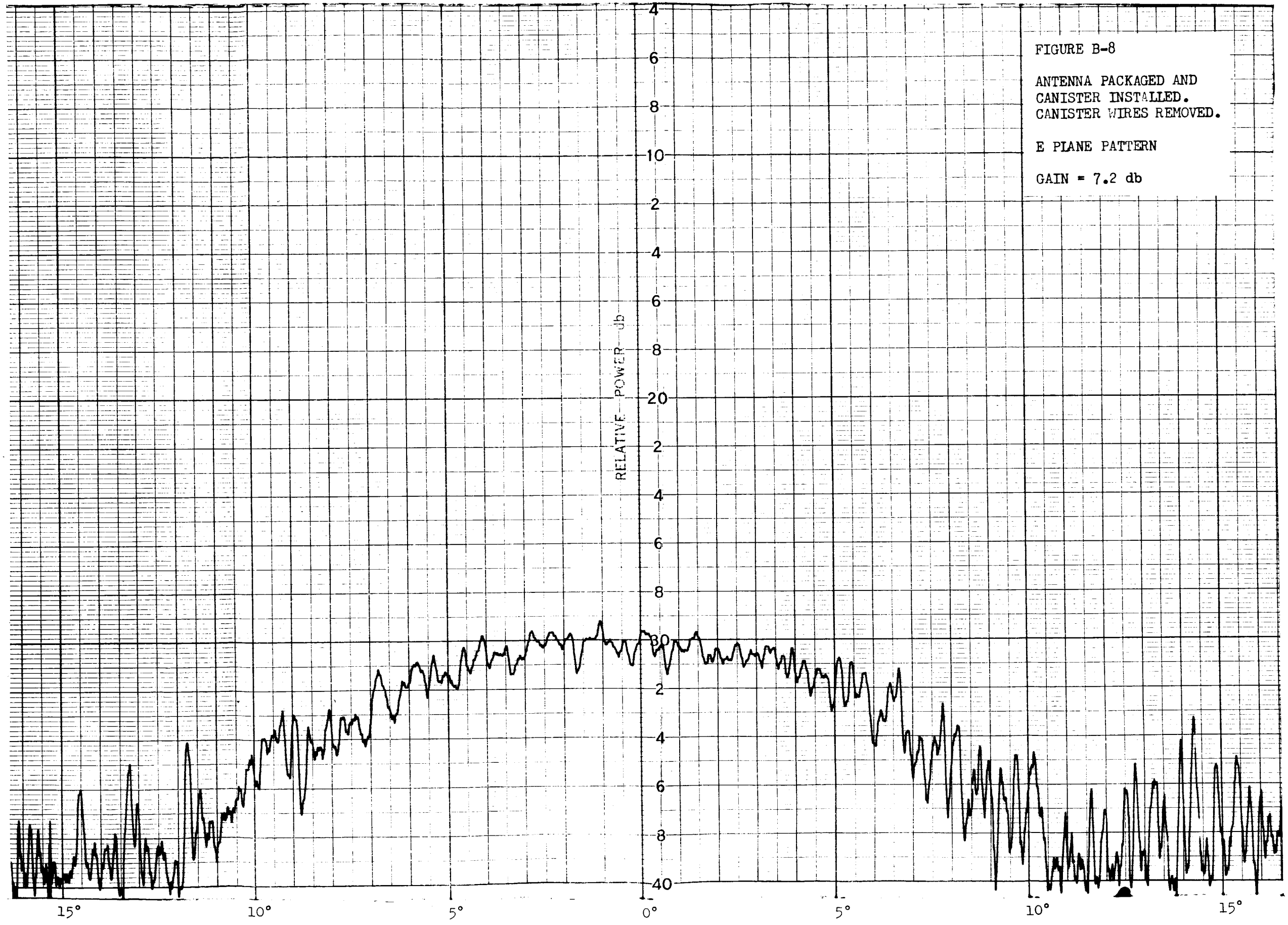

FIGURE B-8

ANTENNA PACKAGED AND CANISTER INSTALLED. CANISTER WIRES REMOVED.

E PLANE PATTERN

GAIN = 7.2 db

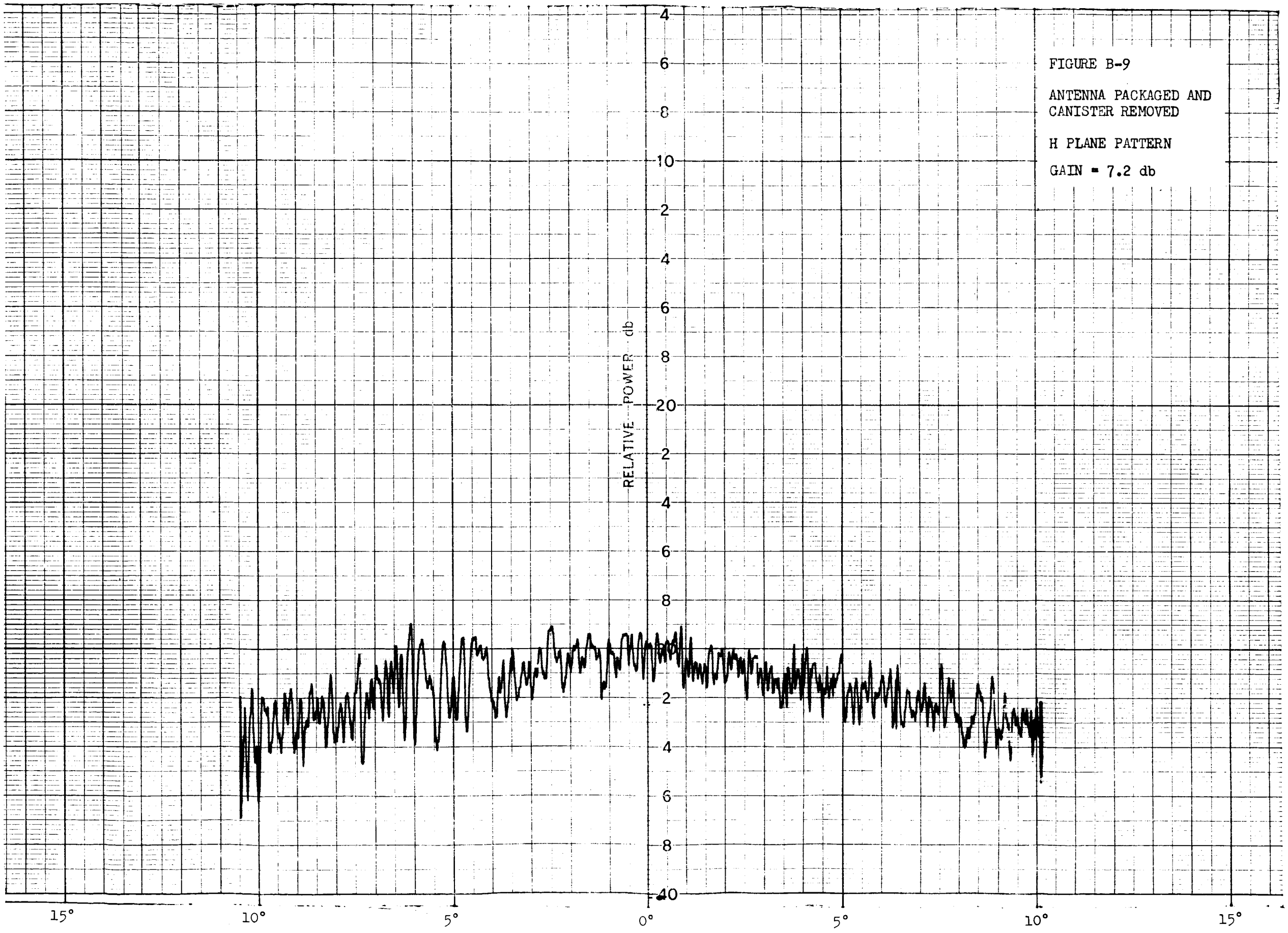

FIGURE B-9

ANTENNA PACKAGED AND CANISTER REMOVED

H PLANE PATTERN

GAIN = 7.2 db

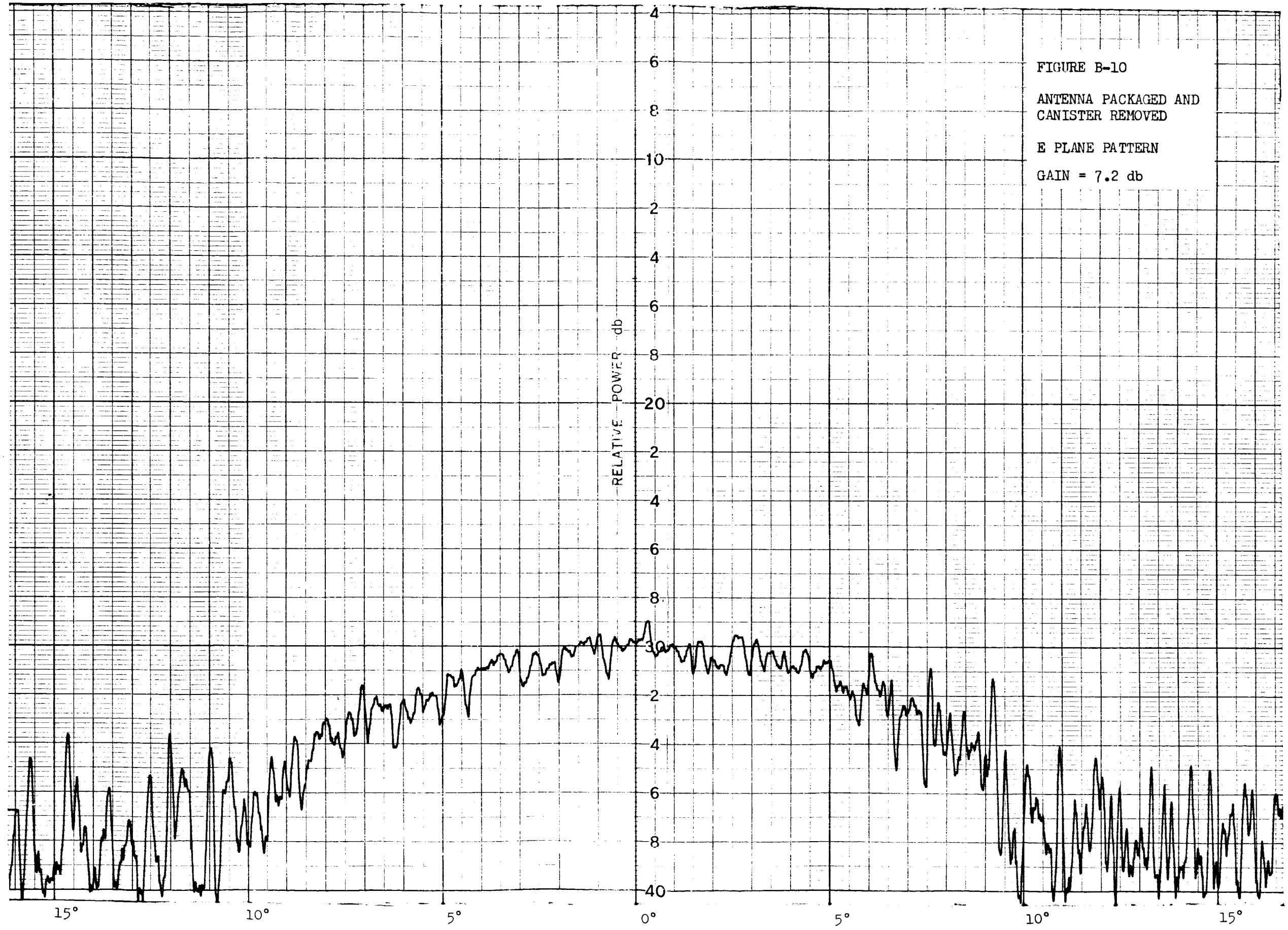

FIGURE B-10

ANTENNA PACKAGED AND CANISTER REMOVED

E PLANE PATTERN

GAIN = 7.2 db

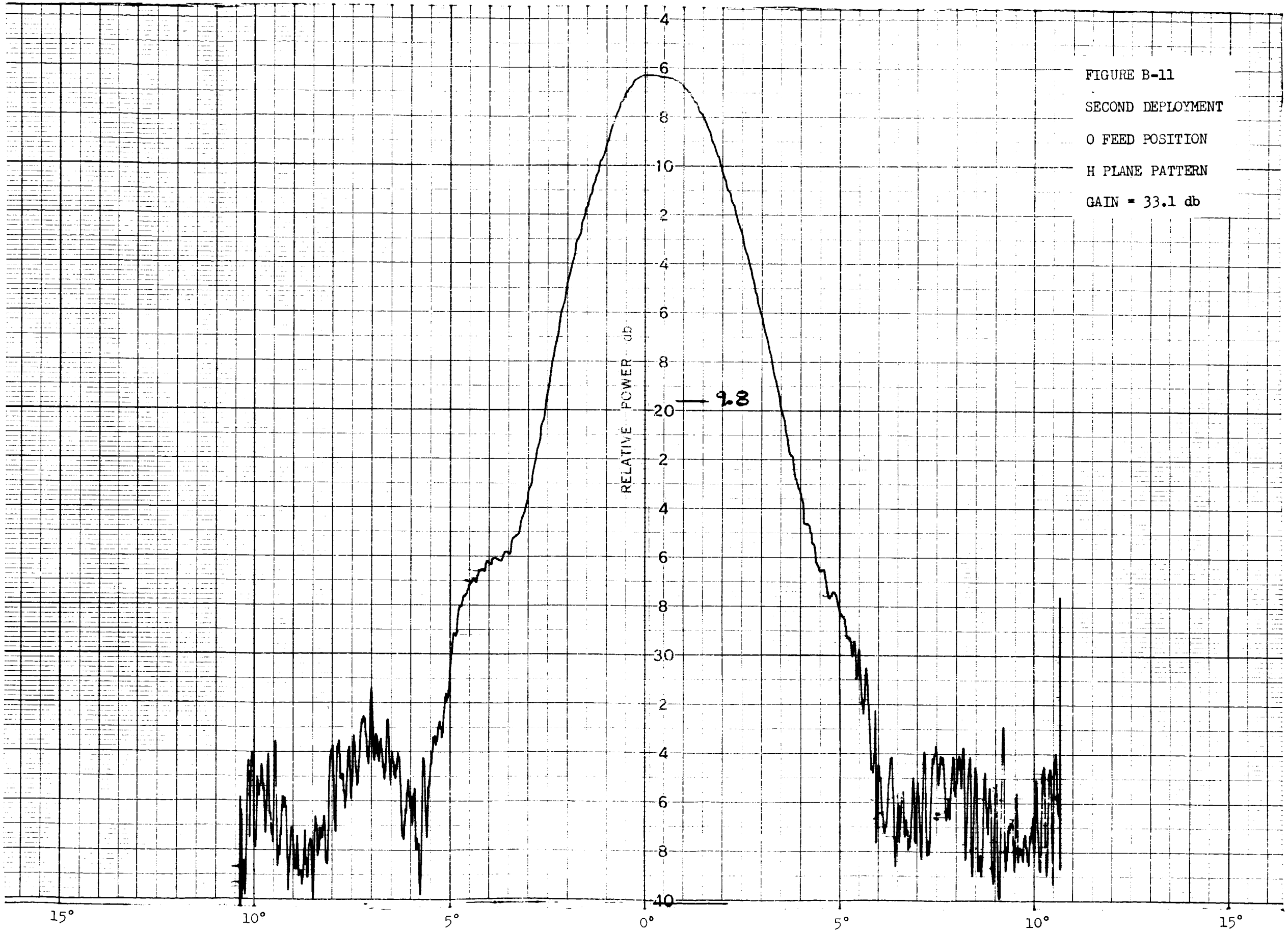

FIGURE B-11

SECOND DEPLOYMENT

O FEED POSITION

H PLANE PATTERN

GAIN = 33.1 db

FIGURE B-12

SECOND DEPLOYMENT

O FEED POSITION

E PLANE PATTERN

GAIN = 33.1 db

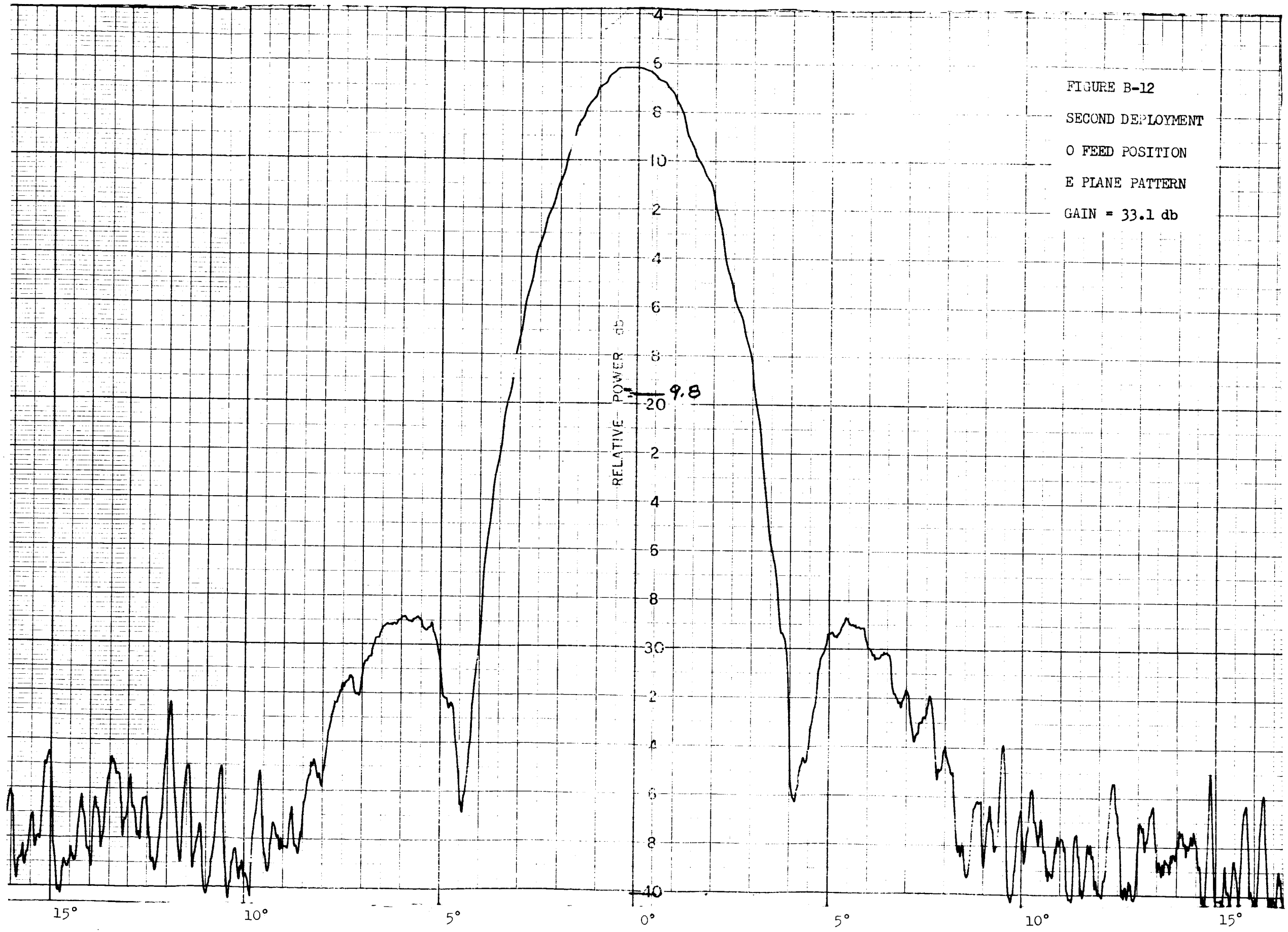

FIGURE B-13

SECOND DEPLOYMENT

0 + 90° FEED POSITION

H PLANE PATTERN

GAIN = 31.2 db

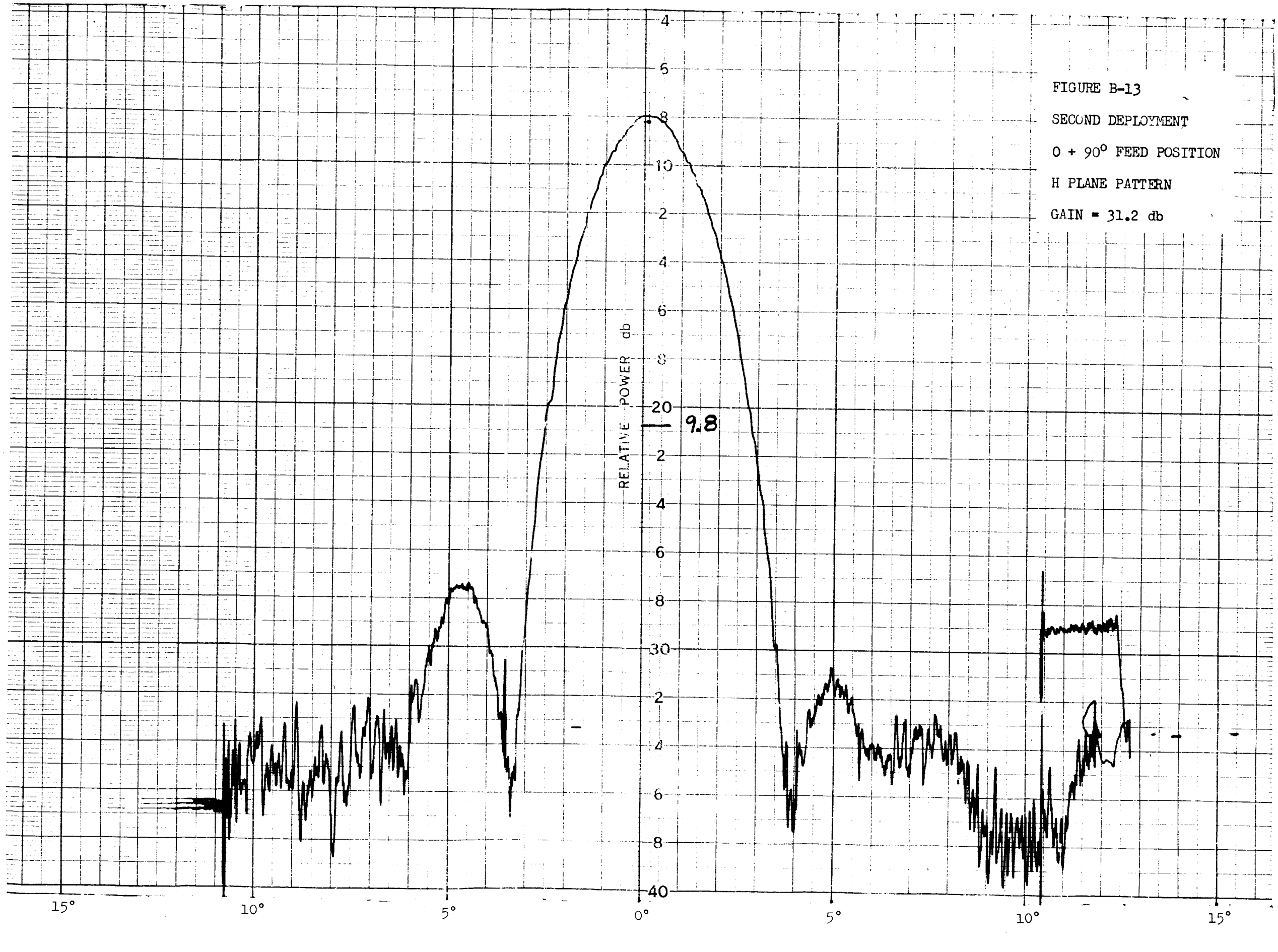

FIGURE B-14

SECOND DEPLOYMENT

0 + 90° FEED POSITION

E PLANE PATTERN

GAIN = 31.2 db

RELATIVE POWER db

9.8

4 6 8 10 2 4 6 8 20 2 4 6 8 30 2 4 6 8 40

15° 10° 5° 0° 5° 10° 15°

FIGURE B-15

THIRD DEPLOYMENT

O FEED POSITION

H PLANE PATTERN

GAIN = 33.2 db

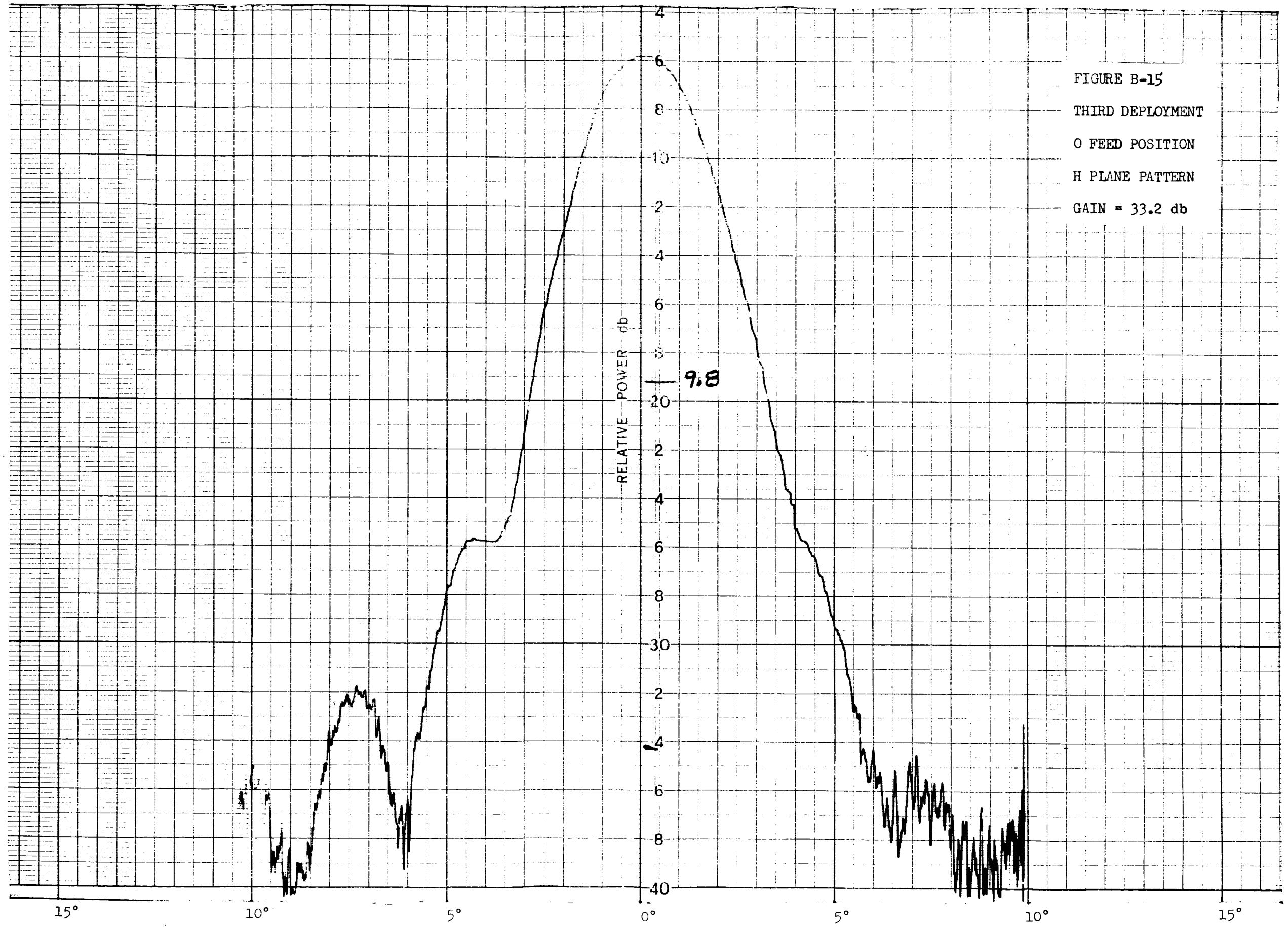

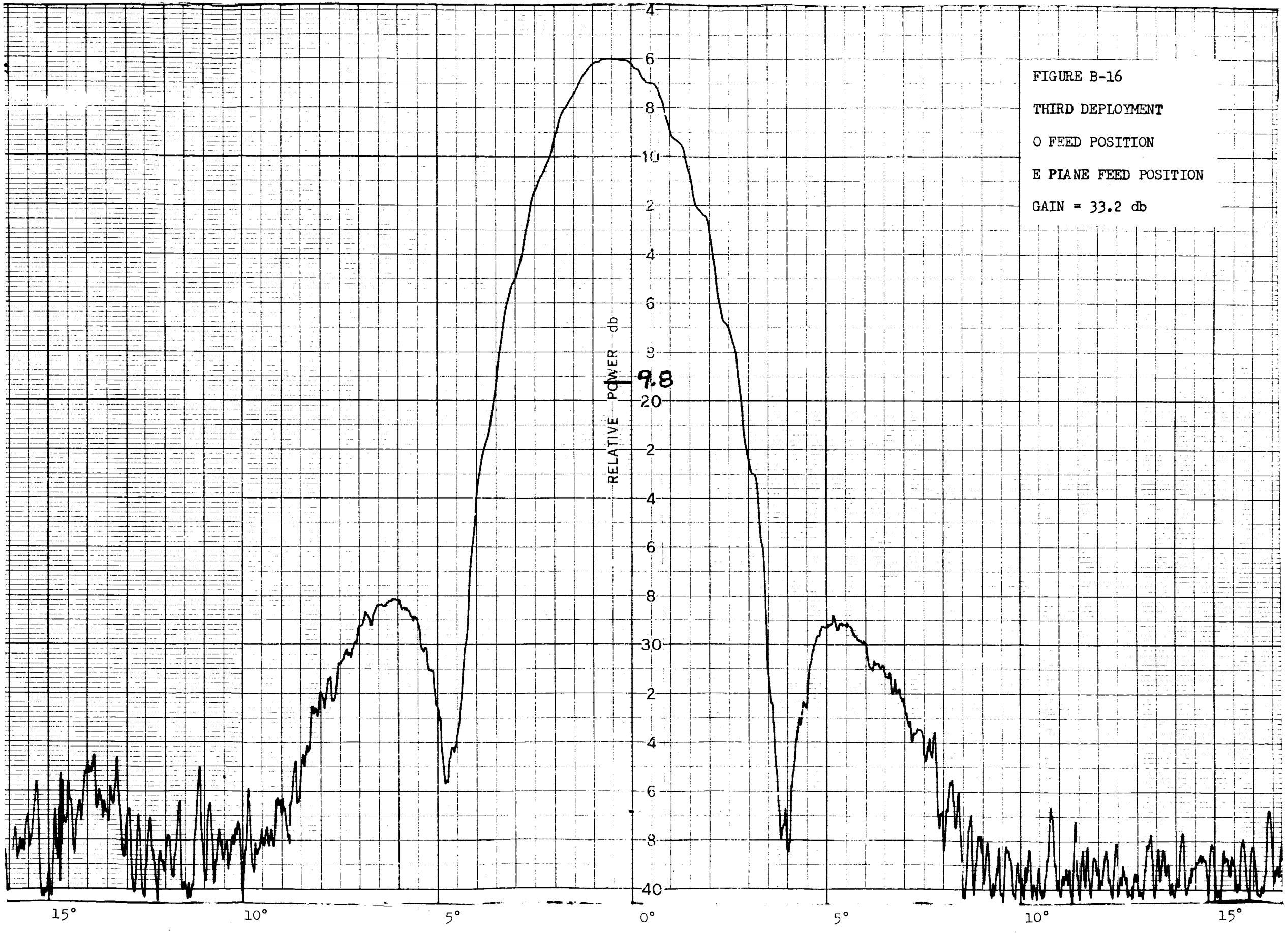

FIGURE B-16

THIRD DEPLOYMENT

O FEED POSITION

E PIANE FEED POSITION

GAIN = 33.2 db

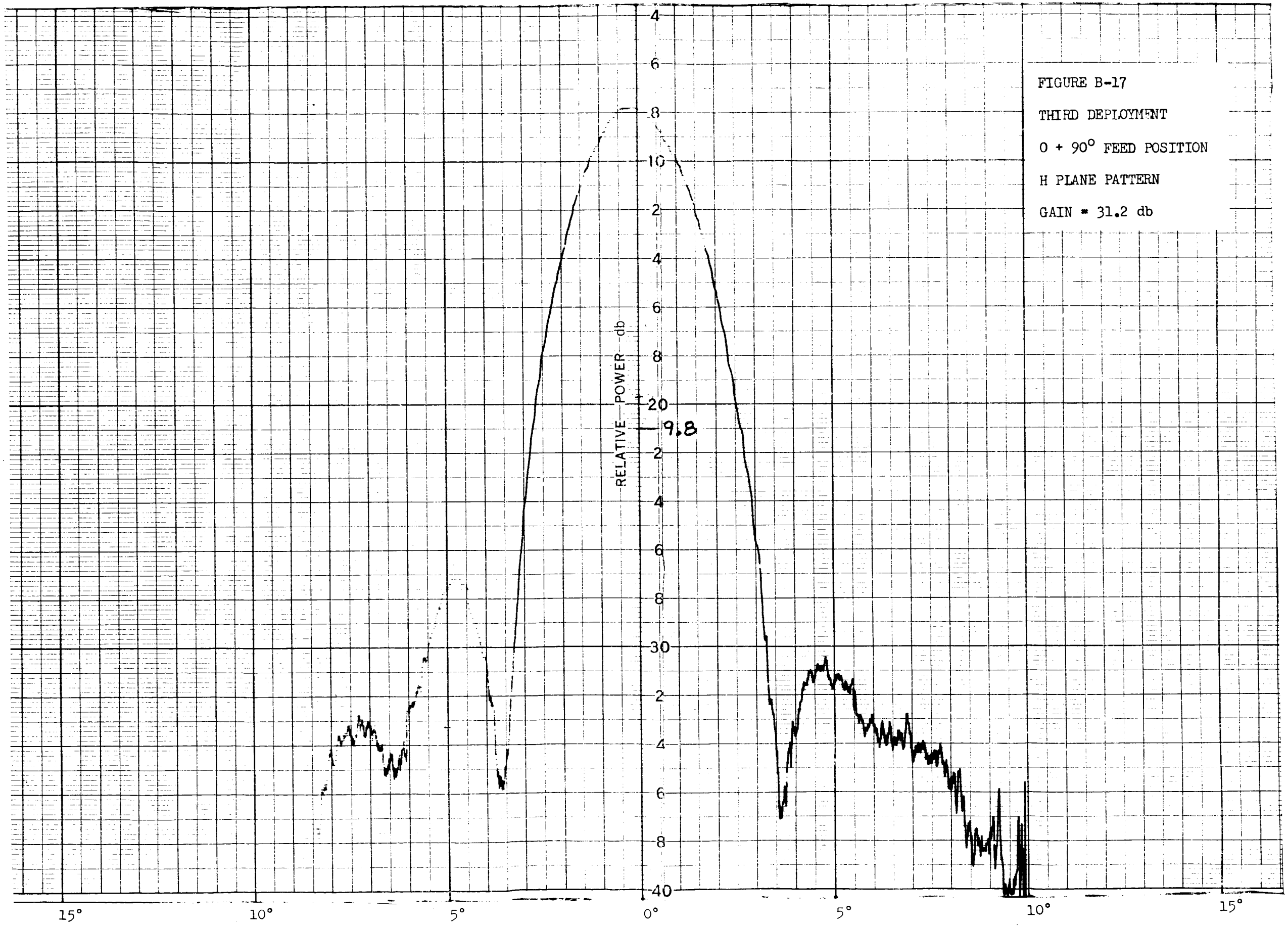

FIGURE B-17

THIRD DEPLOYMENT

0 + 90° FEED POSITION

H PLANE PATTERN

GAIN = 31.2 db

FIGURE B-18

THIRD DEPLOYMENT

0 + 90° FEED POSITION

E PLANE PATTERN

GAIN = 31.2 db

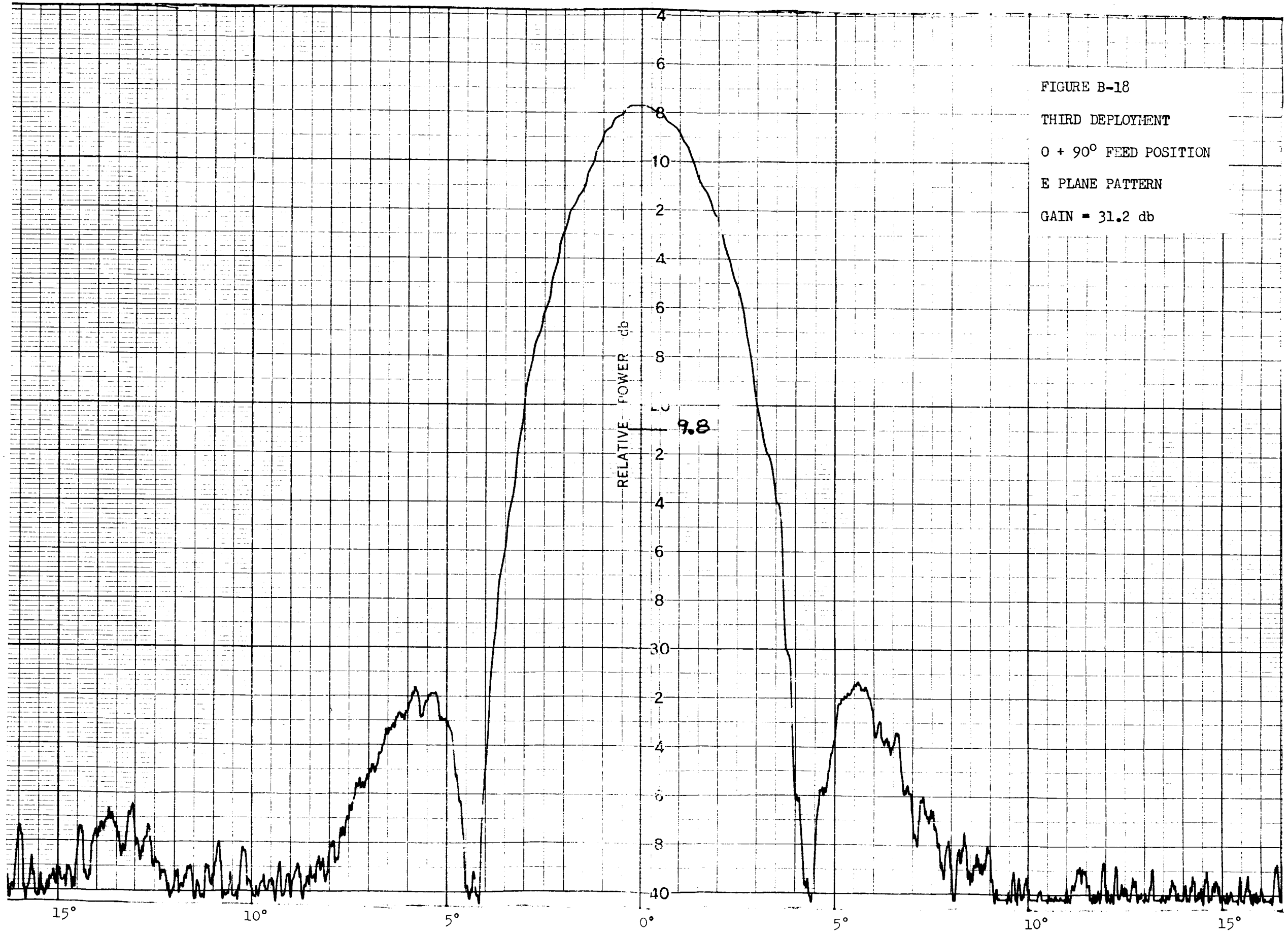

APPENDIX C

ENGINEERING DRAWINGS

The enclosed envelope is for storage of the following engineering drawings:

SK-DW-33065 FEED MODIFICATION

528A-055 RIB ASSY DEPLOYMENT MECHANISM

528A-056 MODIFICATION, DRUM LOCK AND CABLE ROUTING

528A-057 DRUM LOCK DETAILS

528A-058 SPACER

528A-059 BUMPER

528A-060 STIFFENER

528A-061 DRUM LOCK MODIFICATION DETAILS